December 2016

Ultrastructural Changes During Pollen Wall Development and Germination in Arabidopsis Thalaiana

Katrina Olsen
University of Wisconsin-Milwaukee

ULTRASTRUCTURAL CHANGES DURING POLLEN WALL DEVELOPMENT AND GERMINATION IN *ARABIDOPSIS THALIANA*

by

Katrina Olsen

A Dissertation Submitted in

Partial Fulfillment of the

Requirements for the Degree of

Doctor of Philosophy

in Biological Sciences

at

The University of Wisconsin-Milwaukee

December 2016

ABSTRACT

ULTRASTRUCTURAL CHANGES DURING POLLEN WALL DEVELOPMENT AND GERMINATION IN *ARABIDOPSIS THALIANA*

by

Katrina Olsen

The University of Wisconsin-Milwaukee, 2016
Under the Supervision of Heather A. Owen

The *Arabidopsis thaliana* meiotic mutant 6491 has been identified as displaying temperature sensitive male reduced- fertility. It has been determined that callose wall formation is defective, both in temporal and structural areas. There is irregular rippling in the plasma membrane and aberrant formation of the exine portion of the pollen wall. A developmental study using brightfield, epifluorescence, and transmission electron microscopy of the early stages of wall formation in 6491 has been completed, along with a similar study of *Arabidopsis thaliana (L.) heynh*, ecotype Wassilewskija (WS). Due to the temperature-sensitive nature of the mutant line, a further study of both lines was completed at three different growth temperatures, all within the acceptable growth range of *A. thaliana.* Techniques for visualization included Hoffman modulation contrast microscopy to examine structure and aniline blue staining observed by epifluorescence microscopy to examine callose wall formation. Several potentially damaging structural differences were noted in both lines, dependent upon the temperature at which the plants had been grown.

Further examination of pollen walls was undertaken, focusing on breakout of the pollen tube through the stiff patterned portion of the pollen wall layer known as exine. It has generally been accepted that pollen tubes exited through the interaperture space, where less biomechanical force

would be required to breach the wall. However, it is now known that certain species of *Arabidopsis thaliana* are omniaperturate, breaking through the wall at a point closest in contact with the stigma. Pollen from a known omniaperturate line, *Arabidopsis thaliana* ecotype Landsberg *erecta* (Ler), was dusted onto male sterile-1 (MS-1) mutant plants in the same background. Brightfield and transmission electron microscopy were used to determine structural changes occurring within the grain and wall that would allow a pollen tube to breach such a resilient structure as exine.

I dedicate this work

To my family and their love that is never ending,

To my daughter, Delaney, whose brightness, strength, and compassion gives me hope for the future of our world,

And to Heather Owen, who held a belief in me stronger than my own, who guided with infinite patience, care, intelligence, and perseverance, and to whom I owe a gratitude everlasting

TABLE OF CONTENTS

LIST OF FIGURES

LIST OF ABBREVIATIONS

Ba	Baculae
C	Celsius
Ca	Callose
Co	Collar
Cy	Cytoplasm
En	Endothecium
End	Endintine
Ep	Epidermis
ER	Endoplasmic reticulum
Ex	Exine
Exi	Exintine
Fl	Foot layer
GB	Golgi body
GSI	Gametophytic self-incompatibility
HTG	High Temperature Group
Int	Intine
Ler	Landsberg *erecta*
LTG	Low Temperature Group
M	Mitochondria
Mi	Microsporocyte
ML	Middle layer

mRNA	Messenger ribonucleic acid
Ms	Microspore
MTG	Mid-Range Temperature Group
MVBs	Multivesicular bodies
N	Nucleus
Nex	Nexine
Nm	Nanometer
Pb	Pectin bulge
Pc	Pollen coat
Pcd	Programmed cell death
PG	Pollen grain
PME	Pectin methylesterases
PR	Primexine
SAPs	Sporopollenin acceptor particles
Sb	Spherical bodies
Sc	Sperm cell
SCR	S-locus cysteine-rich protein
SEM	Scanning electron microscope
Sfl	Stratified fibrillar layer
SI	Self-incompatibility
SLG	S-locus glycoprotein
SP11	S-locus protein 11

SRK	S-locus receptor kinase
SSI	Sporophytic self-incompatibility
St	Stigma
T	Tapetum
Tc	Tectum
TEM	Transmission electron microscope
Te	Tetrads
TRY	Tryphine
µm	Micrometer
V	Vacuole
Vc	Vegetative cell
Ves	Vesicle
WS	Wassilewskij ecotype
WT	Wild-type

Introduction

Reproductive success in angiosperms such as *Arabidopsis thaliana* depends largely upon the development, release, and germination of pollen grains. The diploid microsporocytes of the male reproductive structures undergo substantial developmental changes from inception within the microsporangia, undergoing meiosis and cytokinesis to each produce four haploid microspores, through one or two (in *Arabidopsis*) mitotic divisions of each microspore to become male gametophytes (pollen grains), to dehiscence of the anther allowing release of the mature pollen, and finally attachment of pollen grains to the female stigma on which they germinate. In the early stages of this process, the cells that ultimately become pollen grains develop a species-specific outer covering called the exine. The exine is a highly reticulate layer that serves a number of functions, among them protection and species recognition in reproduction.

Mechanisms involved in the development and degradation of the exine and the rest of the pollen wall are not yet fully understood. Examination of the morphological changes occurring on an ultrastructural level during the development and degradation of the pollen wall can help elucidate these processes.

Background

Arabidopsis seeds germinate (principal growth stage zero) approximately three days after sowing. The first inflorescences emerge at twenty-six days (principal growth stage five). At forty-eight days siliques open, making seed collection possible (principal growth stage eight) (Boyes et al., 2001). On mature plants, male reproductive structures in *Arabidopsis thaliana* are found on the six stamens. The stamen consists of the filament and the anther, which is the site of pollen grain development. A diploid microsporocyte mass, along with four concentric rings of

non-reproductive tissue, constitutes the microsporangium. In *Arabidopsis*, the microsporangium is located within the locule in each of the four anther lobes. The non-reproductive layers of the microsporangium from deepest to most superficial, are the tapetum, middle layer, endothecium, and epidermis (Baldwin, Coen, & Dickinson, 1992; Heslop-Harrison, 1971; Owen & Makaroff, 1995).

The tapetum is perhaps the most valuable of the non-reproductive layers in the anther in terms of pollen development. This is a secretory tissue, providing support and nutrition to the microsporocytes which undergo meiosis to produce the microspores that undergo further developmental steps to ultimately become pollen grains. It plays additional important roles, secreting sporopollenin, a complex biopolymer that is used in the construction of the exine, and later in development producing materials of the pollen coat. Early in anther development the tapetal cells play a part in regulating the proliferation of microsporocytes. EXCESS MICROSPOROCYTES 1 (EMS1) (Zhao, Wang, Speal, & Ma, 2002) is expressed in the tapetal cell membrane during early development. Microsporocytes synthesize TAPETUM DETERMINANT 1 (TPD1) (Yang et al., 2003), a small protein ligand shown to bind EMS1. The activation of EMS1 by TPD1 induces tapetal cells to proliferate, which, in turn, represses further microsporocyte cell divisions (Feng & Dickinson, 2010; Jia, Liu, Owen, & Zhao, 2008). Another important function of the tapetum is to secrete AtMYB103 (Zhang et al., 2007) a transcription factor that regulates the gene *A6* in *Arabidopsis.* The protein coded for by *A6* has been shown to act as a callase (Hird et al., 1993), contributing to the dissolution of the callose wall that holds the four microspores produced by meiosis and cytokinesis of each microsporocyte together in tetrads. Finally, prior to degeneration of the tapetum, the cells release pollen coat material that is one of the components of the pollen wall, as development of the

pollen is completed. The materials deposited include esters and lipidic volatile compounds (Mayfield, Fiebig, Johnstone, & Preuss, 2001). In addition to the materials secreted from the tapetum, in *Arabidopsis* and other members of the Brassicaceae remnants of the degenerated tapetum cells are also deposited on the mature pollen grains and the pollen coat is called the tryphine.

In addition to the pollen coat, the mature pollen wall is composed of two main layers, the exine and intine (Figure 1). The exine can be further divided into the sexine and nexine, and the intine includes endintine and exintine layers. The species-specific patterning found on the exine of Brassicaceae is formed by the arrangement of the tectum and bacula.

Pollen Wall Development

Development of the pollen wall can be divided into twelve distinct stages (Owen & Makaroff, 1995). A brief overview of these stages follows and is shown in Figure 2. In premeiosis, diploid microsporocytes are enveloped by a cellulosic wall. Plasmodesmata initially connect the microsporocytes as well as the tapetal cells to each other, but these connections are lost as microsporocytes begin secreting callose, a β- 1,3 glucan, within their primary cell walls during premeiosis II. Plasmodesmatal connections between microsporocytes are replaced by larger connections called cytomictic channels as the callose is deposited. Functions of the cytomictic channels are still uncertain, but it has been proposed that they help to synchronize development of the microsporocytes (Heslop-Harrison, 1964). The presence of callose can be identified by staining with aniline blue, which binds specifically to β-1,3-glucan. During microsporogenesis, callose forms a special cell wall between the cellulosic cell wall and the plasma membrane, until

Figure 1 Transmission electron micrograph of a cross-section of exine architecture in pollen grains. The electron-dense exine of WT *Arabidopsis* pollen grains is made up of the Tc (tectum), Ba (baculae). Also shown Nex 1 and Nex 2 (Nexine), Int (Intine), PM (Plasma membrane), and Cy (Cytoplasm) Bar = 0.25um

Figure 2. Modified from Paxson-Sowders, et al. 1997, after Scott, 1994. Hoffman modulation contrast micrographs of single anther locules from 0.5 um semi-thin sections shown directly above corresponding regions of a pollen wall development model. **A** Early Meiosis. Each of the centrally located microsporocytes produces a callose wall. **B** Late Meiosis. Pre-patterned period, no observable structures exist at the microsporocyte surface within the callose wall. **C** Cytokinesis. Ingrowths of callose from the microsporocyte wall separate the daughter nuclei. **D** Early tetrad stage. Primexine matrix forms between the microspore plasma membrane and callose wall. **E** Mid tetrad stage. Formation of probaculae by deposition of sporopollenin at raised sites on plasma membrane. **F** Late tetrad stage. Probaculae become more consolidated. **G** Upon callose wall dissolution, microspores are released from tetrads. **H** Ring vacuolate stage. Tapetum-derived sporopollenin adds to the bacula and tectum, the foot layer and intine form. Bar = 10 um

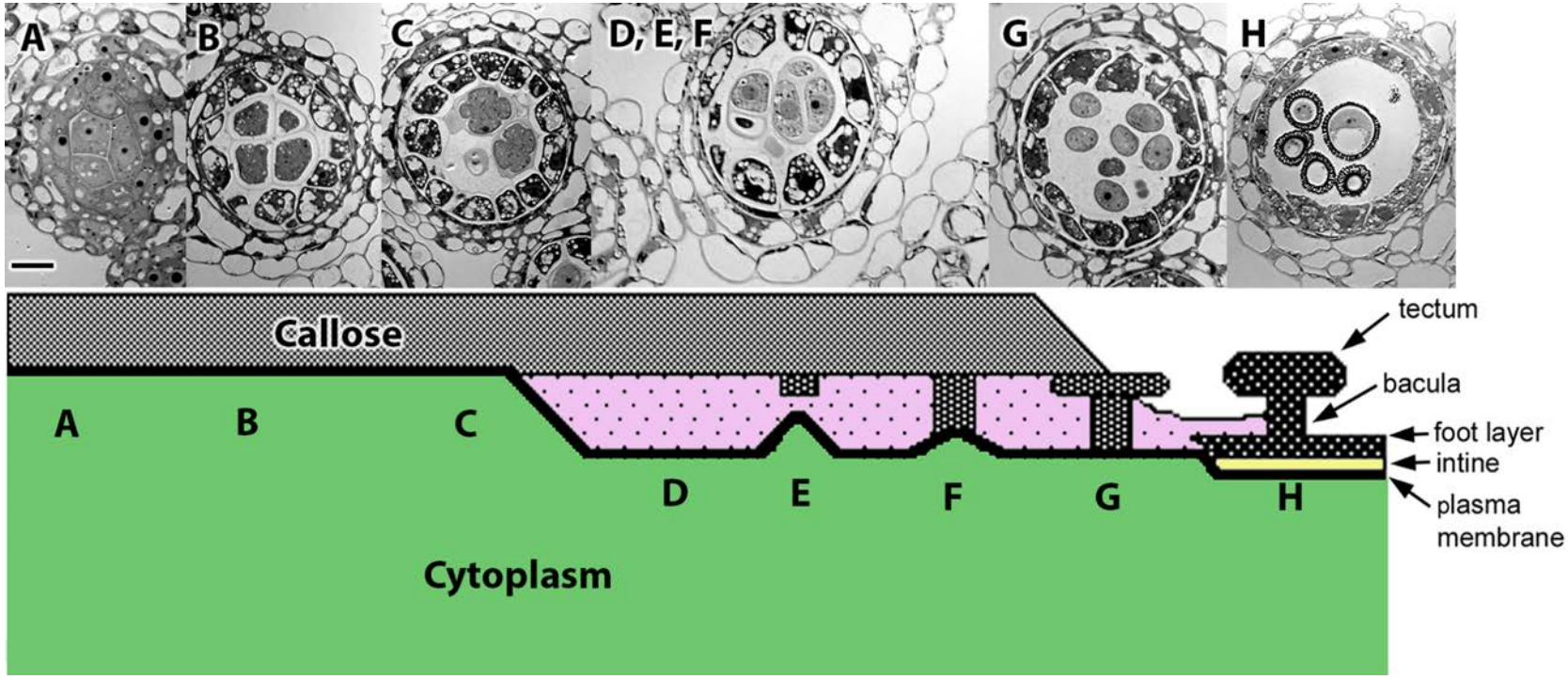
A
B
C
D, E, F
G
H
Callose
A
B
C
D
E
F
G
H
Cytoplasm
tectum
bacula
foot layer
intine
plasma membrane

it undergoes degradation later in development. Callose may serve to isolate and protect the microsporocytes while they are developing, especially from the influence of surrounding tissues (Knox & Heslop-Harrison, 1970). Callose continues to increase and all plasmodesmatal connections are terminated as the channels are filled in with callose. During meiosis each microsporocyte undergoes Meiosis I and Meiosis II to produce four haploid nuclei, followed by simultaneous cytokinesis during which centripetal furrows of callose form, originating from the parental wall and separating each coenocytic microsporocyte into a tetrad of microspores. The special cell wall is maintained until the late tetrad stage of development, when it is degraded by callase from the tapetum. Meiosis marks the beginning of the processes involved in exine patterning, but not yet to the point where pattern is visible through microscopic means. Several meiotic mutants have been thoroughly characterized and many have shown some type of defect or aberration in the exine. It has been suggested that callose may act as a template for the reticulate patterning of the exine (Waterkeyn & Bienfait, 1970); however, this has yet to be conclusively supported.

During the tetrad stage, components involved in exine formation appear and form the scaffolding for the unique patterns found on mature pollen grains. The scaffolding appears first as structures called probacula, radially directed rods that continue to develop and contribute to the formation of exine. At first, the microspore plasma membrane is held tight against the callose, and then electron-dense material is deposited and periodically spaced between the callose and membrane. This appears to cause a rippling or undulating of the membrane. It is thought the material being deposited is primexine matrix. Primexine has been reported as a microfibrillar material composed largely of cellulose, some proteins, and neutral and acidic polysaccharides (Heslop-Harrison, 1968). There are no confirmed models on how primexine

helps to establish patterning of the exine. One possibility is that primexine acts as an "anchor" to sporopollenin. Enzymes within primexine, referred to as sporopollenin acceptor particles (SAPs), may be associated with sporopollenin reception (Gabarayeva & Grigorjeva, 2004). Exine formation depends upon some kind of intracellular function or functions that will nucleate sporopollenin deposition at specific places along the plasma membrane.

There are several male-sterile mutants in *Arabidopsis* that result in defective primexine formation and support the idea that primexine helps to establish patterning of the exine. Among these is *defective in exine formation1 (dex1),* a mutation that results in random and delayed deposits of sporopollenin that do not appear to anchor to the plasma membrane (Paxon-Sowders, Dodrill, Owen, & Makaroff, 2001). Normal exine patterning does not occur in *dex1* mutants. *Ruptured pollen grain 1 (rpg1)* mutants have randomly deposited sporopollenin on both the plasma membrane and primexine, establishing a slightly functional exine (Guan et al., 2008). The primexine found in the *nef1 (no exine formation)* mutant seems to be the most defective, producing a thin primexine layer with no probacula present (Ariizumi et al., 2004). In *transient defective exine 1 (tde1),* fertility is normal, even with a phenotype that includes defective primexine and probacula development, as well as sporopollenin that is deposited in irregular aggregates. The *Tde1* line displays a normal exine pattern later in development, indicating the initial formation processes were affected, but not those necessary for proper exine formation (Ariizumi et al., 2008).

The rippling of the microspore membrane occurs throughout the plasma membrane, except where the apertures will form. Apertures are openings within the exine that allow for water influx at the point of adhesion between the pollen grain and stigma and, in many cases, an area for the pollen tube to easily escape (Edlund, Swanson, & Preuss, 2004). Apertures are formed

during the tetrad stage of development and, at maturity, are generally covered by the lipophilic inner pollen wall layer called the intine, but sporopollenin is either thinner or absent. The intine, which is deposited later in development, consists of polymers and celluloses, which are constructed from the microspores (Hasegawa, Bressan, Zhu, & Bohnert, 2000). Some studies have suggested that the presence of endoplasmic reticulum within the microspore cytoplasm at the sites of the future apertural openings (also known as "colpal shields") acts to restrict the deposition of primexine in these regions (Heslop-Harrison, 1963).

The undulations of the plasma membrane seem to be associated with the formation of spacers that are present in the depressions of the membranes (Fitzgerald & Knox, 1995). The depressions are evenly spaced, except for the sites of apertures, and are visible as the thickening of primexine matrix continues. As development proceeds, the primexine matrix becomes heterogeneous along the now straight plasma membrane. What occurs next is matter of great speculation. Electron-dense material appears within the primexine matrix, closest to the callose wall. This material accumulates and forms structures that appear to be developing exine, specifically the probacula. The electron-dense material is likely sporopollenin (Paxon-Sowders et al., 2001). Sporopollenin is composed of polyhydroxylated unbranched aliphatic units with small quantities of oxygenated aromatic rings and phenylproanoids (Ahlers, Thom, Lambert, Kuckuk, & Wiermann, 1999). The path the sporopollenin takes at this point in development is still being elucidated. It is the belief of this lab that this sporopollenin is produced from the microspore alone, with additional deposition of sporopollenin produced by the tapetum after the callose wall is degraded by callase. Other possibilities include all sporopollenin traversing the thick callose wall from the tapetum (Ariizumi & Toriyama, 2007).

The primexine continues to develop, as more sporopollenin is deposited. The sporopollenin becomes polymerized and the protectum (columns of the proexine) and probacula become fully formed. The tapetal cells release callase into the locule and the callose wall is degraded. With the dissolution of the callose wall, the microspores are now released from the tetrad formation. After the callose is gone, the tapetal cells also release sporopollenin, adding to the exine. The microspores increase in size, and two mitotic divisions follow. The first of these gives rise to the vegetative cell and the generative cell, and a second division of the generative cell in *Arabidopsis* results in the formation of the two sperm cells. The mature pollen grains are now tricellular and accumulate tryphine on the surface of the exine. The tryphine is comprised of long- and short-chain lipids, lipases and Gly-rich oleosins (Mayfield et al., 2001), along with the remnants of the degenerated tapetal cells. GRP17, a Gly-rich oleosin, is the most abundant protein in *Arabidopsis* tryphine (Mayfield & Preuss, 2000). Tryphine can help protect the pollen grain from desiccation and pathogen attack and also serves important roles in pollen reception, recognition and germination. The final stage is the release of the pollen grains through dehiscence, a rupturing of the stomium or furrow between the two locules on each side of the anther (Scott, Spielman, & Dickinson, 2004). Prior to dehiscence, the middle layer and tapetum degenerate, while fibrous bands are deposited in the endothecial cells. A bilocular anther is generated, and stomium cell breakage follows (Sanders et al., 1999), allowing release of pollen from the anthers.

Plant Reproduction and Structure

As mentioned previously, pollen grain development takes place in the male portion of the plant called the anther. The anther and filament together comprise the stamen of the flower. The primary female structures involved in plant reproduction are the ovary, style and stigma,

collectively known as the gynoecium (or pistil). After dehiscence, pollen grains are transported to the stigma via biotic and abiotic vectors. The *Arabidopsis* stigma contains approximately 150 elongated epidermal cells, specialized for recognition of compatible pollen grains (Sessions & Zambryski, 1995). Upon contact a series of interactions occur between the desiccated pollen grain and stigma with the pollen-stigma interface physically changing and becoming stronger as pollination continues. The initial contact and binding is thought to be exine-mediated, possibly of a chemical basis involving polymers in the exine (Edlund et al., 2004). The process has not yet been fully studied and remains an unknown in the pollination pathway. What is known is that the compatibility response is different depending upon whether the stigma is of the dry or wet type. A wet stigma is covered in a layer of secretions containing carbohydrates and lipids (Zinkl, Zwiebel, Grier, & Preuss, 1999). Any pollen grain landing on the stigma has the ability to be hydrated. The compatibility response is initiated later in development rather than at the point of contact. In a dry stigma such as that of *Arabidopsis*, at the point of adhesion between the pollen grain and stigma, the pollen coat mobilizes from its original place between the tectum and bacula of the grain to form a "foot layer" (Figure 3) between the two structures (Edlund, 2004). Other components such as water and nutrients pass from the papillae through the pollen coat to contact the grain and contribute to the formation of the foot layer. It is during this time in adhesion when a compatibility response is initiated.

Self Incompatibility (SI) is an important evolutionary advance that allows for recognition and rejection between stigma and pollen of certain angiosperms. To encourage the successful advancement of a species, new genetic information should be integrated, thereby allowing for

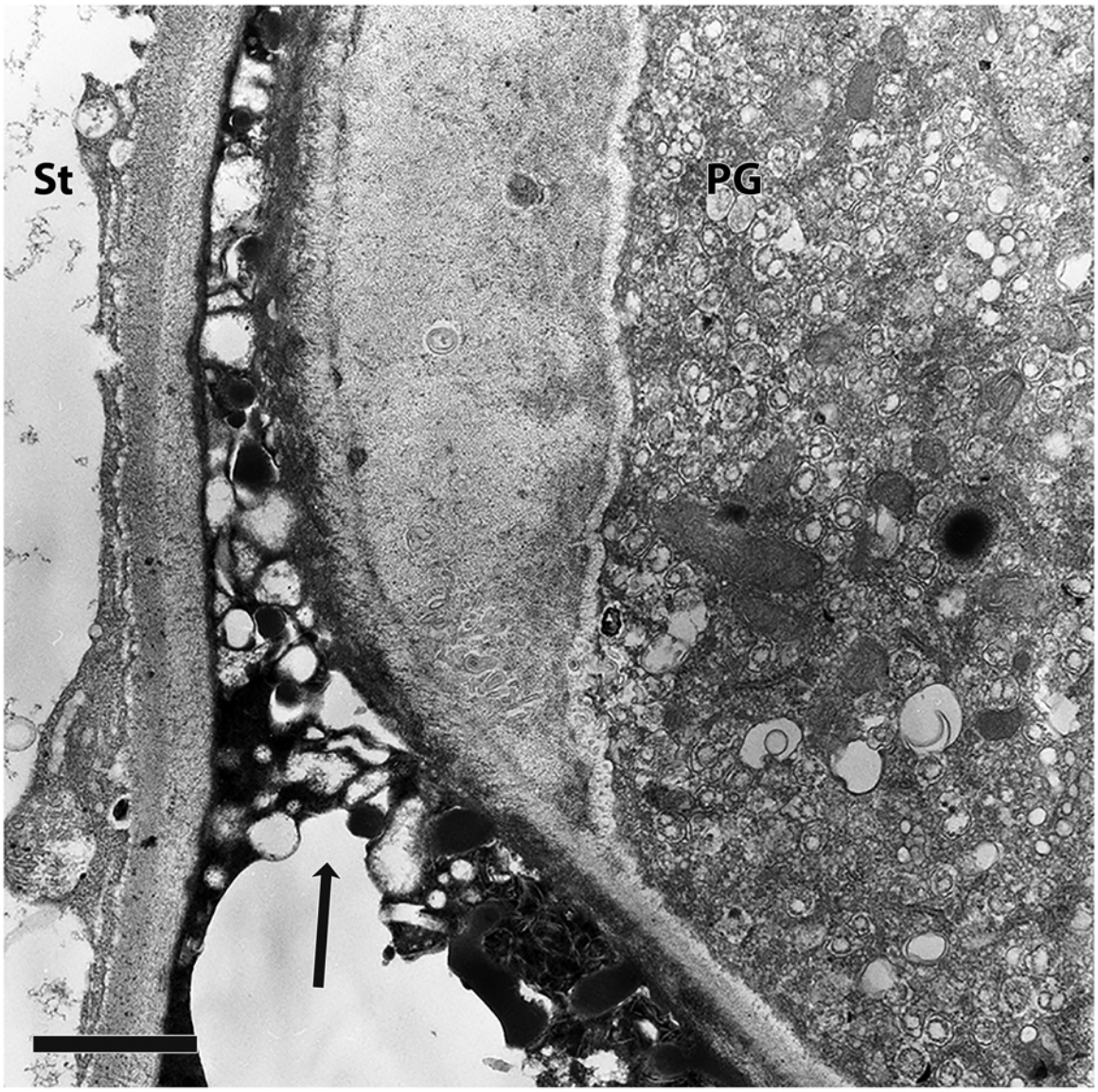

Figure 3. Pollination in Arabidopsis. Transmission electron micrograph showing the point of contact between a pollen grain (PG) and a stigma papillus (St). A foot of lipid-rich material (arrow) collects between the two surfaces. Bar = 1 µm

species survival through adaptation as necessary. Continued inbreeding or selfing may increase the number of mutations in a population, and selfing becomes disadvantageous when the offspring suffer reduced fitness (Tsuchimatsu & Suwabe, 2010). There are several types of SI, but two distinct systems are most prevalent; Gametophytic Self-Incompatibility (GSI) and Sporophytic Self-incompatibility (SSI). Both systems are controlled by the S locus, a multiallelic locus that contains linked transcriptional units that are inherited as a single unit. The S-locus contains two protein-coding regions; one is expressed in the pistil and is called the female determinant and the other is expressed in the pollen grain and called the male determinant. Although both GSI and SSI are similar in having a two-gene recognition system, the male and female determinants are different. Most species of *Arabidopsis* do not exhibit the SI response, but rather self-fertilize. Notable exceptions are *Arabidopsis lyrata* and *Arabidopsis halleri* (Kusaba et al., 2001). In *A. thaliana* mutations have occurred that retained the molecular signaling components necessary for the SI response, but removed the ability to carry out the process (Nasrallah, Nasrallah, Liu, Sherman-Broyles, & Boggs, 2004).

GSI occurs in families such as the Papaveraceae, Solanaceae and Rosaceae and is the most prevalent form of SI in angiosperms. In GSI the phenotype of the pollen is determined by its own gametophytic haploid genotype (Franklin-Tong & Franklin, 2003). Each pollen grain arises from the diploid mother cell undergoing meiosis and producing a tetrad of haploid microspores. Thus the pollen grain has one allele, while the stigma contains two. If the alleles are of the same haplotype, rejection should occur.

SSI occurs in the Brassicaceae and has been well characterized, with more than 50 haplotypes (in *B. oleracea*) and both the male and female determinants identified. The male determinant is S-locus protein 11 or S-locus cysteine rich protein (SP11/SCR), a small pollen coat protein that

induces incompatible reactions in the stigma papilla cells (Schopfer, Nasrallah, & Nasrallah, 1999). SP11/SCR is expressed post-meiotically in both the pollen grain and anther tapetum (Bower et al., 1996), although in some S-alleles it is expressed solely in the tapetal cells (Shiba et al., 2001). Prior to degradation of the tapetum, SCR is localized to the pollen grain surface (Iwano et al., 2003).

The female determinant is S-locus receptor kinase (SRK). The expression of *SRK* begins in flower buds and peaks when the buds reach maturity. SRK is found in the stigma plasma membrane (Stephenson et al., 1997) and *SRK* mRNA undergoes splicing, resulting in several transcripts. One of those transcripts encodes eSRK, which comprises the extracellular domain of SRK. A transmembrane domain and an intracellular domain are also present (Seiji Takayama & Isogai, 2005).

SRK is predicted to be synthesized in the endoplasmic reticulum, then sent through the Golgi and finally localized to small vesicles in close proximity to the plasma membrane (Ivanov & Gaude, 2009). Only small amounts of SRK are present at the plasma membrane and those small amounts are distributed in SI domains or zones. SRK is abundant in the endosomes and colocalizes with THIOREDOXIN H-LIKE 1 (THL1). THL1 and THIOREDOXIN H-LIKE2 (THL2) act as inhibitors to SRK, keeping SRK in an inactive state until self-pollen germination. The activity of THL1 and THL2 is inhibited upon SCR ligand binding (Bower et al., 1996).

Another protein that co-segregates with SP11/SCR and SRK is S-locus glycoprotein (SLG), but it is thought that SLG is not required for the SI response (Seiji Takayama et al., 1987). SLG is thought to act as an enhancer of SRK activity (Nasrallah, 2000), but is not necessary in all haplotypes. This was supported through a gain-of-function experiment using *B. rapa* expressing

both *SLG*$_{28}$ and *SRK*$_{28}$. S$_{28}$ pollen was rejected, but there was a stronger incompatibility reaction with both proteins (SLG and SRK) than with SRK alone.

The SSI system is initiated when the pollen grain lands on the stigma and the pollen coat flows to the point of adhesion. SP11/SCR travels from the pollen coat, penetrates the papilla cell wall with the help of an unknown pollen coat protein and, if both determinants are from the same haplotype, binds the extracellular domain of SRK. This will activate SRK in an S-haplotype-specific manner (S. Takayama et al., 2001). The activation is based upon the physical interaction between SRK and SCR and the activation of the SRK kinase domain. An intracellular signaling cascade eventually leads to the rejection of self-pollen. The events occurring within the cascade have not yet been conclusively determined, but evidence is supportive of the following pathway.

The binding of SP11/SCR to SRK causes phosphorylation and activation of the kinase domain in SRK. *M* locus protein kinase (MLPK) appears to form a complex with SRK at the plasma membrane (Murase et al., 2004), which in turn could activate downstream events. Armadillo-repeat-containing 1 (ARC1) binds the SRK-MLPX complex at the kinase domain of SRK, resulting in the phosphorylation of ARC1, an E3 ubiquitin ligase. Activation of ARC1 may target and negatively regulate factors that promote the self-compatibility response (Samuel et al., 2008).

Exo70A1 is a protein that is ubiquitinated by ARC1 and sent to the proteosome. It is one of the possible factors that contributes to the SI response when negatively regulated by ARC1. Exo70A1 is necessary in the stigma for the SC response. If a SI response is to occur, then Exo70A1 would likely have to be removed from the plasma membrane, much as ARC1 is

suspected of doing. After activation of the SRK complex at the plasma membrane, the complex dissociates, with SRK and possibly some other components going to the endosomes.

The point of adhesion is where the pollen tube germinates and either comes through the aperture or breaks through the exine, then travels down the stigma. Pollen tubes of many species will exit only through the thinned areas of the pollen wall, where the exine is absent. However, preliminary studies have shown that pollen tubes in *Arabidopsis* will breakout through interaperture spaces in some ecotypes, despite the presence of the thick sporopollenin in these patterned regions (Edlund et al., 2004). In *Arabidopsis*, the breakout point seems to be determined by the most direct route to the point of adhesion. In order for the pollen tube to exit the pollen grain, the pollen wall must be weakened, a force or pressure must be present to push out through the wall, or a combination of the two must be present. While the pollen tube is breaking out, a pectin bulge forms underneath the point of adhesion to the stigma. The pollen tube elongates and grows between the papillar cells of the stigma into the style. The two sperm travel down the tube until they reach the ovule, where one sperm fertilizes the egg and the other fuses with the 2N central cell nucleus to become the 3N endosperm.

All of the genetic analyses to date, and those that will continue to be completed in the future, will contribute to the elucidation of pathways involved in pollen wall development. Along with genetic analysis, morphological analysis of structures involved in pollen development, germination, and degradation will provide a much-needed component to the overall picture of plant reproduction in *Arabidopsis thaliana*. To that end, the aims of this study are three-fold:

1. To examine aberrations in pollen development of both a novel pollen wall mutant and wild-type *Arabidopsis* within a narrow range of temperatures.
2. To characterize a novel pollen wall mutant at the ultrastructural level.
3. To examine at the ultrastructural level how the very deviant non-aperture breakout behavior that is observed in some ecotypes of Arabidopsis occurs.

These aims will be addressed separately in each of the following three chapters.

References

Ahlers, F., Thom, I., Lambert, J., Kuckuk, R., & Wiermann, R. (1999). H NMR analysis of sporopollenin from *Typha angustifolia*. *Phytochemistry, 50*, 1095-1098.

Ariizumi, T., Hatakeyama, K., Hinata, K., Inatsugi, R., Nishida, I. S., Shusei, & Kato, T. (2004). Disruption of the novel plant protein NDF1 affects lipid accumulation in the plastids of the tapetum and exine formation of pollen, resulting in male sterility in *Arabidopsis thaliana*. *The Plant Journal, 39*, 170-181.

Ariizumi, T., Kawanabe, T., Hatakeyama, K., Sato, S., Kato, N., Tabata, S., & Toriyama, K. (2008). Ultrastructural characterization of exine development of the *transient defective exine 1* mutant suggests the existence of a factor involved in constructing reticulate exine architecture from sporopollenin aggregates. *Plant and Cell Physiology, 49*, 58-67.

Ariizumi, T., & Toriyama, K. (2007). Pollen exine pattern formation is dependent on three major developmental processes in *Arabidopsis thaliana*. *International Journal of Plant Developmental Biology, 1*, 106-115.

Baldwin, T., Coen, E., & Dickinson, H. (1992). The ptl1 gene expressed in the transmitting tissue of Antirrhinum encodes an extensin-like protein. *The Plant Journal, 2*(5), 733-739.

Bower, M. S., Matias, D. D., Fernandes-Carvalho, E., Mazzurco, M., Gu, T., Rothstein, S. J., & Goring, D. R. (1996). Two members of the thioredoxin-h family interact with the kinase domain of a Brassica S locus receptor kinase. *The Plant Cell, 8*(9), 1641-1650.

Boyes, D. C., Zayed, A. M., Ascenzi, R., McCaskill, A. J., Hoffman, N. E., Davis, K. R., & Gorlach, J. (2001). Growth stage-based phenotypic analysis of Arabidopsis: A model for high throughput functional genomics in plants. *The Plant Cell, 13*, 1499-1510.

Edlund, A. F., Swanson, R., & Preuss, D. (2004). Pollen and stigma structure and function: The role of diversity in pollination. *The Plant Cell, 16*, S84-S97.

Feng, X., & Dickinson, H. G. (2010). Tapetal cell fate, lineage and proliferation in the *Arabidopsis* anther. *Development, 137*, 2409-2416.

Fitzgerald, M., & Knox, R. (1995). Initiation of primexine in freeze-substituted microspores of Brassica campestris. *Sex. Plant Reprod, 8*, 99-104.

Franklin-Tong, V., & Franklin, F. (2003). Gametophytic self-incompatibility inhibits pollen tube growth using different mechanisms. *Trends Plant Sci., 8*, 598-605.

Gabarayeva, N. I., & Grigorjeva, V. V. (2004). Exine development in Encephalartos altensteinii (Cycadaceae): ultrastructure, substructure and the modes of sporopollenin accumulation. *Rev. Palaeobot. Palynol, 132*, 175-193.

Guan, Y.-F., Huang, X.-Y., Zhu, J., Gao, J.-F., Zhang, H.-X., & Yang, Z.-N. (2008). *RUPTURED POLLEN GRAIN1*, a member of the MtN3/saliva gene family, is crucial for exine pattern formation and cell integrity of microspores in Arabidopsis. *Plant Physiology, 147*, 852-863.

Hasegawa, P. M., Bressan, R. A., Zhu, J., & Bohnert, H. J. (2000). Plant cellular and molecular responses to high salinity. *Annual Review of Plant Physiology and Plant Molecular Biology, 51*, 463-499.

Heslop-Harrison, J. (1963). An ultrastructural study of pollen wall ontogeny in *Silene pendula*. *Grana Palynologica, 4*, 7-24.

Heslop-Harrison, J. (1964). Cell walls, cell membranes and protoplasmic connections during meiosis and pollen development. In H. Linskens (Ed.), *Pollen Physiology and Fertilization* (pp. 29-47). Amsterdam: North-Holland.

Heslop-Harrison, J. (1968). Pollen wall development. *Science, 161*, 230-237.
Heslop-Harrison, J. (1971). Wall pattern formation in angiosperm microsporogenesis. *Society for Experimental Biology Symposium, 25*, 277-300.
Hird, D. L., Worrall, D., Hodge, R., Smartt, S., Paul, W., & Scott, R. (1993). The anther-specific protein encoded by the Brassica napus and Arabidopsis thaliana A6 gene displays similarity to beta-1,3-glucanases. *The Plant Journal, 4*(6), 1023-1033.
Ivanov, R., & Gaude, T. (2009). Endocytosis and Endosomal Regulation of the S-Receptor Kinase during the Self-Incompatibility Response in Brassica oleracea. *Plant Cell, 21*(7), 2107-2117.
Iwano, M., Shiba, H., Funato, M., Shimosato, H., Takayama, S., & Isogai, A. (2003). Immunohistochemical Studies on Translocation of Pollen S-haplotype Determinant in Self-incompatibility of Brassica rapa. *Plant and Cell Physiology, 44*(4), 428-436.
Jia, G., Liu, X., Owen, H. A., & Zhao, D. (2008). Signaling of cell fate determination by the TPD1 small protein and EMS1 receptor kinase. *PNAS, 105*(6), 2220-2225.
Knox, R., & Heslop-Harrison, J. (1970). Direct demonstration of the low permeability of the angiosperm meiotic tetrad using a fluorogenic ester. *Z. Pflanzenphysiol., 62*, 451-459.
Kusaba, M., Dwyer, K., Hendershot, J., Vrebalov, J., Nasrallah, J., & Nasrallah, M. (2001). Self-Incompatibility in the Genus Arabidopsis: Characterization of the S Locus in the Outcrossing A. lyrata and Its Autogamous Relative A. thaliana. *Plant Cell, 13*, 627-643.
Mayfield, J. A., Fiebig, A., Johnstone, S. E., & Preuss, D. (2001). Gene families from the Arabidopsis thaliana pollen coat proteome. *Science, 292*(5526), 2482-2485.
Mayfield, J. A., & Preuss, D. (2000). Rapid initiation of Arabidopsis pollination requires the oleosin-domain protein GRP17. *Nature Cell Biology, 2*(2), 128-130.
Murase, K., Shiba, H., Iwano, M., Che, F. S., Watanabe, M., Isogai, A., & Takayama, S. (2004). A membrane-anchored protein kinase involved in Brassica self-incompatibility signaling. *Science, 303*(5663), 1516-1519.
Nasrallah, J. B. (2000). Cell-cell signaling in the self-incompatibility response. *Curr Opin Plant Biol, 3*(5), 368-373.
Nasrallah, J. B., Nasrallah, M. e., Liu, P., Sherman-Broyles, S., & Boggs, N. A. (2004). Natural variation in expression of self-incompatibility in Arabidopsis thaliana: Implications for the evolution of selfing. *Proceedings of National Academy of Science, 101*(45), 16070-16074.
Owen, H. A., & Makaroff, C. A. (1995). Ultrastructure of microsporogenesis and microgametogenesis in *Arabidopsis thaliana* (L) *heynh* ecotype Wassilewskija (*Brassicaceae*). *Protoplasma, 185*, 7-21.
Paxon-Sowders, D. M., Dodrill, C. H., Owen, H. A., & Makaroff, C. A. (2001). DEX1, a novel plant protein, is required for exine pattern formation during pollen development in *Arabidopsis*. *Plant Physiology, 127*, 1739-1749.
Samuel, M. A., Mudgil, Y., Salt, J. N., Delmas, F., Ramachandran, S., Chilelli, A., & Goring, D. R. (2008). Interactions between the S-Domain Receptor Kinases and AtPUB-ARM E3 Ubiquitin Ligases Suggest a Conserved Signaling Pathway in Arabidopsis. *Plant Physiology, 147*(4), 2084-2095.
Sanders, P. M., Bui, A. Q., Weterings, K., McIntire, K. N., Hsu, Y.-C., Lee, P. Y., Truong, M. T., Beals, T. P., & Goldberg, R. B. (1999). Anther developmental defects in *Arabidopsis thaliana* male-sterile mutants. *Sexual Plant Reproduction, 11*, 297-322.

Schopfer, C., Nasrallah, M., & Nasrallah, J. B. (1999). The male determinant of of self-incompatibility in plants. *Science, 286*, 1697-1700.
Scott, R. J., Spielman, M., & Dickinson, H. G. (2004). Stamen Structure and Function. *Plant Cell, 16*(suppl_1), S46-60.
Sessions, R., & Zambryski, P. (1995). Arabidopsis gynoecium structure in the wild and in ettin mutants. *Development, 121*(5), 1519-1532.
Shiba, H., Takayama, S., Iwano, M., Shimosato, H., Funato, M., Nakagawa, T., Che, F.-S., Suzuki, G., Watanabe, M., Hinata, K., & Isogai, A. (2001). A Pollen Coat Protein, SP11/SCR, Determines the PollenS-Specificity in the Self-Incompatibility of Brassica Species. *Plant Physiology, 125*(4), 2095-2103.
Stephenson, A. G., Doughty, J., Dixon, S., Elleman, C., Hiscock, S., & Dickinson, H. G. (1997). The male determinant of self-incompatibility in Brassica oleracea is located in the pollen coating. *The Plant Journal, 12*(6), 1351-1359.
Takayama, S., & Isogai, A. (2005). Self-incompatibility in plants. *Annual Review of Plant Biology, 56*(1), 467-489.
Takayama, S., Isogai, A., Tsukamoto, C., Ueda, Y., Hinata, K., Okazaki, K., & Suzuki, A. (1987). Sequences of S-glycoproteins, products of the Brassica campestris self-incompatibility locus. *Nature, 326*(6108), 102-105.
Takayama, S., Shimosato, H., Shiba, H., Funato, M., Che, F. S., Watanabe, M., Iwano, M., & Isogai, A. (2001). Direct ligand-receptor complex interaction controls Brassica self-incompatibility. *Nature, 413*(6855), 534-538.
Tsuchimatsu, T., & Suwabe, K. (2010). Evolution of self-incompatibility in *Arabidopsis* by a mutation in the male specificity gene. *Nature, 464*, 1342-1347.
Waterkeyn, L., & Bienfait, A. (1970). On a possible function of the callosic special wall in *Ipomoea purpurea* (L) *Roth*. *Grana, 10*, 13-20.
Yang, C.-Y., Spielman, M., Coles, J. P., Li, Y., Ghelani, S., Bourdon, V., Brown, R. C., & Lemmon, B. E. (2003). TETRASPORE encodes a kinesin required for male meiotic cytokinesis in *Arabidopsis*. *The Plant Journal, 34*, 229-240.
Zhang, Z. B., Zhu, J., Gao, J. F., Wang, C., Li, H., Li, H., Zhang, H. Q., Zhang, S., Wang, D. M., Wang, Q. X., Huang, H., Xia, H. J., & Yang, Z. N. (2007). Transcription factor AtMYB103 is required for anther development by regulating tapetum development, callose dissolution and exine formation in Arabidopsis. *Plant J, 52*(3), 528-538.
Zhao, D.-Z., Wang, G.-F., Speal, B., & Ma, H. (2002). The EXCESS MICROSPOROCYTES1 gene encodes aputative leucine-rich repeat receptor protein kinase that controls somatic and reproductive cell fates in the *Arabidopsis* anther. *Genes & Development, 16*, 2021-2031.
Zinkl, G. M., Zwiebel, B. I., Grier, D. G., & Preuss, D. (1999). Pollen-stigma adhesion in *Arabidopsis*: a species-specific interaction mediated by lipophilic molecules in the pollen exine. *Development, 126*, 5431-5440.

Chapter II

Developmental Study of Meiotic Mutant 6491 and Wild Type *Arabidopsis thaliana* Using Brightfield and Epifluorescence Microscopy

A. Introduction

The establishment of exine pattern begins in meiosis. Several possibilities have been noted that may lead to or be included in exine pattern formation (Ariizumi & Toriyama, 2011; Dawson et al., 1993; Owen & Makaroff, 1995; Regan & Moffatt, 1990). Among these are deposition of primexine matrix, transfer of wall material to the microspore surface via transport along microtubules, endoplasmic reticulum determining location of apertures and invagination of the plasma membrane (Heslop-Harrison, 1971a, 1971b).

Exine patterning is also largely determined by the deposition of callose and primexine at the microspore surface, along with or perhaps mediated by the plasma membrane (Blackmore, Wortley, Skvarla, & Rowley, 2007). The interplay of these and the resulting exine pattern can be greatly affected by the timing of both callose and primexine deposition, as shown in the following literature review.

Mutant Analysis and the Development of the Pollen Wall

Molecular genetics, especially mutant analysis, has led to a more complete understanding of pathways involved in pollen wall development in *Arabidopsis*. Three phases of exine pattern formation have been described (Ariizumi & Toriyama, 2011): synthesis of sporopollenin precursors, primexine formation and callose wall formation. Within each of these stages, several mutants have been characterized.

Callose is synthesized and functions in both gametophytic and sporophytic tissues. Twelve callose synthase genes (also known as *GLUCAN SYNYHASE-LIKE* (*GSL*)) have been identified in *Arabidopsis*. Of these, *GSL1, 2, 5, 8* and *10* function primarily in microgametogenesis (Chen et al., 2009). GSL1 and 5 help prevent microspore degeneration, by forming the callose wall separating the coenocytic microsporocyte into a tetrad of microspores. In studies completed with double mutants of gsl1 and gsl5, a callose wall surrounded microspore mother cells, but did not separate the developing tetrad. This particular phenotype had collapsed and inviable pollen grains (Enns et al., 2005). GSL2 synthesizes callose in the temporary callose wall and functions in exine patterning (Dong, Hong, Sivaramakrishnan, Mahfouz, & Verma, 2005). The temporary callose wall forms between the plasma membrane and cell wall, separating developing microsporocytes until it is dissolved in tetrad stage (Worrall et al., 1992). The *gsl2* mutant line lacked proper exine formation on the surface of microspores, leading to collapsed pollen grains walls forming from only aggregates of tryphine on the surface of mature grains. GSL8 and GSL10 contribute to microspore mitosis and asymmetrical division of the vegetative and generative cell that produces the male gametophye (pollen grain) from each microspore. Neither has been found necessary for microspore development, with *gsl8* and *gsl10* mutants having normal exine, normal callose deposition in microspores, and normal polarization of microspores prior to asymmetric division. A mutation in either gene is demonstrated after cytokinesis following the first mitotic division of the microspore begins. Dwarf phenotypes and mononuclear rather than bicellular pollen grains were observed (Toller, Brownfield, Neu, Twell, & Schulze-Lefert, 2008).

Several male-sterile mutants involved in primexine development were covered previously (*dex1, nef1, tde1, rpg1*). *hkm* (*hackly microspore*) (Ariizumi & Toriyama, 2011) is another

primexine mutant that has random aggregates of sporopollenin on both the primexine and plasma membrane. Allelic to the *HKM* gene is *MS1* (*Male Sterility 1*) (Vizcay-Barrena & Wilson, 2006). *ms1* mutants have aberrant pollen wall formation and incomplete deposition of exine, leading to degeneration of microspores. Genes involved in sporopollenin synthesis and, accordingly, exine sculpturing include *MS2* (*Male Sterility 2*) (Aarts et al., 1997) and a number of *LAP* (*Less Adherent Pollen*) genes. The *ms2* mutant has a complete lack of exine layer and nonviable pollen, and has been proposed to be involved in the sporopollenin polymerization pathway. The *lap* mutants have abnormal or non-existent exine, and may be associated with the synthesis of fatty acids and phenolics in the exine (Zinkl, Zwiebel, Grier, & Preuss, 1999).

A number of cytochrome P450s have been shown essential for exine development. CYP704B and CYP703A2 (along with MS2) are all thought to be involved in fatty acid metabolism, a necessary part of sporopollenin synthesis. The mutated genes in each of these three lines resulted in phenotypes with pollen surfaces lacking exine (Dobritsa et al., 2009). Another set of mutants, the *qrt* (*quartet*) mutants, produce tetrads of microspores that do not separate. The failure to separate is caused by a lack of degradation of pectin components in the pollen mother cell wall (Rhee & Sommerville, 1998).

In order to gain a better understanding of pollen wall development, a preliminary morphological characterization of a novel *Arabidopsis* mutant (6491) in which both meiosis and pollen wall patterning are affected has been accomplished using transmission (TEM) and scanning electron microscopy (SEM). Unlike other meiotic mutants, 6491 demonstrates reduced fertility when grown at 20^{o} C, instead of complete sterility. The mutation is also temperature-sensitive. 6491 plants grown at 16˚ C show an increase in fertility when compared to plants

grown at 20° C, while plants grown at 27° C show a marked reduction in fertility in comparison with plants grown at 20° C.

A comparison of wild-type (WT) and mutant pollen grains using SEM demonstrates several differences (Fig. 4 A and B). 6491 grains are more varied in size and rounder than WT pollen, and also lack the consistent regular patterning seen on WT pollen. Apertures appear to be non-existent. Also noted from preliminary data using TEM (not shown), the outer wall of 6491 is thinner than WT and not closely attached to the intine. Although there are fewer differences in the size, shape, and number of microspores in cool grown plants, preliminary data showed differences in the development and thickness of the callose wall between WT and 6491.

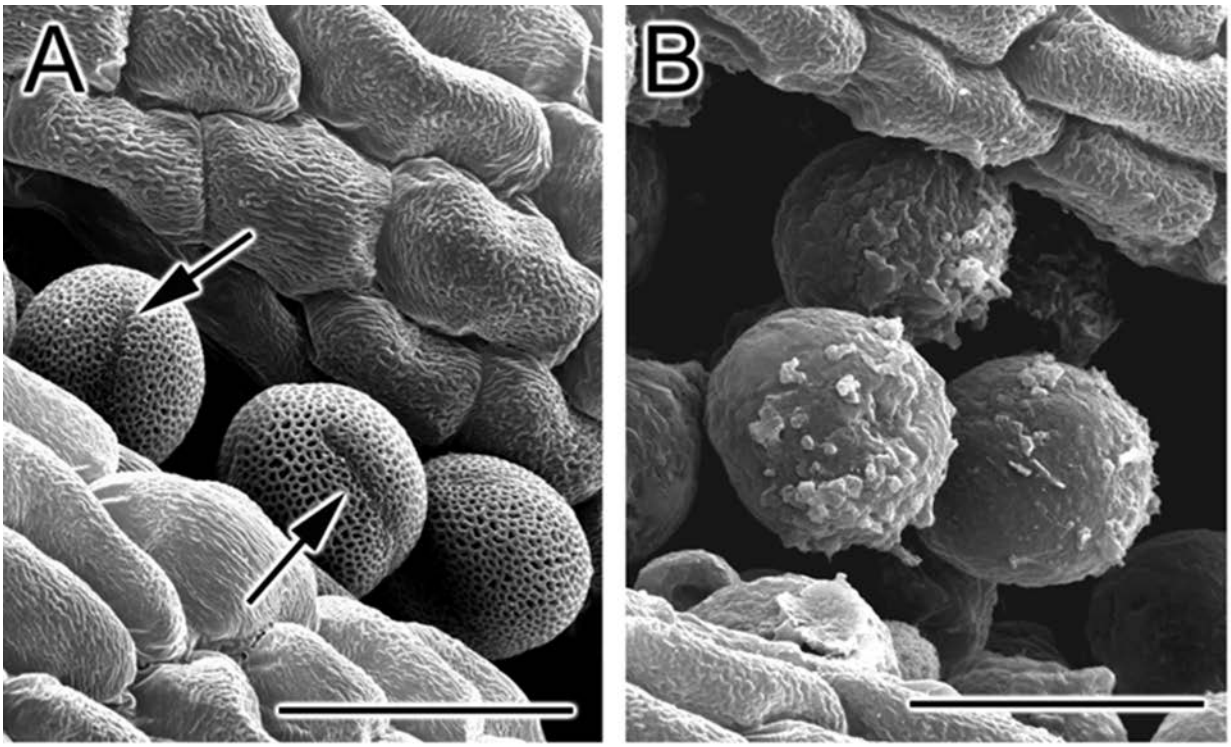

Figure 4. Electron micrographs of mature WT and 6491 pollen grains. **A, B** SEM images of critical point dried dehisced anthers. **A** WT pollen have colpi (arrows) and reticulate exine patterning. **B** Walls of 6491 pollen grains are smooth and lack colpi. Size bar = 20 µm

As part of this project, 6491 was further analyzed. A developmental series examining the ultrastructure of both 6491 and WT *Arabidopsis* within a narrow range of temperatures was completed using images of Azure B stained semi-thin sections. Because of its importance in pollen wall patterning, ultraviolet fluorescence micrographs of semi-thin sections stained with aniline blue were also examined for an in depth look at the deposition of the callose wall to determine whether there were alterations in deposition between plants grow at different temperatures.

B. Materials and Methods

Plant growth:

Arabidopsis thaliana (L.) heynh, ecotype Wassilewskija (WS) wild-type and 6491, a mutant line in the same background, were used in this work. The mutant 6491 was identified in a screen of a T-DNA mutagenized population (Feldmann & Marks, 1987) and is maintained as a homozygous recessive line. Seeds were grown on damp Metro Mix 360 commercial potting mix in a growth chamber with a 16/8 light and dark cycle. Three different temperature treatments were sustained: 16° C, 20° C, or 27° C.

Semi-thin slide preparation:

Material was prepared for semi-thin sectioning according to (Owen & Makaroff, 1995). Whole inflorescences were removed from plants and fixed overnight at room temperature in 2.5% (v/v) gluteraldehyde in 0.1 M HEPES buffer (pH7.2) and 0.02% (v/v) Triton X-100. Buds were rinsed three times with 0.1 M HEPES buffer (pH7.2) and post-fixed overnight in 1% OsO_4. After rinsing twice with distilled, deionized water, buds were dehydrated in a graded acetone series of 10% increments and infiltrated in Spurr's resin or modified Spurr's resin. Spurr's resin was modified by the addition of Quetol 651 according to Table 3 (Ellis, 2006), except 0.05g 2(dimethyl-amino)

ethanol was used in place of 0.02 g N, N-dimethylbenzylamine (Holdorf et al., 2012). Following infiltration in 100% resin, individual buds were removed from inflorescences, and placed into numbered flat embedding molds in developmental order. Semi-thin sections (0.5 µm) were cut with a diamond knife on an RMC MT 7000 ultramicrotome and heat-fixed to microscope slides. Semi-thin sections to be used in the analysis of general development were stained with Azure B in 1% (w/v) sodium bicarbonate at pH 9 (Hoefert, 1968). Coverslips (#1.5) were mounted over the sections with Spurr's resin that had been partially polymerized at room temperature to increase its viscosity. After the coverslips were added the slides were kept in horizontal position at room temperature until the Spurr's resin was completely polymerized, prior to microscopic observation. Visualization of callose was completed on sections from which plastic had been removed with sodium methoxide (Fulcher, McCully, Setterfield, & Sutherland, 1976) followed by mounting in 0.05% (w/v) aniline blue in phosphate buffer (Smith & McCully, 1978).

All slides of semi-thin sections were examined with a Nikon 80i light microscope equipped with Hoffman optics for the Azure B stained sections, and epifluorescence illumination with a Nikon UV-2E/C filter set (excitation filter 325-375, dichroic 400 LP, emitter 435-485) for callose imaging. Images were captured with a QImaging Retiga 2000-R digital camera using Q Capture Pro V.5.1 software.

C. Results

A study of microsporogenesis and early microgametogenesis was carried out on wild-type *Arabidopsis thaliana*, and a mutant of the same line (WS), referred to as 6491. This analysis was used as a means to elucidate differences present between wild-type and the mutant 6491 grown at 20^{o} C, and structural differences arising from growth at lower and higher temperatures in both

the wild-type and mutant. Eight developmental stages were examined, encompassing premeiosis I through second mitotic division of pollen grain stage.

Wild-type *A. thaliana* grown at 20° C

In premeiosis I, five differentiated tissues are present in each of the four anther lobes, one of which is shown in Figure 5 A. Tightly packed microsporocytes are surrounded successively by tapetum, middle layer, endothecium and epidermis. Microsporocytes and tapetal cells display a nucleus and nucleolus, although not all structures are visible in every cell, due to varying planes of section. The microsporocytes have thin walls, with little separation between adjacent microsporocytes. A larger separation between cytoplasm and microsporocyte wall appears in premeiosis II (Fig. 5 B). A thickening callose wall (Peirson, Owen, Feldmann, & Makaroff, 1996; Smith & McCully, 1978) continues to isolate the microsporocytes. The nucleoli are no longer evident and numerous small vacuoles have appeared within the cytoplasm of the microsporocytes. Tapetal cells have retained a distinct nucleus and developed large vacuoles.

Each microsporocyte is fully encased in a thick callose wall, is rounded in appearance, and fairly consistent in size during meiosis (Fig. 5 C). Tapetal cells have few distinguishable cellular structures, multiple vacuoles continue to develop within the tapetal cytoplasm, and separations between the cells appear. Many of the tapetal cells are binucleate. Cytokinesis (Fig. 5 D) begins with an ingrowth of the callose wall surrounding the coencytic microsporocytes. Cells are multinucleate, containing four nuclei, although they may not all be visible. Nuclei move to the periphery of the cell. Cleavage furrows deepen and separate each microsporocyte into four microspores (tetrad). Tapetal cell walls degrade and the number of vacuoles continue to grow.

Fig. 5 Semi-thin sections through wild-type *Arabidopsis thaliana WS* anthers, stained with Azure B. Bar = 10 µm**. A** Premeiosis I. Four anther cell layers surround microsporocytes (Mi). From deepest to superficial the cell layers are the tapetum (T), endothecium (En), Middle layer (ML), and Epidermis (Ep). **B** Premeiosis II. Microsporocytes (Mi) are separated by developing callose wall (arrow). Tapetal (T) cells begin to separate and are vacuolated. **C** Meiosis. Microsporocytes (Mi) have increased separation tangentially and radially. **D** Cytokinesis. Centripetal ingrowths of callose (arrow) form and begin to separate microsporocytes. **E** Tetrads. Tetrads (Te) are completely enclosed within callose (Ca) and tapetal cells are highly vacuolate with increased separation. **F** Released microspores. Individual microspores (Ms) are free within the locule of the anther. Tapetal (T) cells stain darkly and are irregular in size. **G** Ring-vacuolate microspores. Patterned exine (Ex) is on the surface of microspores. A large vacuole (V) has displaced cytoplasm to one side of the microspore. **H** Pollen grains. Pollen grains (PG) have well-patterned exine and the vegetative cell (Vc) is visible.

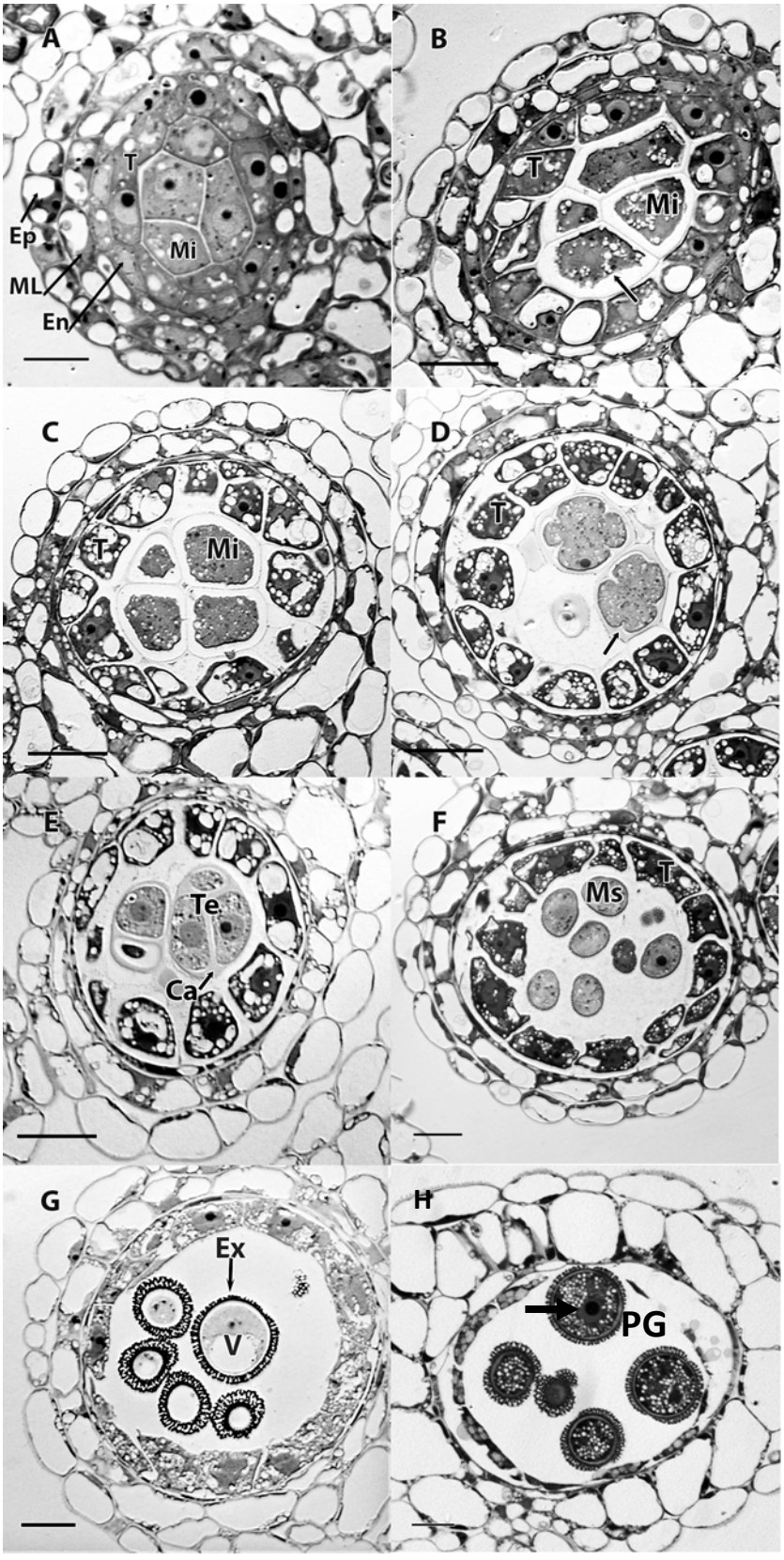
A
T
Ep
Mi
ML
En
B
T
Mi
C
T
Mi
D
T
E
Te
Ca
F
Ms
T
G
Ex
V
H
PG

At tetrad stage, groups of four mononucleate microspores are enclosed by a thick callose wall (Fig. 5E). Nucleoli are visible within the nuclei of the microspores. The tapetal protoplasts are pulled away from the remaining cell wall. Next the callose wall disappears, and the microspores are free in the locule of the anther. Microspores in released microspore stage (Fig. 5F) have a substance that stains darkly with Azure B appearing in a defined pattern on the surface of each microspore. Indentations within developing exine suggest the site of future apertures. Darkly staining drops and tiny vacuoles are visible in the cytoplasm of each microspore. Small vacuoles appear to coalesce into one large vacuole in ring vacuolate stage (Fig. 5G). The darkly stained exine is well-formed and distinctly patterned. Microspores are now more round in appearance. Tapetal cells have no visible cell wall and contain numerous clusters of small vacuoles. In pollen grain stage (Fig. 5H), the grains have distinct exine with baculae and tectum visible. The cytoplasm is highly vacuolate and a vegetative cell is visible.

***A. thaliana* mutant 6491 grown at 20º C**

Premeiosis I in 6491 (Fig. 6 A) appears similar to WT, with visible changes first occurring in Premeiosis II. At this stage, an increase in thickness of the cell wall is present (Fig. 6 B), but to a lesser degree than noted in WT. A delay in 6491 tapetal development is also noted by the slower increase in vacuoles within tapetal cells (Fig. 6 B-C). Meiosis in 6491(Fig. 6 C) has numerous morphological differences from WT. Most notable is the thinness of the microsporocyte cell walls in comparison to WT and resulting lack of separation of the microsporocytes (Fig. 6 C). The microsporocytes are non-uniform in size and shape and have not taken on the rounded appearance noted in WT. The tapetal cells show no separation, either radially or tangentially, and the vacuoles that are beginning to form are larger and fewer in number than WT.

Fig. 6 Semi-thin sections through mutant 6491 *Arabidopsis thaliana* anthers grown at 20° C, stained with Azure B. Bar = 10 µm. **A** Premeiosis I. Four anther cell layers surround microsporocytes (Mi). Microsporocytes are thin-walled. From deepest to superficial the cell layers are the tapetum (T), endothecium (En), Middle layer (ML), and Epidermis (Ep). **B** Premeiosis II. Microsporocytes (Mi) are separated with increasing distance (arrow). Tapetal (T) cells have large vacuoles. **C** Meiosis. Microsporocytes (Mi) are irregular in size and shape. **D** Cytokinesis. Centripetal ingrowths of callose (arrow) form and begin to separate microsporocytes. Cytoplasm of microsporocytes is vacuolate. **E** Tetrads. Tetrads (Te) are completely enclosed within callose (Ca), irregular in size and shape and tapetal cells have large vacuoles. **F** Released microspores. Individual microspores (Ms) are free within the locule of the anther with a great variety of sizes. Tapetal (T) cells are almost completely void of structure. **G** Ring-vacuolate microspores. Individual microspores (Ms) have a large vacuole (V) that has displaced cytoplasm to one side of the microspore. Some grains appear collapsed. **H** Pollen grains. Pollen grains (PG) have some exine (Ex) and the vegetative cell (Vc) is visible.

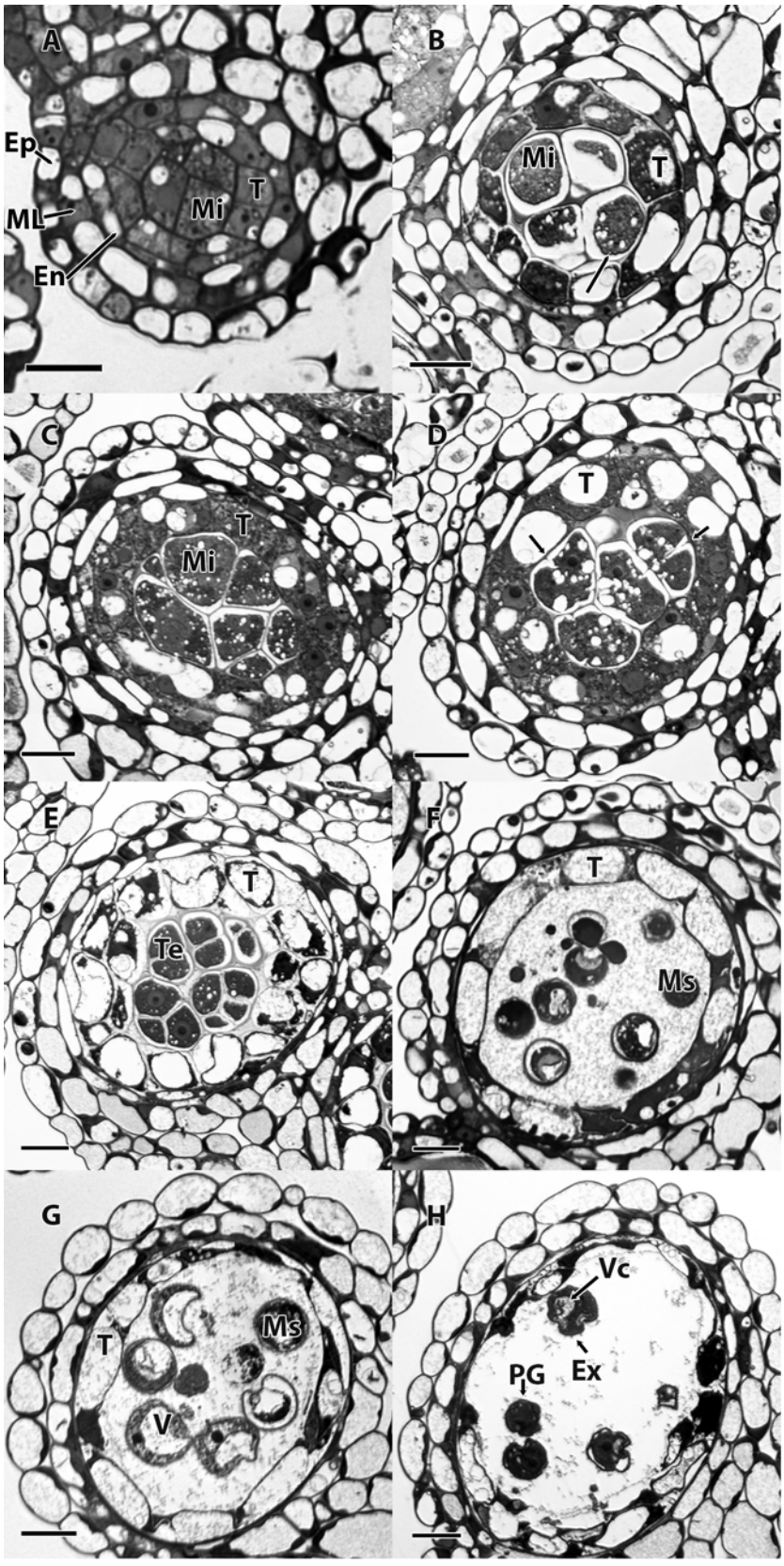
A
Ep
ML
En
Mi
T
B
Mi
T
C
T
Mi
D
T
E
T
Te
F
T
Ms
G
Ms
T
V
H
Vc
Ex
PG

Progressing into cytokinesis, the irregularly shaped microsporocytes develop centripetal in-growths (Fig. 6 D). The cytoplasm is unequally distributed, with many vacuoles throughout. Unlike WT, the nuclei of 6491 have not moved to the periphery of the dividing cells. The tapetal cells are irregular, some with large vacuoles and little notable cellular structure, and others with no visible vacuoles. The tapetal cells still lack any sign of separation or division. In tetrad stage, the microspores in 6491 have darkly staining cytoplasm (Fig. 6 E), a thin wall, and little regularity in size or shape. While division in some tapetal cells is evident, most of the cells are lacking any visible cellular structure. The microspores, which are greatly varied in size, shape and structure are released into the locule of the anther (Fig. 6 F). Some microspores are collapsed and others more closely resemble microspores of WT. In ring vacuolate stage (Fig. 6 G), the vacuoles have coalesced into one larger vacuole, similar to WT. However, many of the microspores are misshapen, do not appear to have consistent patterning on the outer wall, and are devoid of any recognizable cellular structure. The pollen grains which have arisen from the microsporocytes of 6491 are mostly collapsed, darkly staining, and few in number (Fig. 6 H). The tapetum has largely disappeared, leaving remnants of the cells which are generally empty of structure.

Structural changes arising from alterations in growing temperatures of WT and 6491 *Arabidopsis thaliana*

It has been reported that 6491 displays reduced fertility when grown at higher temperatures. As a control it was necessary to grow WT, which led to the finding that the WT phenotype was different at temperatures close to the accepted growing range. General trends were noted in both 6491 and WT. The lower growth temperature of 16^{o} C led to a delay in the timing of certain well

characterized stages of development (Peirson et al., 1996), while the higher temperature of 27° C appeared to result in more catastrophic structural issues overall.

WT *Arabidopsis thaliana* grown at 16° C, 20° C, and 27° C

Structural alterations from the midrange growth temperature (20° C) plants are apparent at each stage of development of the 16° C (low temperature group) and 27° C (high temperature group). WT plants grown at 16° C display cytoplasm that stains more darkly throughout pollen development, while the cytoplasm in the higher temperature group plants appears more vacuolated. Differences are evident in tapetal cells at most stages at both higher and lower temperatures. Premeiosis I (Fig. 7 A-C) is similar in all three temperature groups. Premeiosis II has the first noticeable differences, primarily microsporocytes that are irregularly shaped with thinner cell walls (Fig. 7 D-F). Callose deposition is delayed at both higher and lower temperatures through meiosis (Fig. 7 G-I). There appears to be premature tapetal disintegration in the high temperature group (Fig. 7 I). Cytoplasmic distribution is unequal (Fig. 7 J-K), with centripetal in-growths that are delayed and irregular, and the haploid nuclei are not arranged as expected for the tetrad stage.

At tetrad stage (Fig. 8 A-C), the differences in tapetal development are quite evident. In both lower (LTG) and higher temperature groups (HTG), the tapetal cells generally contain a single cell-filling vacuole, or ruptured vacuoles, and little separation is apparent between the cells. The tetrads within the locule of the lower temperature group are irregular, the protoplast of the microspores has retracted from the cell wall and the thickness of the callose is uneven. The higher temperature group also shows uneven callose thickness.

Fig. 7 Semi-thin sections through wild-type *Arabidopsis thaliana MS* anthers, stained with Azure B and subjected to three different growing temperatures. **A, D, G, J** Low Temperature Group (LTG) grown at 16° C. **B, E, H, K** Mid-Range Temperature Group (MTG) grown at 20° C. **C, F, I, L** High Temperature Group (HTG) grown at 27° C. Bar = 10 µm. **A-C** Premeiosis I. Premeiosis I is similar across all three temperature groups. **D-F** Premeiosis II. Microsporocytes (Mi) have differing degrees of separation across three groups. **G-I** Meiosis. Microsporocytes (Mi) are irregular in size and shape in LTG. LTG and HTG have vacuolated cytoplasm. **J-L** Cytokinesis. Centripetal ingrowths of callose (arrow) form and begin to separate microsporocytes, varying in size and shape primarily in LTG and HTG. Tapetal cells in LTG contain single large vacuoles, while HTG tapetal cells show signs of hypertrophy.

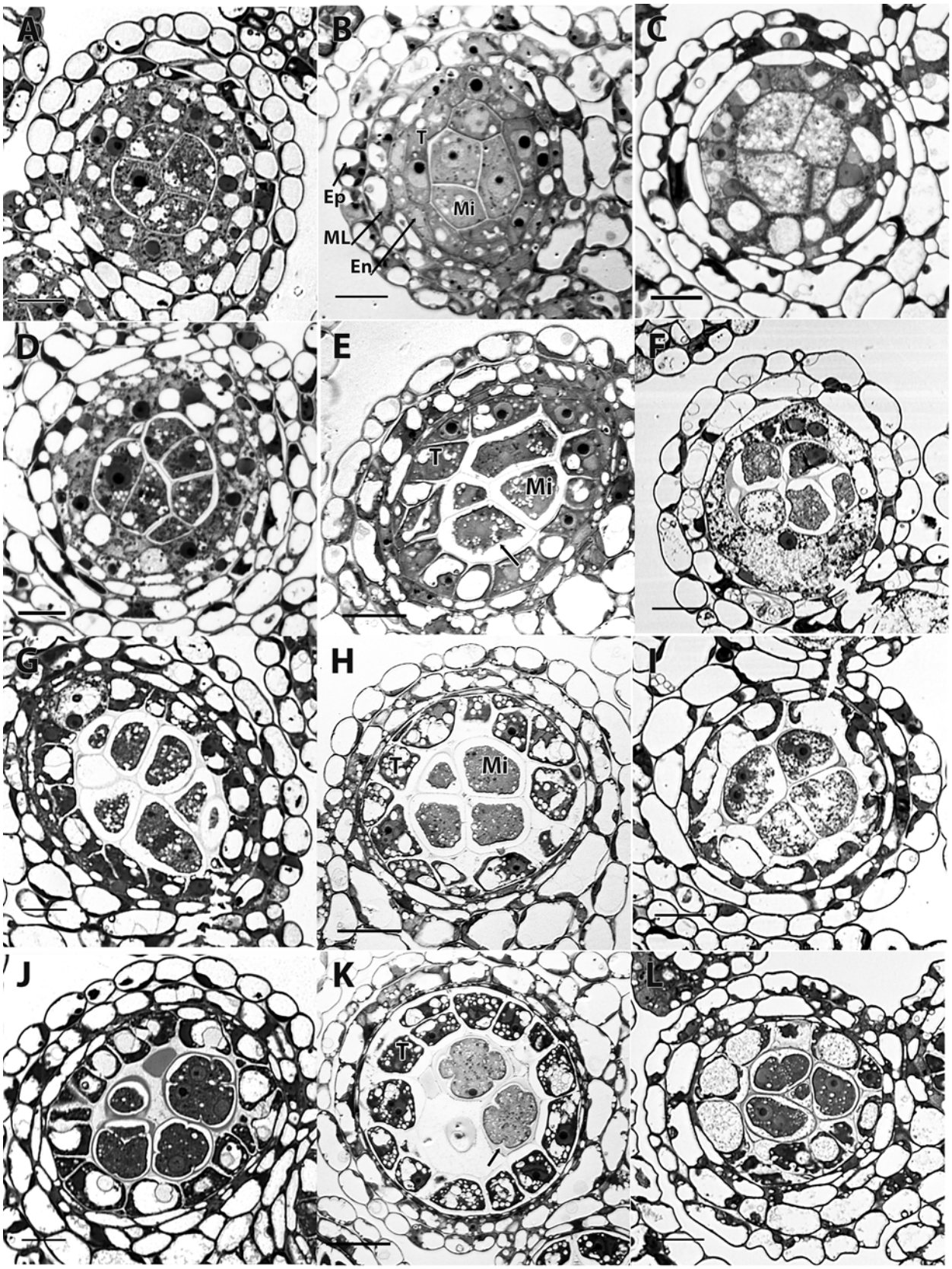
A
B
T
Ep
Mi
ML
En
C
D
E
T
Mi
F
G
H
T
Mi
I
J
K
T
L

Fig. 8 Semi-thin sections through wild-type *Arabidopsis thaliana MS* anthers, stained with Azure B and subjected to three different growing temperatures. **A, D, G, J** Low Temperature Group (LTG) grown at 16° C. **B, E, H, K** Mid-Range Temperature Group (MTG) grown at 20° C. **C, F, I, L** High Temperature Group (HTG) grown at 27° C. Bar = 10 µm. **A-C** Tetrads. Tetrads (Te) are completely enclosed within callose (Ca), LTG and HTG microsporocytes are irregular in size and shape. **D-F** Released microspores. Individual microspores (Ms) are free within the locule of the anther with a great variety of sizes. Microspores in LTG appear collapsed, while HTG are vacuolated. **G-I** Ring-vacuolate microspores. Individual microspores (Ms) have a large vacuole (V) that has displaced cytoplasm to one side of the microspore. Tapetum in LTG and HTG appears largely diminished. **J-L** Pollen grains. Pollen grains (PG) in LTG and HTG are irregular in size with large vacuoles remaining.

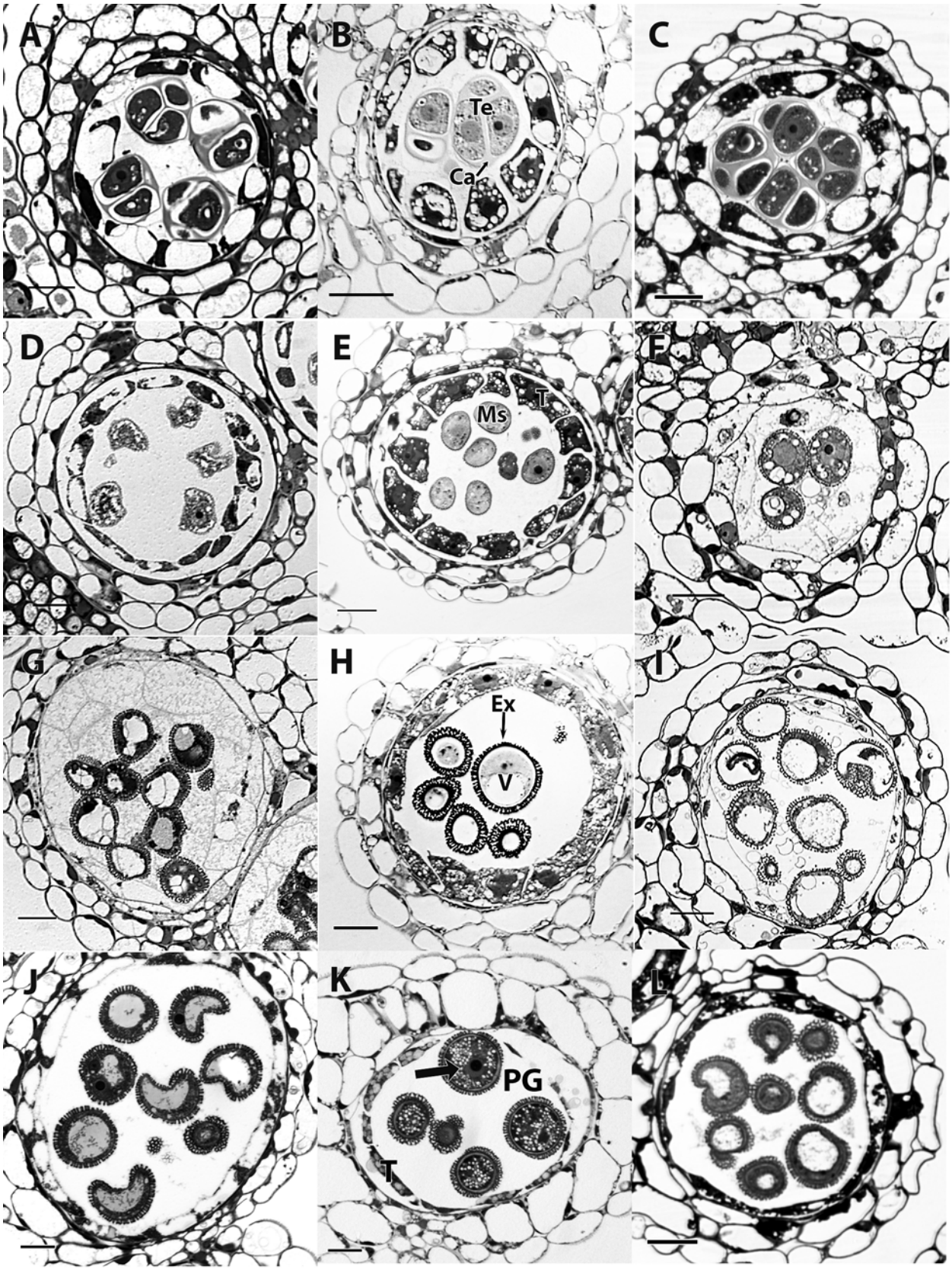
A
B
Te
Ca
C
D
E
Ms
T
F
G
H
Ex
V
I
J
K
PG
T
L

The released microspores (Fig. 8 D-F) are notably different between the three temperature groups. The higher temperature group has highly vacuolated cytoplasm and what appears as developed exine. The microspores have become rounded earlier than the midrange group. The lower temperature group shows several collapsed microspores. Ring vacuolate and pollen grain stages (Fig. 8 G-L) show the resulting phenotype differences between the three temperatures groups. Although each group appears to have some grains resembling WT, the number is considerably less in the higher and lower temperature groups than in the midrange group.

6491 grown at 16° C, 20° C, and 27° C

6491 has little synchrony in development throughout all of the examined stages (Figures 9 and 10, A-L). Several different stages of development could be found not only within the same bud, but also within the same anther. Unlike WT, the lower temperature group proceeded with the most "regular" development, and resulted in the highest number of grains similar in appearance to WT, albeit considerably less than WT grown at midrange temperature.

The structural differences between the three 6491 temperature groups are evident beginning with Premeiosis II (Fig. 9 D-F). Wall thickness around microsporocytes is varied and separation of microsporocytes is unequal. As development proceeds into meiosis (Fig. 9 G-I), there is little resemblance to the comparable stages of WT. From cytokinesis on, the higher temperature group appears to have development that is at first severely impacted, and then aborted. (Fig. 9 L and 10 C, F, I, L).

Tetrad formation in the midrange (MTG) and lower temperature groups (Fig. 10 A-B) occurs, with microspores of varying sizes and shapes resulting (Fig. 10D-E). Ring vacuolate stage (Fig. 10 G-H) in the midrange temperature appears closer to what is seen in WT than low temperature.

Fig. 9 Semi-thin sections through 6491 *Arabidopsis thaliana* anthers, stained with Azure B and subjected to three different growing temperatures. **A, D, G, J** Low Temperature Group (LTG) grown at 16° C. **B, E, H, K** Mid-Range Temperature Group (MTG) grown at 20° C. **C, F, I, L** High Temperature Group (HTG) grown at 27° C. Bar = 10 µm. **A-C** Premeiosis I. Microsporocytes appear to have a greater separation in HTG. **D-F** Premeiosis II. Microsporocytes (Mi) have differing degrees of separation across three groups, and all have irregular shapes. **G-I** Meiosis. Microsporocytes (Mi) are highly vacuolated in HTG, with little obvious organelle structure. **J-L** Cytokinesis. Centripetal ingrowths are separating microsporocytes into irregular sizes and shapes. HTG microsporocytes appear to be collapsing.

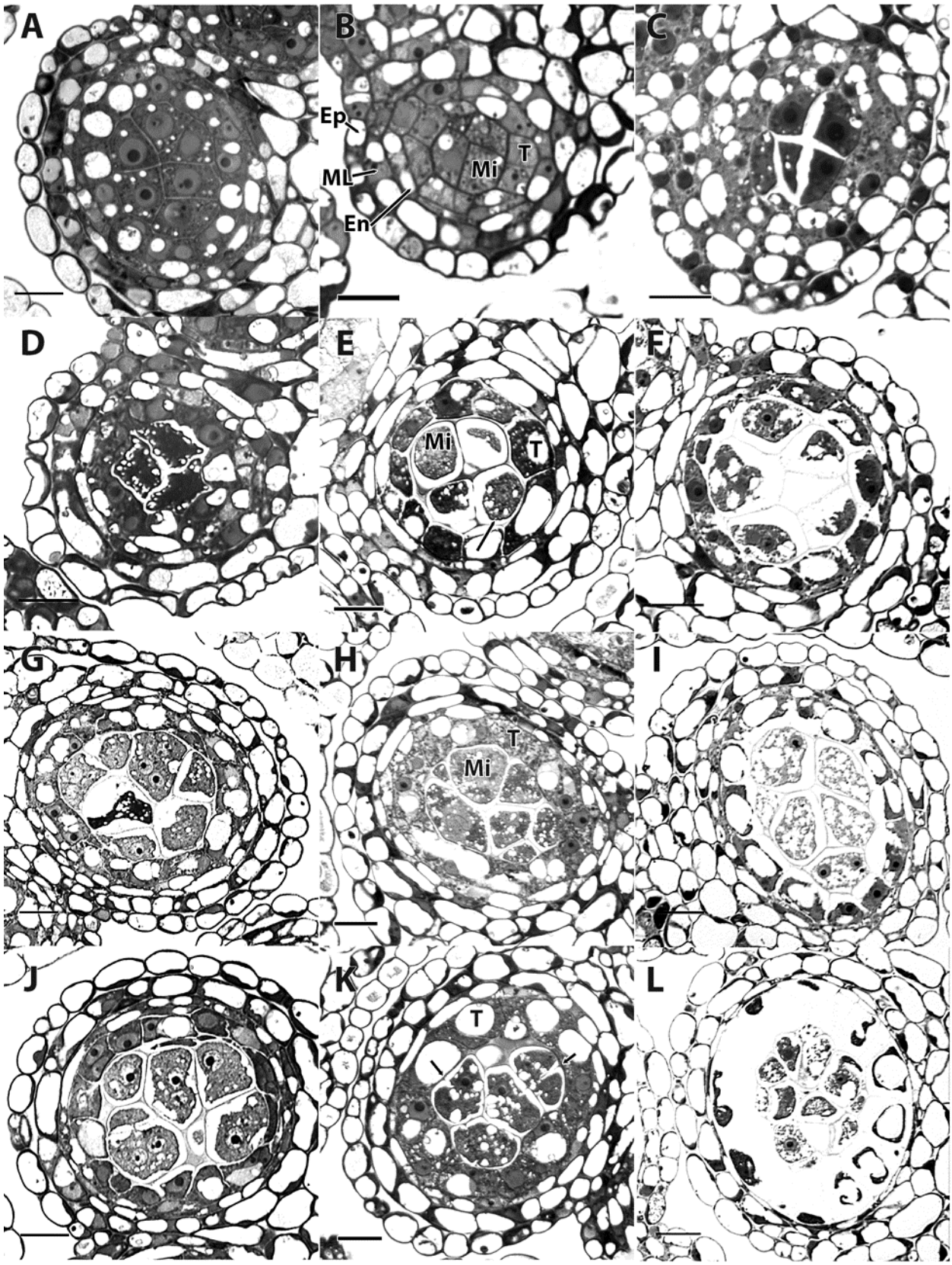
A
B
Ep
ML
En
Mi
T
C
D
E
Mi
T
F
G
H
T
Mi
I
J
K
T
L

Fig. 10 Semi-thin sections through 6491 mutant *Arabidopsis thaliana* anthers, stained with Azure B and subjected to three different growing temperatures. **A, D, G, J** Low Temperature Group (LTG) grown at 16° C. **B, E, H, K** Mid-Range Temperature Group (MTG) grown at 20° C. **C, F, I, L** High Temperature Group (HTG) grown at 27° C. Bar = 10 µm. **A-C** Tetrads. Tetrads (Te) are completely enclosed within callose (Ca), LTG and HTG microsporocytes are irregular in size and shape. **D-F** Released microspores. Individual microspores (Ms) are free within the locule of the anther with a great variety of sizes. Microspores in LTG appear collapsed, while HTG are vacuolated. **G-I** Ring-vacuolate microspores. Individual microspores (Ms) have a large vacuole (V) that has displaced cytoplasm to one side of the microspore. Tapetum in LTG and HTG appears largely diminished. **J-L** Pollen grains. Pollen grains (PG) in LTG are irregular in size with large vacuoles remaining. HTG pollen grains appear collapsed.

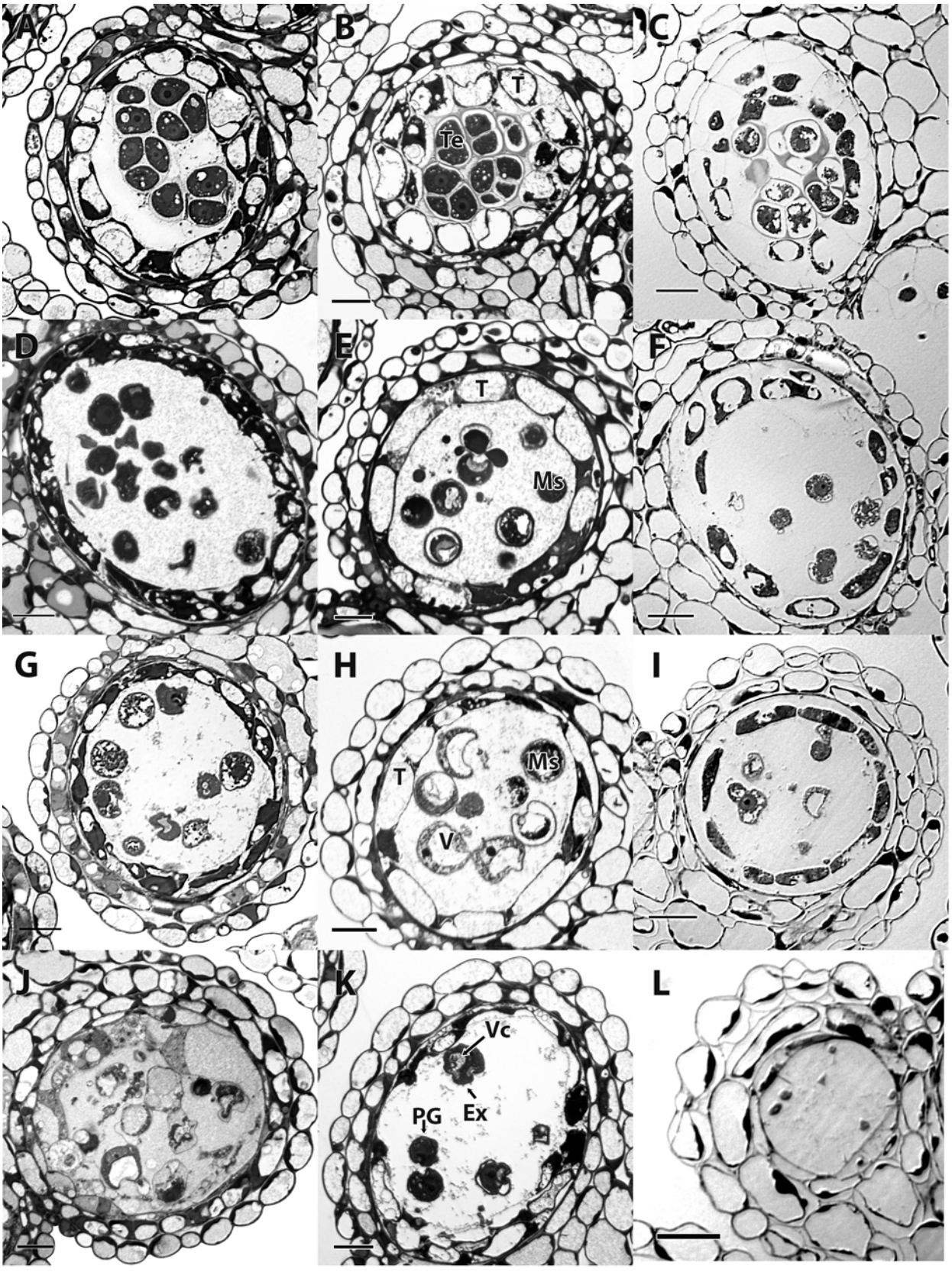
A
B
T
Te
C
D
E
T
Ms
F
G
H
T
Ms
V
I
J
K
Vc
Ex
PG
L

The resulting pollen grains (Fig. 10 J-K) in the HTG appear to be collapsed, while the grains in LTG and Mid-group appear to be closer to what WT looks like.

Aniline Blue Staining of the Callose Wall

Because of the differences in appearance of the walls surrounding microsporocytes and tetrad-stage microspores, the production of microspores of varying size, and the importance of the callose wall during meiosis and pollen exine patterning, the appearance of callose was investigated at microsporocyte through tetrad developmental stages using aniline blue (Hoefert 1968). To accomplish this, semi thin sections were cut from WT and 6491 anther locules grown at 16° C, 20° C, and 27° C and stained with aniline blue which binds specifically to callose (Figures 11 A-L and 12 A-L). Callose development generally corresponds with the cell wall thicknesses noted in the previous figures and results. However, when comparing the Azure B stained semi thins in earlier figures (Figures 5-10) to the sections stained specifically for callose, there are a few unexpected results. Figure 11 B-K shows WT grown at 20° C, with results similar to previously published data (Peirson et al., 1996). Figures 9 F and 10 E-F show what appears to be a thick callose wall, but comparison to Figures 11 F and 12 E-F indicate the lack of thick callose in the same area. Figures 11 G, I, J and K show callose wall that is not just thinner than WT at 20° C, but surrounding microsporocytes and microspores that appear misshapen.

Callose in 6491 in all temperature groups does not appear similar to WT 20° C at equivalent stages. In general, the callose wall in 6491 is considerably thinner in all stages and aniline blue staining shows what appears to be incomplete or irregular cytokinesis (Fig. 12 G-I) and tetrad (Fig. 12 J-L) formation. Figures 11 D, 12 A and 12 E have callose of punctate appearance.

Fig. 11 Semi-thin sections through wild-type *Arabidopsis thaliana MS* anthers subjected to three different growing temperatures, stained with Aniline Blue and viewed with epifluorescence. **A, D, G, J** Low Temperature Group (LTG) grown at 16° C. **B, E, H, K** Mid-Range Temperature Group (MTG) grown at 20° C. **C, F, I, L** High Temperature Group (HTG) grown at 27° C. Bar = 10 µm. **A-C** Premeiosis. Both LTG and HTG are lacking callose, while MTG shows the beginning of callose deposition between microsporocytes. **D-F** Meiosis. LTG and HTG callose wall has a punctate appearance. **G-I** Cytokinesis. Centripetal in-growths of callose separate microsporocytes. The LTG appear to have callose walls separating the microsporocytes in an irregular manner, while the HTG walls are incomplete. **J-L** Tetrad. Callose walls appear complete, although microsporocytes in the LTG and HTG are irregular in size and shape.

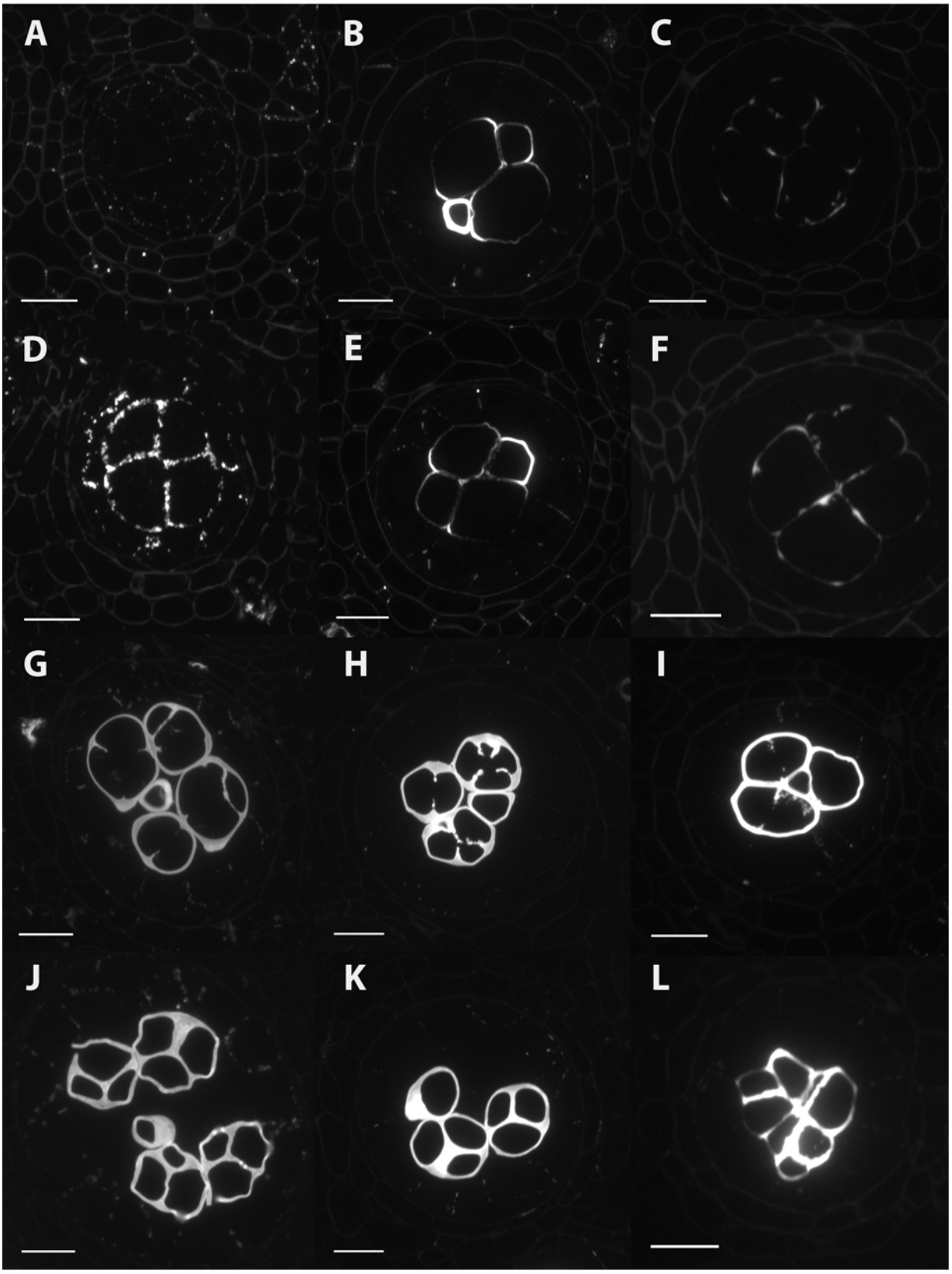
A
B
C
D
E
F
G
H
I
J
K
L

Fig. 12 Semi-thin sections through 6491 mutant *Arabidopsis thaliana* anthers subjected to three different growing temperatures, stained with Aniline Blue and viewed with epifluorescence. **A, D, G, J** Low Temperature Group (LTG) grown at 16° C. **B, E, H, K** Mid-Range Temperature Group (MTG) grown at 20° C. **C, F, I, L** High Temperature Group (HTG) grown at 27° C. Bar = 10 µm. **A-C** Premeiosis. Both LTG and MTG show the beginning of callose deposition. **D-F** Meiosis. Callose walls that completely enclose microsporocytes are apparent in the LTG. Callose in the MTG is punctate, while very little callose is apparent in HTG. **G-I** Cytokinesis. Centripetal in-growths of callose are beginning to separate microsporocytes in the LTG. Separation in the MTG and HTG is incomplete. **J-L** Tetrad. Callose walls appear complete, although microsporocytes in all three groups are irregular in size and shape. Callose walls are uneven in thickness.

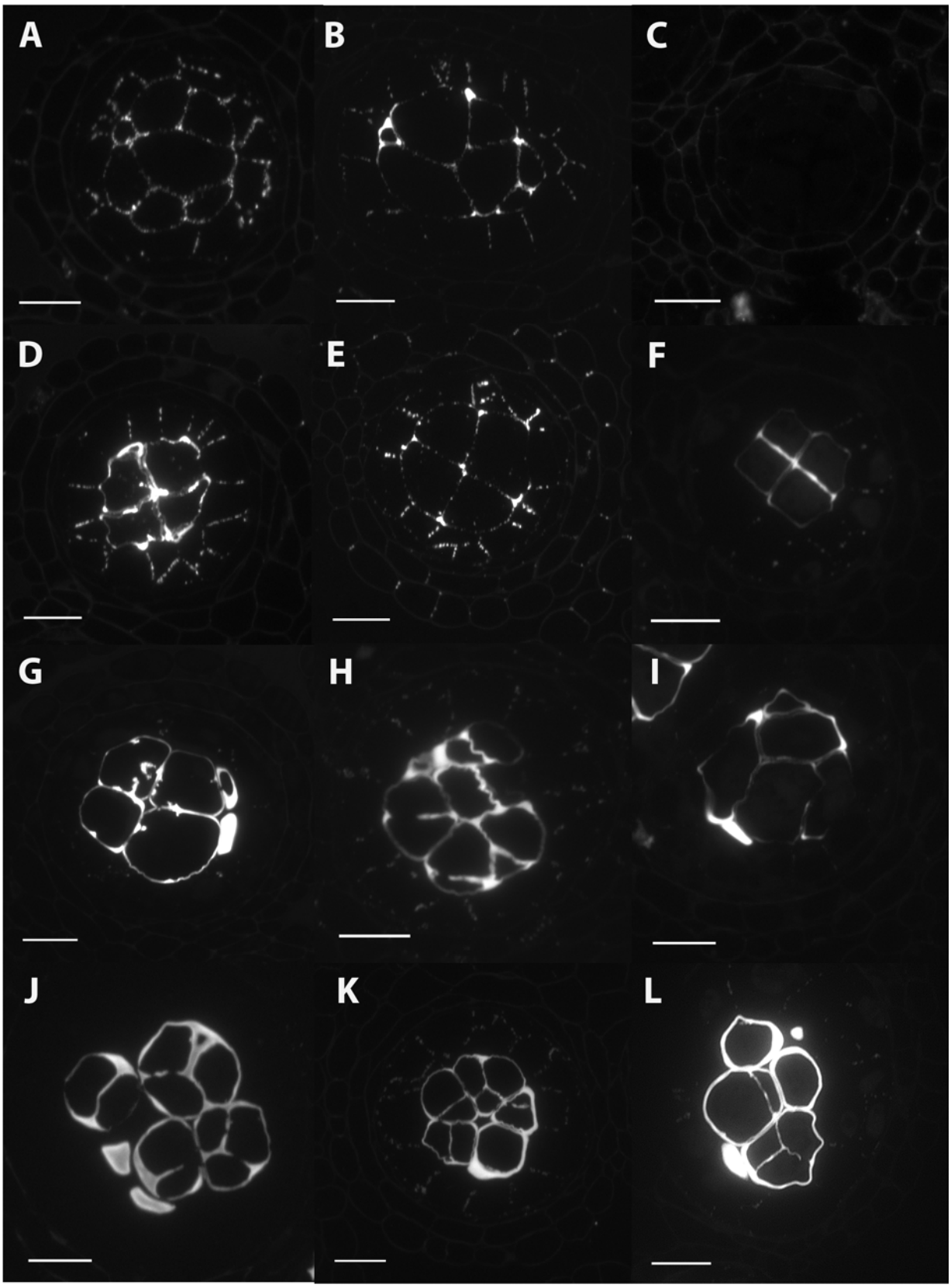
A
B
C
D
E
F
G
H
I
J
K
L

D. Discussion

A cytological study of WT and temperature-sensitive mutant 6491 *A. thaliana* revealed several interesting and previously unnoted factors of interest. Two areas were considered:

1. How development, specifically microsporogenesis and microgametogenesis, of the meiotic mutant 6491 differs from WT
2. How pollen development in WT and 6491 is affected by changes within an ambient temperature range

Wild-type *A. thaliana* Development compared to Mutant Line 6491

Previous developmental studies of WT (Peirson et al., 1996) showed results similar to those of WT grown at the same temperature found in this study. The initial comparison of WT development to 6491 development was carried out on plants grown at 20^{o} C. The mutant line had visible changes beginning in early meiosis (Premeiosis II). Most of the differences in phenotype appear to be a result of a mutation that leads to a defect in how and when the callose layer is produced. Previous examination of 6491 (data not published) has shown it to be a suspected meiotic mutant line that is temperature sensitive with reduced fertility. This conclusion was reinforced and expanded upon by results of the study undertaken for the current project.

Microsporocytes wall themselves off from the surrounding anther cells by producing a callose wall prior to meiosis. Cytomictic channels form and interconnect all of the microsporocytes in the locule as the callose is being produced. This allows for continuity of cytoplasm between the microsporocytes, until the channels are filled in by callose. It is this interconnectedness that may allow for synchrony in development amongst the microsporocytes (Heslop-Harrison, 1966).

As shown in the developmental series (Figures 5 and 6) and the aniline blue stained sections (Figures 11 B-K and 12 B-K), there is a marked difference in the amount and pattern of callose deposition. The delayed, thinner callose wall evident in 6491 may lead to the altered phenotype of pollen grains which have a smooth surface with little to no reticulate patterning, lack colpi, and pollen grains that are rounder than WT. The irregular shape of coenocytic 6491 microsporocytes (Figure 12 H) in cytokinesis demonstrates the consequences of the mutation already in place, which implicates meiosis as the primary stage of effect. If there is lack of interconnectedness between the developing microsporocytes due to improper timing or deposition of callose, this could result in varying sizes of first microspores, and then the resulting grains (Figure 6 H). A delayed or premature "closing" of this interconnectedness could change the synchrony necessary for an even distribution of cytoplasmic nutrients necessary for proper development. One way of looking at it would be the poor development and stunted growth that is present in a malnourished child versus one with proper nutrition.

Other problems associated with change in callose deposition include too little or too much callose. Not enough callose (thinner wall shown in Figures 12 H-K, as opposed to WT wall in Figures 11 H-K) may cause microspores to be released prematurely, especially if the same amount of callase as in WT is released by the tapetum, causing a faster degeneration of the callose wall. Callose is also suspected of acting as a template for the developing exine, so any alteration in the callose wall would be expected to lead to a defect in the exine. Unfortunately, this level of ultrastructure is not visible with the light microscopy techniques used for this particular portion of the study.

Developmental Changes in WT and 6491 Grown within an Ambient Temperature Range

Plants are at the mercy of their environment when it comes to unfavorable conditions such as drought, heat, cold and excessive light, These abiotic stresses have a huge impact on crop production, with a projected 23% decrease in crop yield in North America in the next 50 years (Shibasaki & Tan, 2002). Earth has been, and continues to be, undergoing dramatic anthropogenic environmental changes, and for every 1^{o} C increase in seasonal temperature, a loss in the range of 2.5 to 16% of major grain crops can be expected (Battisti & Naylor, 2009). With this knowledge, finding an easy to grow model plant that can be used to study effects of temperature stress becomes highly important. *Arabidopsis* is commonly used to study many biological stressors and like all plant species, a range of growth conditions exists that is considered acceptable and within normal limits.

There have been many studies done on the effect temperature has on plants, but most of these used more accessible tissues such as leaves or roots. However, previous work has shown that floral organs such as petals or stamens appear undamaged after heat shock application, while the developmental tissues had severe defects that led to male sterility. One of the most temperature–sensitive stages is that of the meiosis to microspore transition (Kim, Hong, & Lee, 2001). Furthermore, most heat or cold stress studies are done with fairly drastic changes in temperature from a normal growing range. Alterations of temperature that are considered ambient and still acceptable for growing have yet to be extensively studied in relation to developmental tissues, primarily because little damage is noted to the more visual tissues. One researcher stated that *Arabidopsis* grown within an ambient temperature range of 12^{o} C to 27^{o} C does not have significant induction of stress pathways. And while there is a difference in growth rate,

development, and disease resistance, temperature mediating pathways account for the ability of the plant to overcome the more detrimental results (Wigge, 2013).

Structural changes that occur in pollen development in WT *A. thaliana* and the mutant line 6491 at three different growing temperatures were examined. Temperatures were within a narrow range, generally considered typical ambient temperatures for *Arabidopsis*. The temperature sensitive mutant line 6491 was expected to show structural changes that would challenge its ability to be fertile, and indeed, this was the case. What was unexpected were the results shown by WT in different plants from the same line grown at three different temperatures.

Lower and higher temperature groups of WT *Arabidopsis* appeared to have structural changes beginning in early meiosis. Microsporocytes were irregular in size and shape with thin callose walls. This was especially visible in Figures 11 D and 11 F, when only the callose is being imaged. It has been shown in *Rosa sp*. that there are heat-induced alterations in the meiotic spindles (Pecrix et al., 2011). If this were to also occur in *Arabidopsis*, it might explain the irregular divisions occurring and resulting shapes of the microspores.

The most prominent change in WT at low and high temperatures appears in the tapetum. In the high temperature group, there is premature disintegration of the tapetum beginning in meiosis (Fig. 7 I) and continuing for the remainder of development. Early degeneration of the tapetum will affect the rest of microspore development. The tapetum releases callase to cause disintegration of the callose wall. If the microspores are released prematurely, they will not be fully developed nor have long enough access to the tapetal nutrient source. The tapetum is also responsible for addition of the wall component sporopollenin after microspores are released from the callose wall. Early tapetal degeneration will lead to less sporopollenin being added to the developing pollen grain wall, which could result in a thinner wall that is not as able to protect the

sperm cells or is more vulnerable to bursting from turgor pressure upon rehydration of the pollen grain. Callose also acts as a template for proper patterning of the pollen grain wall. Early disruption of the callose wall will affect the final pattern of the wall and possibly the placement of apertures.

Lower temperatures are thought generally to slow the developmental process. The tapetum remains intact longer, but becomes highly vacuolate with an increase in cell size (hypertrophy) and shows little sign of division (Fig. 7 J). In rice that has been subjected to chilling stress, tapetal cells showed a similar vacuolation and hypertrophy to the anthers in this study (Fig. 8A) (E. A. Mamun, S. Alfred, L. C. Cantrill, R. L. Overall, & B. G. Sutton, 2006). One possible explanation is the reabsorption of sugars into the tapetum from premature disintegration of the callose wall, causing the increase in cell size and vacuoles (E.A. Mamun, S. Alfred, L.C. Cantrill, R. L. Overall, & B.G. Sutton, 2006). Depending upon the severity of the tapetal changes, male sterility is quite often the result.

6491 showed marked changes in structure depending upon the temperature to which it was exposed during growth. Previous unpublished work with 6491 from our lab characterized the line as being a temperature sensitive, reduced-fertile line. It was found that at normal temperatures (20^{o} C) 6491 exhibited reduced fertility, but at higher temperatures (27^{o} C) complete sterility was more often the case. Also noted previously was a smooth, rather than reticulate, pollen grain surface, and round pollen grains that lacked apertures.

Structural changes are evident at all stages of development of 6491. The degree of damage does escalate with an increase in temperature, resulting in collapsed pollen grains and male sterility in the high temperature group. Early in development, the low temperature group actually appeared more disrupted in structure than the midrange group, but seemed to stabilize

prior to dehiscence of the anthers. The lack of proper callose wall formation, indicated by thin walls present in all three temperature groups (Figs. 10 D-F and 12 D-F), prior to and throughout meiosis establishes the issues that will lead to reduced or complete sterility. Also notable is the thick wall layer (indicated by arrows 10 D-E) which appears to be callose, but upon staining with aniline blue, is actually a very thin line of callose (12 D-E). This could be an area where the protoplast has retracted from the cell wall, perhaps due to not having the normal structural support a thicker callose wall would provide or to fixation artifact. Many microsporocytes in the high temperature group appear well on their way to being aborted by meiosis. After meiosis and tetrad stage, the microspores that do form collapse, leading to the complete sterility noted with high temperatures in 6491. Collapse could come from the lack of callose wall support and corresponding accumulation of support material normally apparent. The tapetum in all three groups shows similar changes to those noted in the WT low and high temperature groups, albeit to a higher degree and earlier. The low temperature group has the most "normal" looking tapetum, while the other two groups are more damaged. As noted with WT, the damaged tapetum will lead to grain collapse from lack of sporopollenin normally disbursed to the developing pollen wall. The lack of patterning on mature 6491 pollen grains in dehisced anthers (Fig. 4 B) could be the result of this damage.

Although the gene mutation present in 6491 has not yet been conclusively found, one possibility is that the mutation is causing the gene to be more sensitive to temperature response pathways and leading to a down regulation of that gene and its normal function. Perhaps heat shock proteins that normally help protect proteins by acting as chaperones are somehow being interfered with, although the low temperature at which damage is noted would indicate this is not the case. The gene may be involved directly in pollen wall formation, but the findings that the

tapetum in all three temperature groups is damaged from the earliest stages indicates another area that should be considered. A closer examination of the pollen wall as it is developing may help to narrow down possible gene function, or at the very least see in better detail where and when the differences from WT are occurring.

References

Aarts, M. G. M., Hodge, R., Kalantidis, K., Florack, D., Wilson, Z. A., Mulligan, B. J., Stiekema, W. J., Scott, R., & Pereira, A. (1997). The Arabidopsis MALE STERILITY 2 protein shares similarity with reductases in elongation/condensation complexes. *The Plant Journal, 12*(3), 615-623.

Ariizumi, T., & Toriyama, K. (2011). Genetic regulation of sporopollenin synthesis and pollen exine development. *Annual Review of Plant Biology, 62*, 437-460.

Battisti, D., & Naylor, R. (2009). Historical warnings of future food insecurity with unprecedented seasonal heat. *Science, 323*(5911).

Blackmore, S., Wortley, A. H., Skvarla, J. J., & Rowley, J. R. (2007). Pollen wall development in flowering plants. *New Phytologist, 174*, 483-498.

Chen, X.-Y., Liu, L., Lee, E., Han, X., Rim, Y., Chu, H., Kim, S.-W., Sack, F., & Kim, J.-Y. (2009). The Arabidopsis callose synthase gene *GSL8* is required for cytokinesis and cell patterning. *Plant Physiology, 150*, 105-112.

Dawson, J., Wilson, Z. A., Aarts, M. G. M., Braithwaite, A. F., Briarty, L. G., & Mulligan, B. J. (1993). Microspore and pollen development in six male-sterile mutants of *Arabidopsis thaliana*. *Canadian Journal of Botany, 71*, 629-638.

Dobritsa, A. A., Nishikawa, S.-i., Preuss, D., Urbanczyk-Wochniak, E., Sumner, L. W., Hammond, A., Carlson, A. L., & Swanson, R. J. (2009). *LAP3*, a novel plant protein required for pollen development, is essential for proper exine formation. *Sexual Plant Reproduction, 22*, 167-177.

Dong, X., Hong, Z., Sivaramakrishnan, M., Mahfouz, M., & Verma, D. P. S. (2005). Callose synthase (CalS5) is required for exine formation during microgametogenesis and for pollen viability in Arabidopsis. *The Plant Journal, 42*, 315-328.

Ellis, E. A. (2006). Solutions to the problem of substitution of ERL 4221 for vinyl cyclohexene dioxide in Spurr low viscosiy embedding formulations. *Microscopy Today, 14*, 32-33.

Enns, L. C., Kanaoka, M. M., Torii, K. U., Comai, L., Okada, K., & Cleland, R. E. (2005). Two callose synthases, GSL1 and GSL5, play an essential and redundant role in plant and pollen development and in fertility. *Plant Molecular Biology, 58*, 333-349.

Feldmann, K. A., & Marks, M. D. (1987). *Agrobacterium*-mediated transformation of germinating seeds of *Arabidopsis thaliana*: A non-tissue culture approach. *Molecular and General Genetics, 208*, 1-9.

Fulcher, R. G., McCully, M., Setterfield, G., & Sutherland, J. (1976). β-1,3-Glucans may be associated with cell plate formation during cytokinesis. *Canadian Journal of Botany, 54*(5-6), 539-542.

Heslop-Harrison, J. (1966). Cytoplasmic continuities during spore formation in flowering plants. *Endeavour, 25*, 65-72.

Heslop-Harrison, J. (1971a). The pollen wall: Structure and development. In J. Heslop-Harrison (Ed.), *Pollen: Development and Physiology* (pp. 75-98). London: Butterworths.

Heslop-Harrison, J. (1971b). Wall pattern formation in angiosperm microsporogenesis. *Society for Experimental Biology Symposium, 25*, 277-300.

Hoefert, L. L. (1968). Polychromatic stains for thin sections of beta embedded in epoxy resin. *Stain Technologies, 43*(3), 145-151.

Holdorf, M. M., Owen, H. A., Lieber, S. R., Yuan, L., Adams, N., Dabney-Smith, C., & Makaroff, C. A. (2012). Arabidopsis ETHE1 encodes a sulfur dioxygenase that is essential for embryo and endosperm development. *Plant Physiology, 160*, 226-236.

Kim, S., Hong, C., & Lee, I. (2001). Heat shock stress causes stage-specific male sterility in Arabidopsis thaliana. *Journal of Plant Research, 114*(3), 301-307.

Mamun, E. A., Alfred, S., Cantrill, L. C., Overall, R. L., & Sutton, B. G. (2006). Effects of chilling on male gametophyte development in rice. *Cell Biology International, 30*, 583-591.

Mamun, E. A., Alfred, S., Cantrill, L. C., Overall, R. L., & Sutton, B. G. (2006). Effects of chilling on male gametophyte in rice. *Cell Biology International, 30*, 583-591.

Owen, H. A., & Makaroff, C. A. (1995). Ultrastructure of microsporogenesis and microgametogenesis in *Arabidopsis thaliana* (L) *heynh* ecotype Wassilewskija (*Brassicaceae*). *Protoplasma, 185*, 7-21.

Pecrix, Y., Rallo, G., Folzer, H., Cigna, M., Gudin, S., & Le Bris, M. (2011). Polyploidization mechanisms: temperature environment can induce diploid gamete formation in Rosa sp. *Journal of Experimental Botany, 62*, 3587-3597.

Peirson, B. N., Owen, H. A., Feldmann, K. A., & Makaroff, C. A. (1996). Characterization of three male-sterile mutants of *Arabidopsis thaliana* exhibiting alterations in meiosis. *Sexual Plant Reproduction, 9*, 1-16.

Regan, S. M., & Moffatt, B. A. (1990). Cytochemical analysis of pollen development in wild-type *Arabidopsis* and a male-sterile mutant. *The Plant Cell, 2*, 877-889.

Rhee, S. Y., & Sommerville, C. R. (1998). Tetrad pollen formation in *quartet* mutants of *Arabidopsis thaliana* is associated with persistence of pectic polysaccharies of the pollen mother cell wall. *The Plant Journal, 15*(1), 79-88.

Shibasaki, R., & Tan, G. (2002). Monthly climatologically aided global interpolation of weekly air temperature and precipitation. *Theory Appl. of GIS, 10*, 8-17.

Smith, M., & McCully, M. (1978). Enhancing aniline blue fluorescent staining of cell wall structures. *Stain Technologies, 53*(2), 79-85.

Toller, A., Brownfield, L., Neu, C., Twell, D., & Schulze-Lefert, P. (2008). Dual function of Arabidopsis glucan synthase-like genes GSL8 and GSL10 in male gametophyte development and plant growth. *Plant Journal, 54*(5), 911-923.

Vizcay-Barrena, & Wilson, Z. A. (2006). Altered tapetal PCD and pollen wall development in the *Arabidopsis ms1* mutant. *Journal of Experimental Botany, 57*(11), 2709-2717.

Wigge, P. (2013). Ambient temperature signaling in plants. *Current Opinion in Plant Biology, 16*, 661-666.

Worrall, D., Hird, D. L., Hodge, R., Paul, W., Draper, J., & Scott, R. (1992). Premature dissolution of the microsporocyte callose wall causes male sterility in transgenic tobacco. *The Plant Cell, 4*(7), 759-771.

Zinkl, G. M., Zwiebel, B. I., Grier, D. G., & Preuss, D. (1999). Pollen-stigma adhesion in *Arabidopsis*: a species-specific interaction mediated by lipophilic molecules in the pollen exine. *Development, 126*, 5431-5440.

Chapter III

Ultrastructural Characterization of Early Pollen Wall Development in Meiotic Mutant 6491 and Wild Type *Arabidopsis thaliana*

A. Introduction

Pollen wall development in *Arabidopsis thaliana* follows a specific series of steps that have been well-documented (J. Heslop-Harrison, 1963; J Heslop-Harrison, 1968; Owen & Makaroff, 1995). An ultrastructural characterization of *Arabidopsis thaliana* (L.) Heynh. ecotype Wassilewskija (Owen & Makaroff, 1995) divided microsporogenesis and microgametogenesis into twelve separate stages. Using similar terminology referenced in those characterizations, the development of WT grown at 16^{o} C was compared to development of a temperature-sensitive meiotic mutant of the same ecotype known as 6491, also grown at 16^{o} C.

Previously, semi-thin sections of WT and 6491 were examined, with the results acting as a framework to look at more detailed development in the mutant line 6491. It was noted that the majority of phenotype changes in 6491 appeared to be in place by tetrad stage, thus this study focused on early development, specifically premeiosis through tetrad stages. The examination of ultrastructure involved will allow for information to be added to the incomplete pathways dealing with pollen wall development.

A mutant line such as 6491 is considered a meiotic mutant because of a combination of small and large microspores produced in cytokinesis. In WT, a callose wall is deposited around each microsporocyte prior to meiosis. Large openings, called cytomictic channels, form as callose is being deposited. The channels interconnect all the microsporocytes within a locule, making the cytoplasm contiguous (Heslop-Harrison, 1966). This may allow for the development of the microsporocytes to be synchronized during meiosis. Asynchrony between the microsporocytes may lead to changes in the size, shape, and wall development of microspores within a locule, due

in part from changes in the deposition of the callose wall (Chen et al., 2009; Lu et al., 2014).

Callose, a β-1,3 glucan, has several functions. Callose regulates communication between microsporocytes through plasmodesmata, separates microsporocytes during cytokinesis, and acts as a sealant for sieve plates in dormant phloem to stop the spread of pathogens or in case of mechanical injury (Hong, Delauney, & Verma, 2001; Nishikawa, Zinkl, Swanson, Maruyama, & Preuss, 2005). It has been reported that in tobacco, callose synthase is processed in endoplasmic reticulum, integrated into golgi bodies and transported via actin filaments (Cai, Faleri, Del Casino, Emons, & Cresti, 2011). During early meiosis in *Arabidopsis*, a cytoskeleton of microtubules becomes associated with the nuclear envelope. Microtubules then arrange in a radial pattern in young microspores, extending from the nuclear envelope to the plasma membrane (Sheldon & Dickinson, 1968). This transport system may be a way for callose synthases to be deposited at the site of construction via vesicles traveling along the microtubules, and synthesized into the callose wall. When the cytoskeleton is disrupted, whether through physical or chemical methods, microspores might not evenly separate, pattern anomalies may occur and misplaced apertures may arise from interference in vesicle transport (Dickinson & Sheldon, 1986; Heslop-Harrison, 1971b; Sheldon & Dickinson, 1968). Any change in the thickness, timing, or dissolution of the callose wall may affect the final exine pattern (Chen et al., 2009; Lu et al., 2014), thus it is not surprising that a pollen grain arising from a microspore with an affected cytoskeleton may have a malformed, or even absent pattern on its exine. As previously reported, exine pattern in the mutant line 6491 is disrupted or absent.

In tetrad stage, microspores are enclosed completely within callose and the process resulting in a reticulate exine wall begins. The plasma membrane is first held tight against the callose wall, and then material thought to be primexine is produced that is periodically spaced between

the callose and microspore membrane. The microspore membrane becomes rippled as more primexine is deposited, except at the site of future apertures (Heslop-Harrison, 1963). The primexine matrix appears thickest within the undulations. Electron dense material first appears at the peak portion of the waves in the membrane. More electron dense material is added, taking the shape of probacula and protectum and leading to the reticulate exine wall seen in mature pollen grains of WT *Arabidopsis*. Normal, intact callose is required for proper exine patterning (Dong, Hong, Sivaramakrishnan, Mahfouz, & Verma, 2005). An alteration in callose has been proposed to change the "scaffolding" upon which the exine wall is formed, consequently altering the final exine wall (Dong et al., 2005; Heslop-Harrison, 1971a; Nishikawa et al., 2005).

As shown previously in semi-thin sections of the mutant line 6491, callose is not deposited when, nor how it should be. The callose appears much thinner than WT and microspores lack normal reticulate patterning. The resulting pollen grains lack colpi and are smooth rather than patterned. Examining developing ultrastructure at high magnification in both WT and 6491, will help elucidate changes taking place as the exine wall is formed and contribute information that could help identify the function of the mutated gene in 6491.

B. Literature Review

There are several male-sterile *Arabidopsis* mutants that result in defective primexine formation and support the idea that primexine helps to establish patterning of the exine. Among these is *defective in exine formation1 (dex1)*, a mutation that results in random and delayed deposits of sporopollenin that do not appear to anchor to the plasma membrane (Paxon-Sowders, Dodrill, Owen, & Makaroff, 2001). Normal exine patterning does not occur in *dex1* mutants. The *ruptured pollen grain 1 (rpg1)* mutant results in microspores that have randomly deposited

sporopollenin on both the plasma membrane and primexine, establishing a slightly functional exine (Guan et al., 2008). *RPG1* helps maintain plasma membrane integrity and timely undulation of microspore membrane. *Exine formation defect* (*efd*) has a properly undulated membrane but primexine formation is impaired and exine formation is mostly absent (Hu, Wang, Zhang, & Sun, 2014). The primexine found in the *nef1 (no exine formation)* mutant seems to be the most defective, producing a thin primexine layer with no probacula present (Ariizumi et al., 2004). In *transient defective exine 1 (tde1),* fertility is normal, even with a phenotype that includes defective primexine and probacula development, as well as sporopollenin that deposits in irregular aggregates. The *tde 1* mutant displays a normal exine pattern later in development, indicating the initial formation processes were affected, but not those necessary for proper exine formation (Ariizumi et al., 2008).

The establishment of exine pattern is a largely untapped area of information in pollen development. Callose at tetrad stage has been shown to be important in the establishment of exine pattern (Albert, Ressayre, & Nadot, 2011; Chen et al., 2009; Dong et al., 2005; Heslop-Harrison, 1968; Nishikawa et al., 2005; Zhang et al., 2007). 6491 displays abhorrent exine patterning, but the appearance of this defect seems to present itself least when grown at 16^{o} C. For this reason, an ultrastructural study of 6491 grown at 16^{o} C was undertaken to examine the details of the callose/ microspore plasma membrane during early exine development.

C. Materials and Methods

Plant growth:

Arabidopsis thaliana L. Heynh, ecotype Wassilewskija (WS) wild-type and 6491, a mutant line in the same background, were used in this work. The mutant 6491 was identified in a screen of a T-DNA mutagenized population (Feldmann & Marks, 1987) and is maintained as a

homozygous recessive line. Seeds were grown on damp Metro Mix 360 commercial potting mix in a growth chamber with a 16/8 light and dark cycle at 16^{o} C.

Transmission electron microscopy sample preparation:

Material was prepared for ultrathin sectioning essentially according to (Owen & Makaroff, 1995). Whole inflorescences were removed from plants and fixed overnight at room temperature in 2.5% (v/v) gluteraldehyde in 0.1 M HEPES buffer (pH7.2) and 0.02% (v/v) Triton X-100. Buds were rinsed three times with 0.1 M HEPES buffer (pH7.2) and post-fixed overnight in 1% OsO_4. After rinsing twice with distilled, deionized water, buds were dehydrated in a graded acetone series of 10% increments and infiltrated in Spurr's resin or modified Spurr's resin. Spurr's resin was modified by the addition of Quetol 651 according to Table 3 (Ellis, 2006), except 0.05g 2(dimethyl-amino) ethanol was used in place of 0.02ml N, N-dimethylbenzylamine (Holdorf et al., 2012). Following infiltration in 100% resin, individual buds were removed from inflorescences, and placed in numbered flat embedding molds in developmental order.

Ultrathin (silver to pale gold) sections were cut with a diamond knife on an RMC MT 7000 ultramicrotome and picked up on 200 mesh copper grids. Sections were stained with 2% aqueous uranyl acetate and Reynold's lead citrate, then imaged with a Hitachi H-600 transmission electron microscope operating at 75kv. Images were captured on Kodak 4489 electron microscope film. Following development, digital images were acquired by scanning the film with an Agfa V750 Pro flatbed scanner in transmitted light mode.

D. Results

Arabidopsis thaliana L.- Heynh, ecotype Wassilewskija (WS) wild-type and 6491, a mutant line in the same background were grown at 16^{o} C and an ultrastructural survey of the early developmental stages was undertaken. Focus of this study was primarily development of the

exine wall. Transmission electron microscopy was completed on six stages for both WT and mutant lines, to compare the presence and timing of ultrastructural differences.

Wild-type *A. thaliana* grown at 16º C

The results from WT *Arabidopsis* are shown in figures thirteen through twenty-one. In premeiosis I (Fig. 13 A), microsporocytes have thin walls, with little separation between adjacent microsporocytes. Both the microsporocytes and cells comprising the tapetal layer contain nuclei and nucleoli. There are numerous small vacuoles present within the microsporocytes, and larger vacuoles in the tapetal cells. Rough endoplasmic reticulum is present in the microsporocytes, appearing to connect directly to the nuclear envelope. A larger separation between plasma membrane and microsporocyte wall appears in premeiosis II (Fig. 13 B). A layer of callose (confirmed by aniline blue fluorescence in semi-thin sections, data shown previously) is deposited by the microsporocytes between their cell walls and plasma membranes. Fewer vacuoles are present within the microsporocyte cytoplasm, but an increase in endoplasmic reticulum is apparent. Each microsporocyte is fully encased in a callose wall of uneven thickness, is more rounded in appearance, and fairly consistent in size during meiosis (Fig. 13 C). Irregular undulations are present in the microsporocyte plasma membrane. An increase in endoplasmic reticulum is present near the nuclear envelope and deep to the plasma membrane. During cytokinesis (Fig. 14 A), it appears as though there is an uneven distribution of cytoplasm and organelles within the microsporocytes. The callose wall has grown inward, following the cleavage furrows evident at this stage. Nuclei have moved to the periphery of each microsporocyte. Large amounts of endoplasmic reticulum are present, as are numerous large vacuoles. Mitochondria are both elongate and round in appearance. Numerous small vesicles can be seen at the periphery between the plasma membrane of the microsporocytes and callose wall

Fig. 13 Transmission electron micrographs of cross-sections thru anthers of wild-type *A. thaliana* grown at 16^{o} C showing three stages of early development. **A** Premeiosis I. Microsporocytes (Mi) have little separation between them. Rough endoplasmic reticulum (arrow) is present close to nucleus (N). Microsporocytes are surrounded by the tapetum (T) and vacuoles (V) are present. **B** Premeiosis II. Microsporocytes (Mi) are separated by developing callose wall. Tapetal (T) cells begin to separate and are vacuolated. **C** Meiosis. Microsporocytes (Mi) have increased separation tangentially and radially and a callose wall (Ca) encloses the microsporocytes. Irregular undulations (arrowhead) are present in the microsporocyte plasma membrane. Bar = 5 µm.

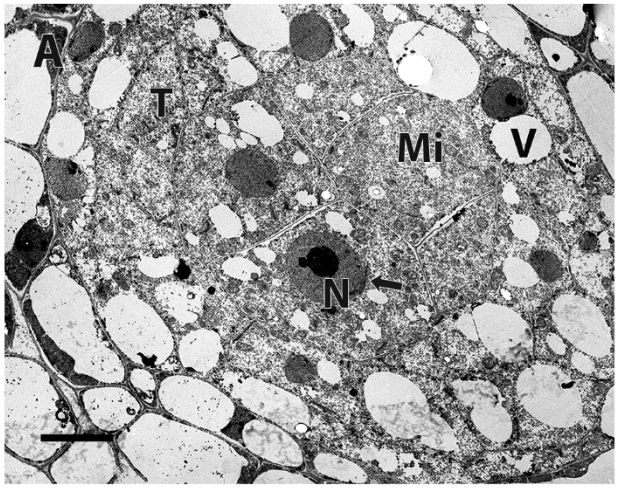
A
T
Mi
V
N

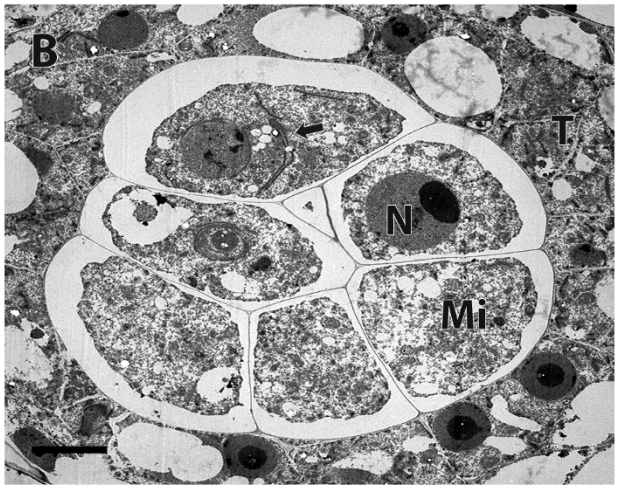
B
T
N
Mi

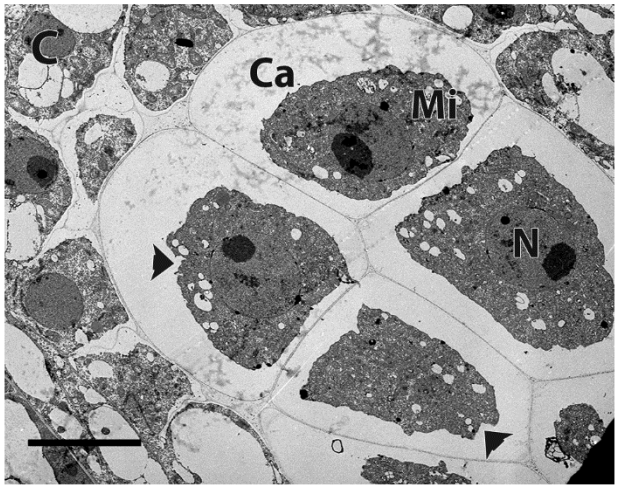
C
Ca
Mi
N

Fig. 14 Transmission electron micrographs thru cross-sections of anthers of wild-type *A. thaliana* grown at 16^{o} C showing three stages of later development. **A** Cytokinesis. Microsporocytes (Mi) undergoing cytokinesis with cleavage furrows (arrows) forming. Nuclei (N) and vacuoles (V) are present. Bar = 1 µm. **B** Tetrads. Microspores (Ms) are separated by a callose wall in a Tetrad (Te). **C** Pollen grains. Pollen grains are vacuolated and enclosed by the exine wall (Ex). Tryphine (Try) is found on the exine wall. Bar = 5 µm.

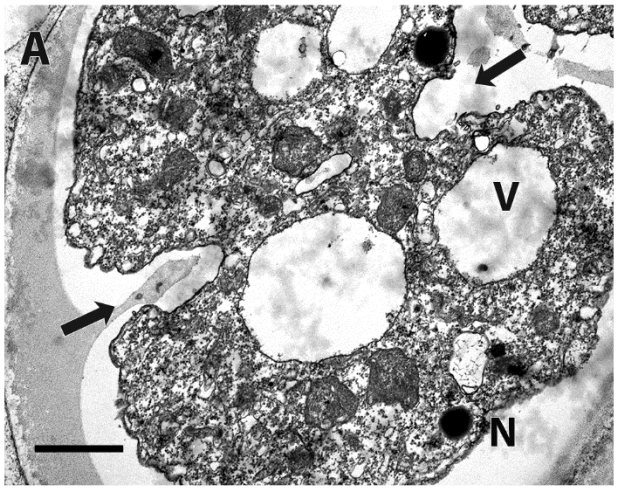
A
V
N

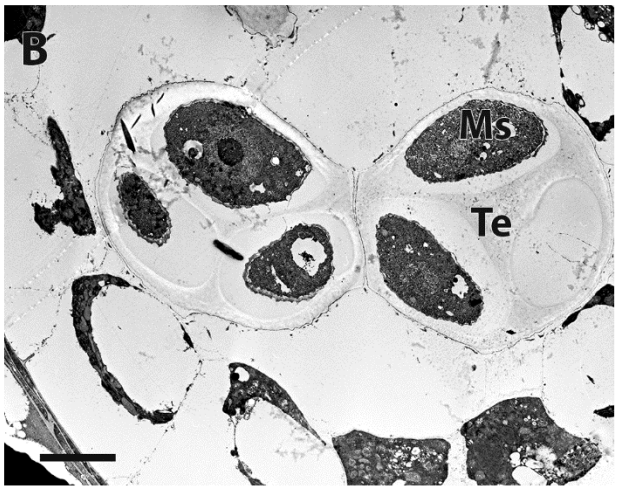
B
Ms
Te

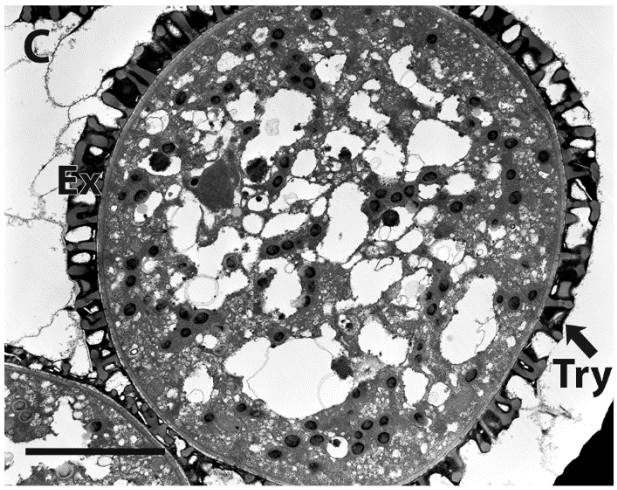
C
Ex
Try

(Fig. 15). Some vesicles can also be found within the callose layer. Golgi bodies are in close proximity to the vesicles. Tapetal cells are enlarged with vacuoles present and large gaps within the tapetal cell membranes (Fig. 16).

During tetrad stage (Fig. 14 B), the four haploid microspores are encased within a callose wall, comprised of both the original callose wall secreted by the microsporocytes and a newer layer deposited throughout cytokinesis. Undulations are present in the plasma membrane (Fig. 17), with deposits of an electron dense substance occurring at fairly regular intervals within the depressions of the plasma membrane, at the periphery between plasma membrane and callose wall. As shown previously in literature (Paxson-Sowders, Dodrill, Owen, & Makaroff, 2001), this microsporocyte-produced material is primexine. Later, more electron-dense material is accumulating in a radial direction at the peak portions of the plasma membrane, forming probaculae of the future exine wall (Fig. 18). The electron dense material gathered at the peaks of membrane undulations is likely sporopollenin, supported by previous literature. Deposits of sporopollenin appear to be coming from the microspore, and going no further than the border between primexine and callose. It has been shown that later in development sporopollenin also comes from tapetal cells to help complete the exine wall of a pollen grain (Fig. 14C).

The pollen grain wall shows several distinct layers (Fig. 19). The distinctive and species-specific reticulate exine is comprised of radially arranged baculae and transverse portions called tectum. This layer is referred to as the sexine. Comprising the deeper layer of the exine is the nexine. Covering large areas of the superficial sexine is tryphine (also known as pollen coat). Within the tryphine are electron-lucent structures of a crystalline form. The multilamellar intine has two distinct layers, an exintine and endintine. Exintine is granular with pectin and protein inclusions and endintine is a microfibrillar cellulosic layer facing inward (Huang et al., 2009).

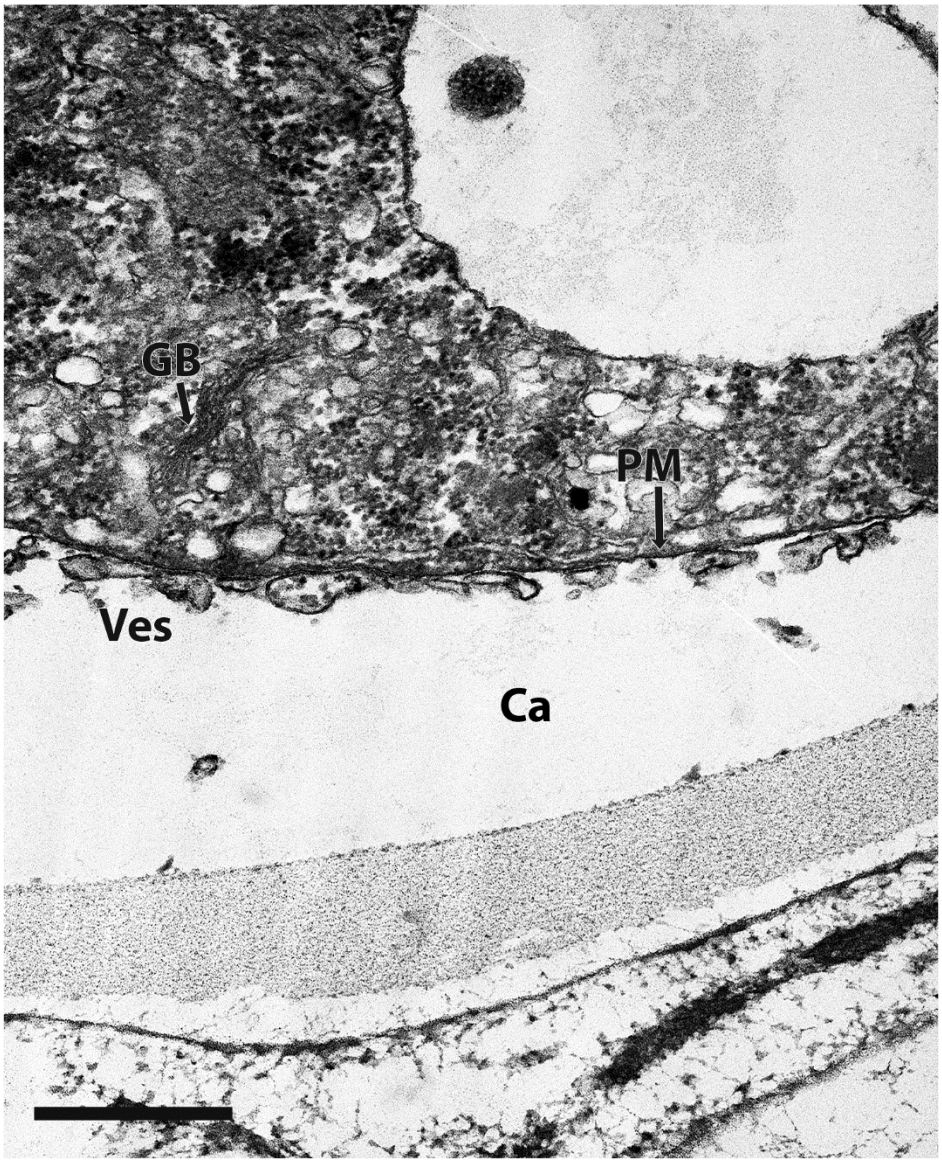

Fig. 15 Transmission electron micrograph thru cross section of an anther of Wild-type *A. thaliana* grown at 16^{o} C in cytokinesis stage. In a microsporocyte, vesicles (Ves) are present at the interface of the plasma membrane (PM) and callose wall (Ca). Numerous golgi body (GB) are within the cytoplasm. Bar = 0.5 µm.

Fig. 16 Transmission electron micrograph thru cross section of an anther of Wild-type *A. thaliana* grown at 16^{o} C in cytokinesis stage. Vacuolated tapetal cells (T) surround microspores (Ms) completing cytokinesis with irregular shapes and sizes. Bar = 5 µm.

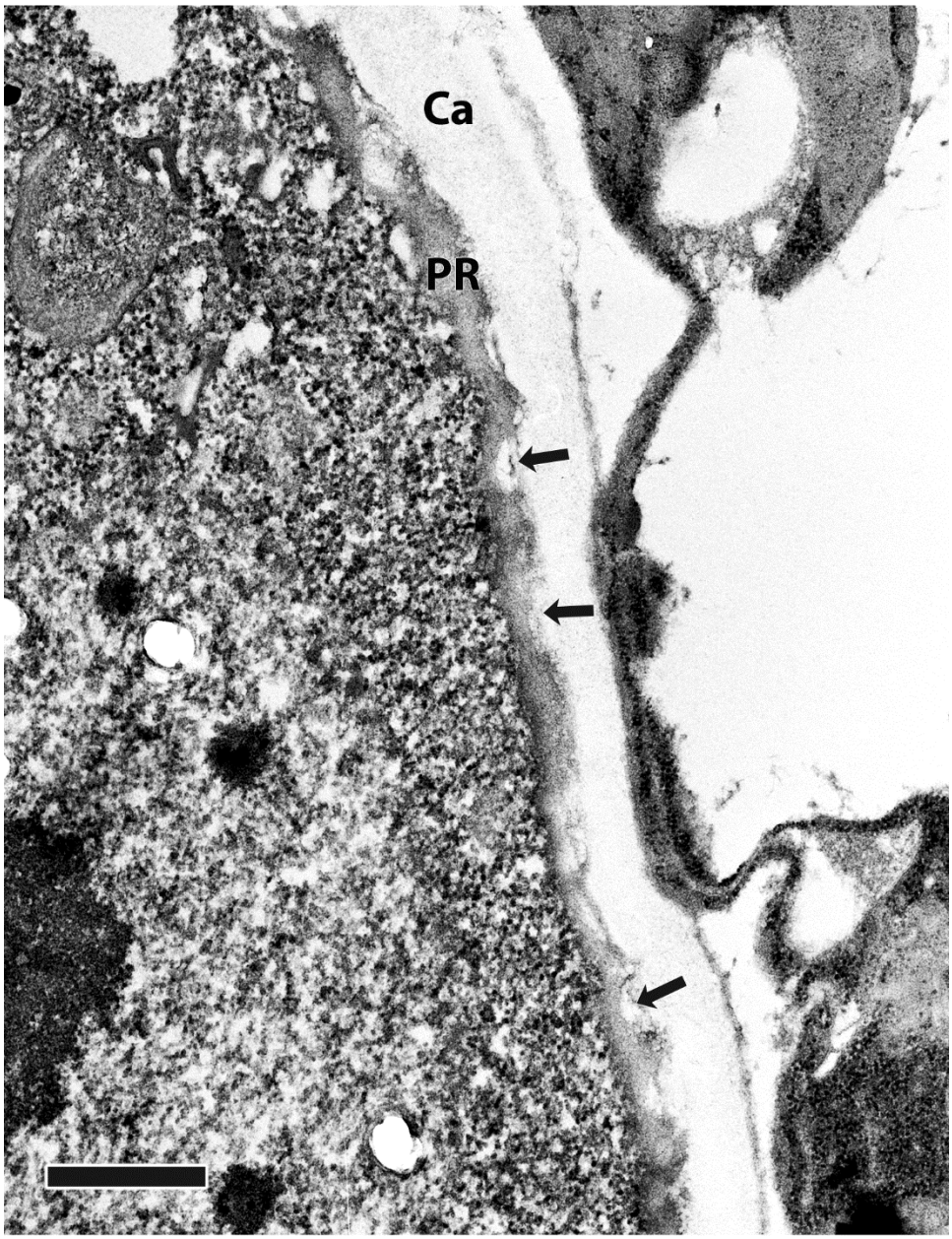

Fig. 17 Transmission electron micrograph thru cross section of an anther of Wild-type *A. thaliana* grown at 16º C in tetrad stage. Primexine (PR) is deposited at the interface of plasma membrane and callose wall (Ca). Undulations are found in the plasma membrane (arrows). Bar = 0.5 µm.

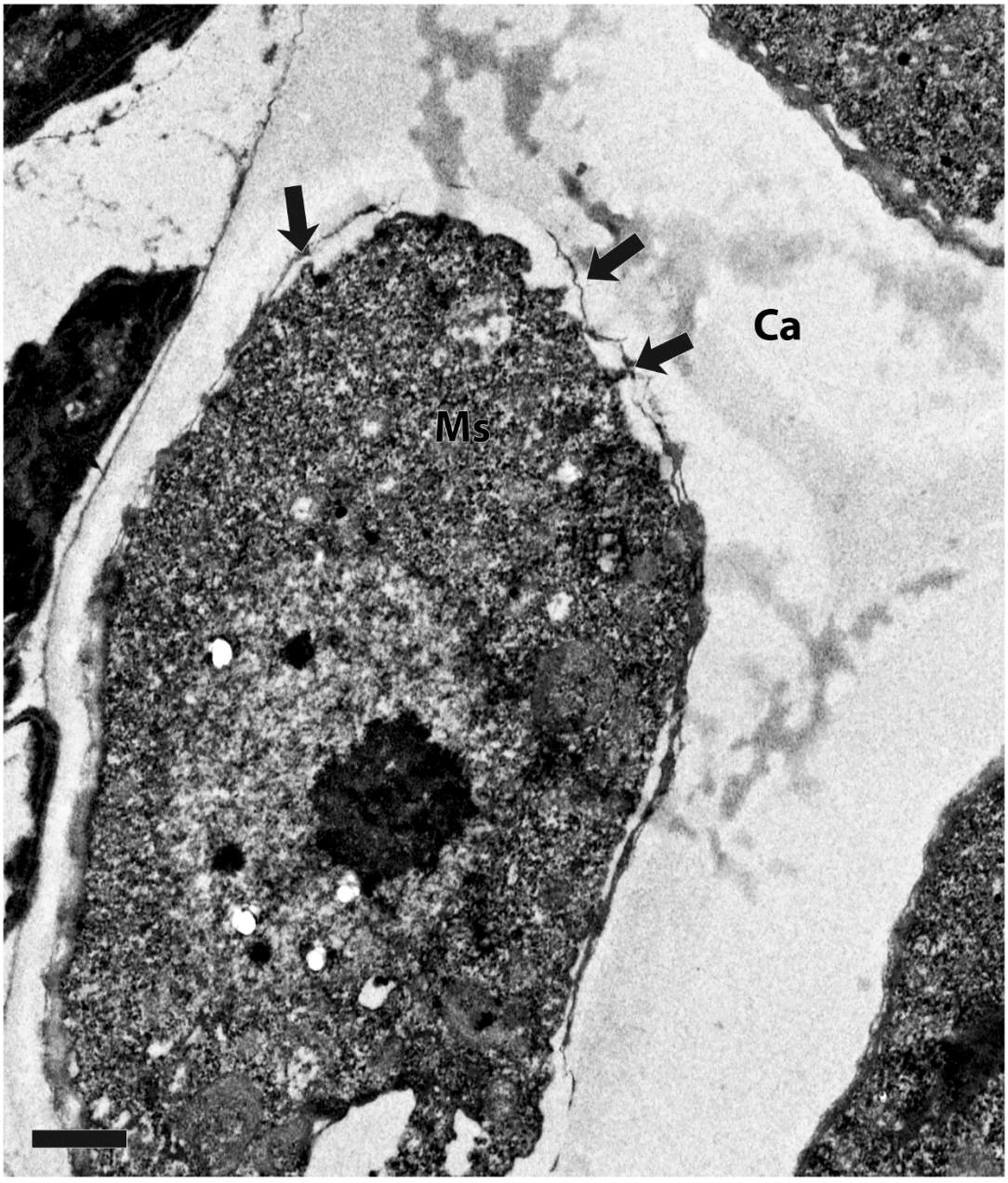

Fig. 18 Transmission electron micrograph thru cross section of a tetrad of Wild-type *A. thaliana* grown at 16º C. Sporopollenin (arrows) from the microspore (Ms) is accumulating in distinct peaks at the interface of the callose wall (Ca) and plasma membrane. Bar = 1 µm.

Fig. 19 Transmission electron micrograph thru cross section of a pollen grain wall of Wild-type *A. thaliana* grown at 16^{o} C. Electron lucent structures (asterisk) are present within the pollen coat (Pc) on the exine wall. The exine is made up of bacula (Ba) and tectum. The deeper layer of the exine is the nexine (Nex) and deep to that is the intine, comprised of two layers, the exintine (Exi) and endintine (End). Bar = 0.5 µm

Vesicles are noted within the endintine, seemingly traversing the layer in a superficial direction (Fig. 20). The thickness of the intine and the proportions of the exintine and endintine varies along the plasma membrane, especially at the area of apertures (Fig. 21).

***A. thaliana* mutant 6491 grown at 16º C**

The results from the ultrastructural survey of the mutant 6491line are shown in figures twenty-two through twenty-nine. During premeiosis I (Fig. 22 A) the microsporocytes have little to no separation and are vacuolated. The tapetal cells have large vacuoles, and nuclei with nucleoli. In premeiosis II (Fig. 22 B), there is a bit more separation between the microsporocytes, but not the same separation seen in WT at a similar stage. Plasmodesmata are present between the tapetal cells (Fig. 23) and vacuoles within the tapetal cells seemed to have decreased in number. Rough endoplasmic reticulum is noted in proximity to the nucleus. Tapetal cells have an increased number of vacuoles, but they are smaller in size than seen during premeiosis I. The tapetal cells have little separation tangentially or radially. A callose layer (confirmed previously through aniline blue fluorescence) within the cell wall is visible in meiosis (Fig. 22 C), separating each microsporocyte. Condensing chromosomes are present within the nuclei. Irregular undulations are forming along the plasma membrane.

Division of microsporocyte cytoplasm is unequal during cytokinesis (Fig. 24 A). Cleavage furrows are followed by deposition of callose within the furrows. Elongated mitochondria and rough endoplasmic reticulum are present throughout the cytoplasm. Late in cytokinesis (Fig. 25), more distinct undulations are noted in the plasma membrane. A layer of an electron-dense material is forming between the callose wall and the plasma membrane, with the densest deposits

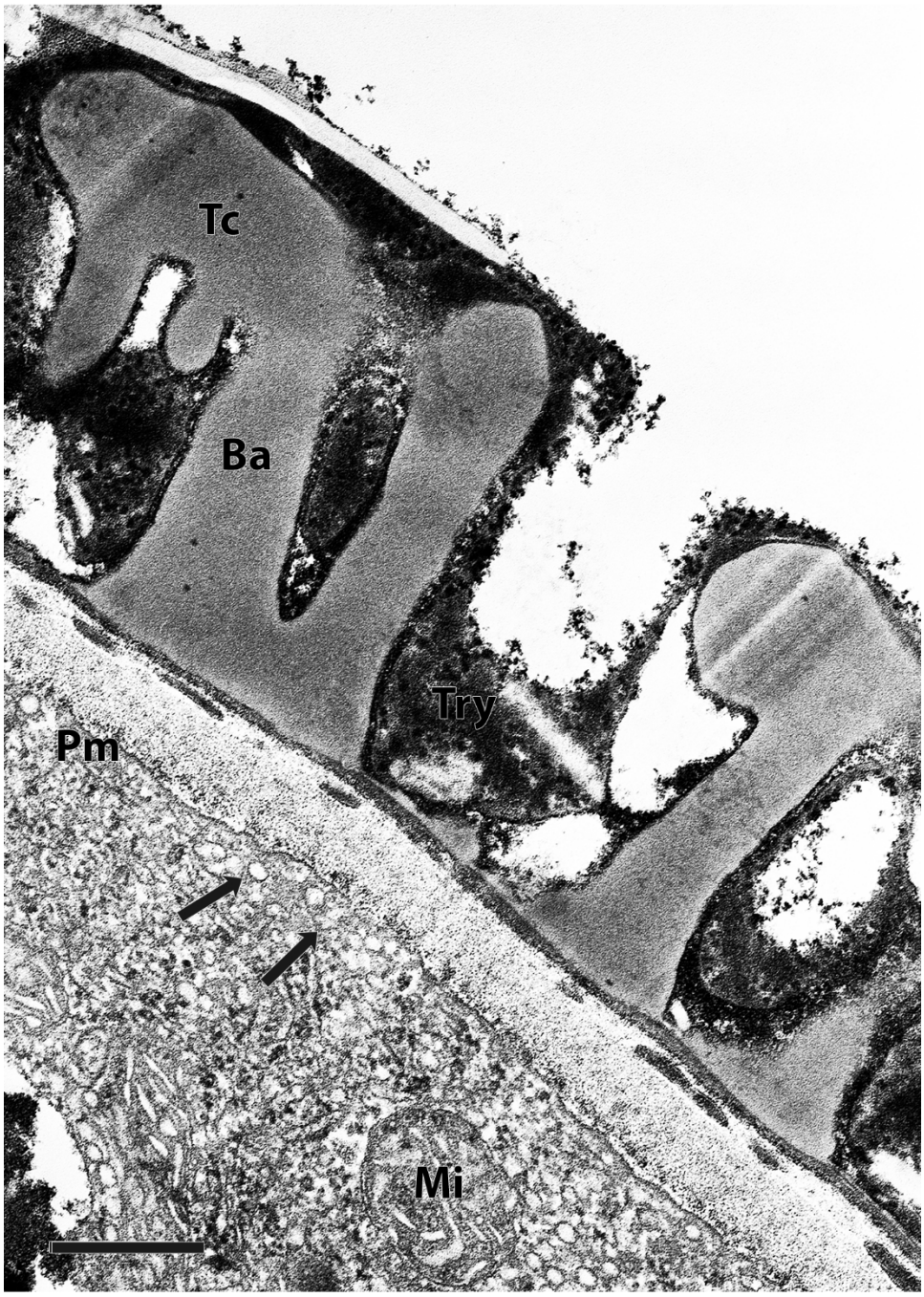

Fig. 20 Transmission electron micrograph of a cross section thru pollen grain wall of Wild-type *A. thaliana* grown at 16º C. Tectum (Tc) and baculae (Ba) of the exine are visible, along with the tryphine (Try) layer. Multiple vesicles (arrows) are present at the interface of plasma membrane (Pm) and intine. Mitochondria (Mi) are found throughout the cytoplasm. Bar = 5 µm.

Fig. 21 Transmission electron micrograph cross-section thru Wild-type *A. thaliana* pollen grain grown at 16° C. Two sperm cells (Sc) are present. Also visible are three apertures (arrows) within the exine wall. Bar = 5 µm

Fig. 22 Transmission electron micrographs of cross-sections thru anthers of mutant line 6491 *A. thaliana* grown at 16^{o} C. **A** Premeiosis I. Microsporocytes (Mi) have little separation between them. Some large vacuoles are present in tapetal cells (T). **B** Premeiosis II. Microsporocytes (Mi) show little separation. Nucleus and nucleolus are present, as is endoplasmic reticulum (arrow) by nuclear membrane. **C** Meiosis. A callose wall separates microsporocytes. Bar = 5 µm.

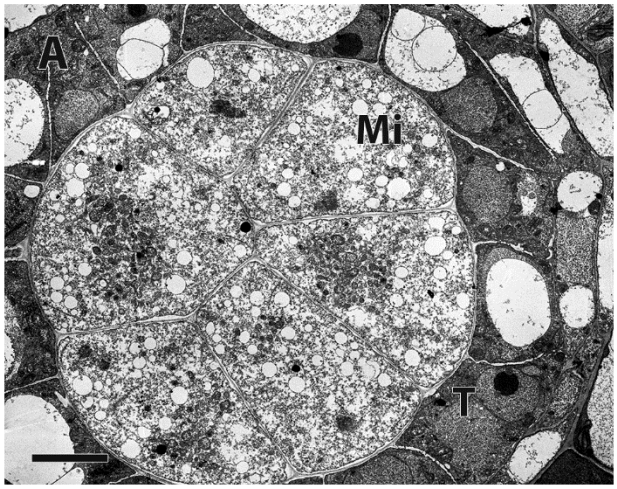
A
Mi
T

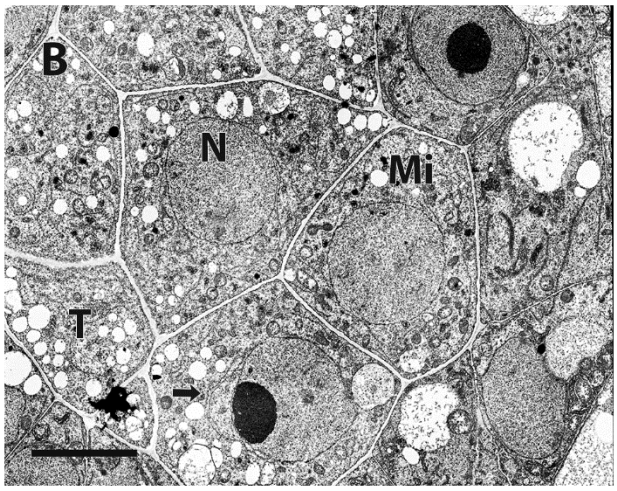
B
N
Mi
T

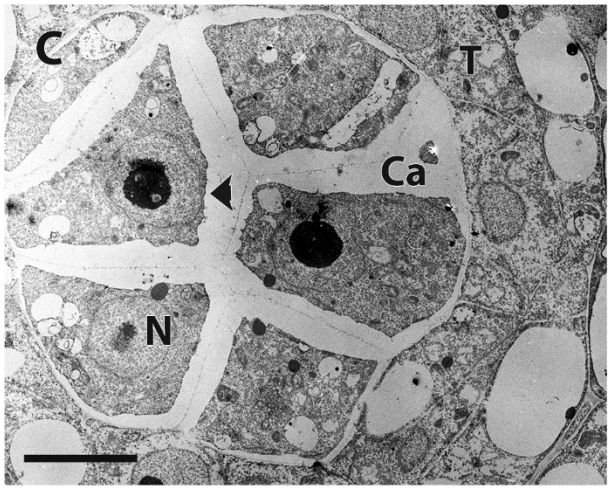
C
T
Ca
N

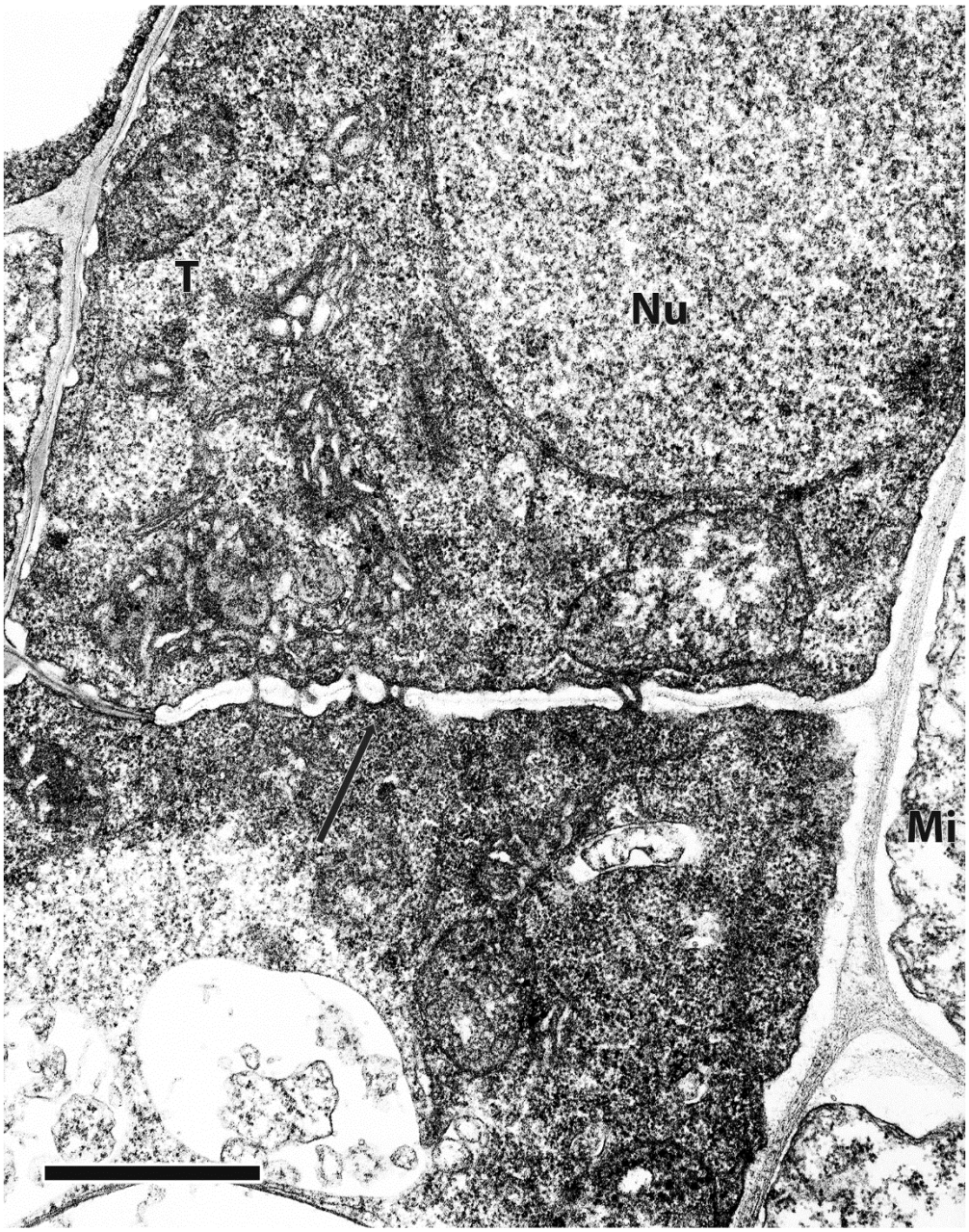

Fig. 23 Transmission electron micrograph of cross- section thru anther of mutant line 6491 *A. thaliana* grown at 16^{o} C. Plasmadesmata (arrows) are present between tapetal cells during premeiosis II. Nucleus (Nu) is visible. Bar = 1µm.

Fig. 24 Transmission electron micrographs of cross- section thru anther of mutant line 6491 *A. thaliana* grown at 16^{o} C showing late stages of development. **A** Cytokinesis. Microsporocytes (Mi) undergoing cytokinesis with cleavage furrows (arrows) forming. Nuclei and vacuoles (V) are present. Small mitochondria (M) are present in cytoplasm of microsporocyte. Bar = 1 µm. **B** Tetrads. Microspores (Ms) are enclosed by callose wall in a Tetrad (Te). Highly vacuolated cytoplasm in microsporocytes. **C** Pollen grains. Pollen grains have an even, non-reticulated exine wall (Ex). There is no recognizable cellular structure within the pollen grains. Bar = 5µm

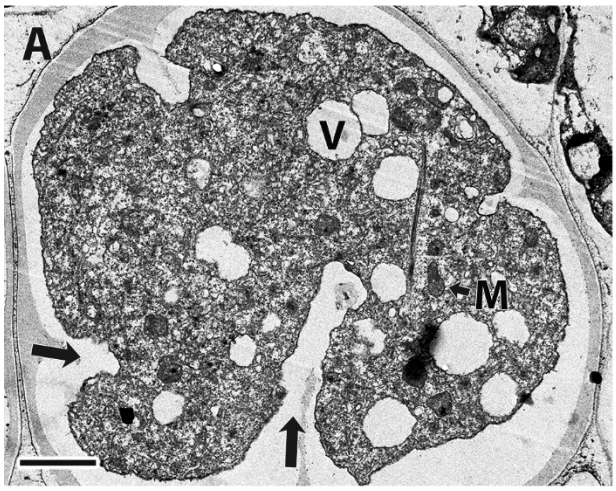
A
V
M

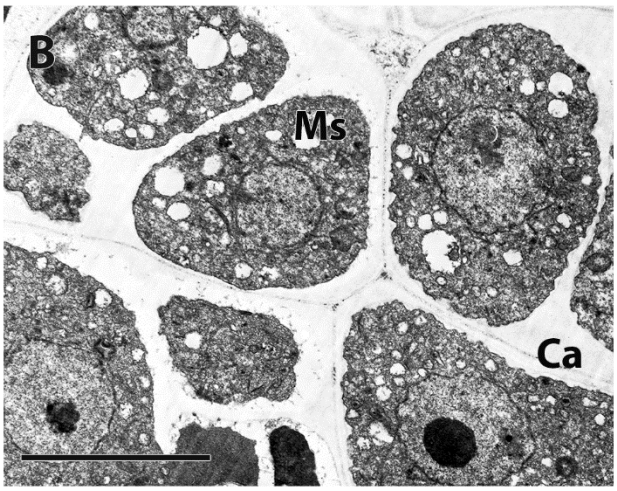
B
Ms
Ca

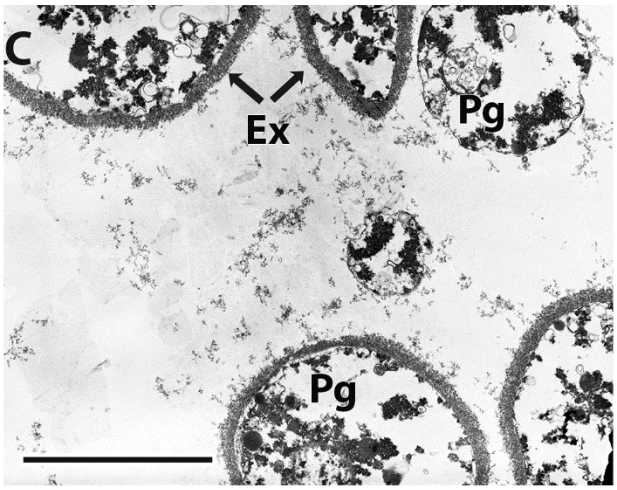
C
Ex
Pg
Pg

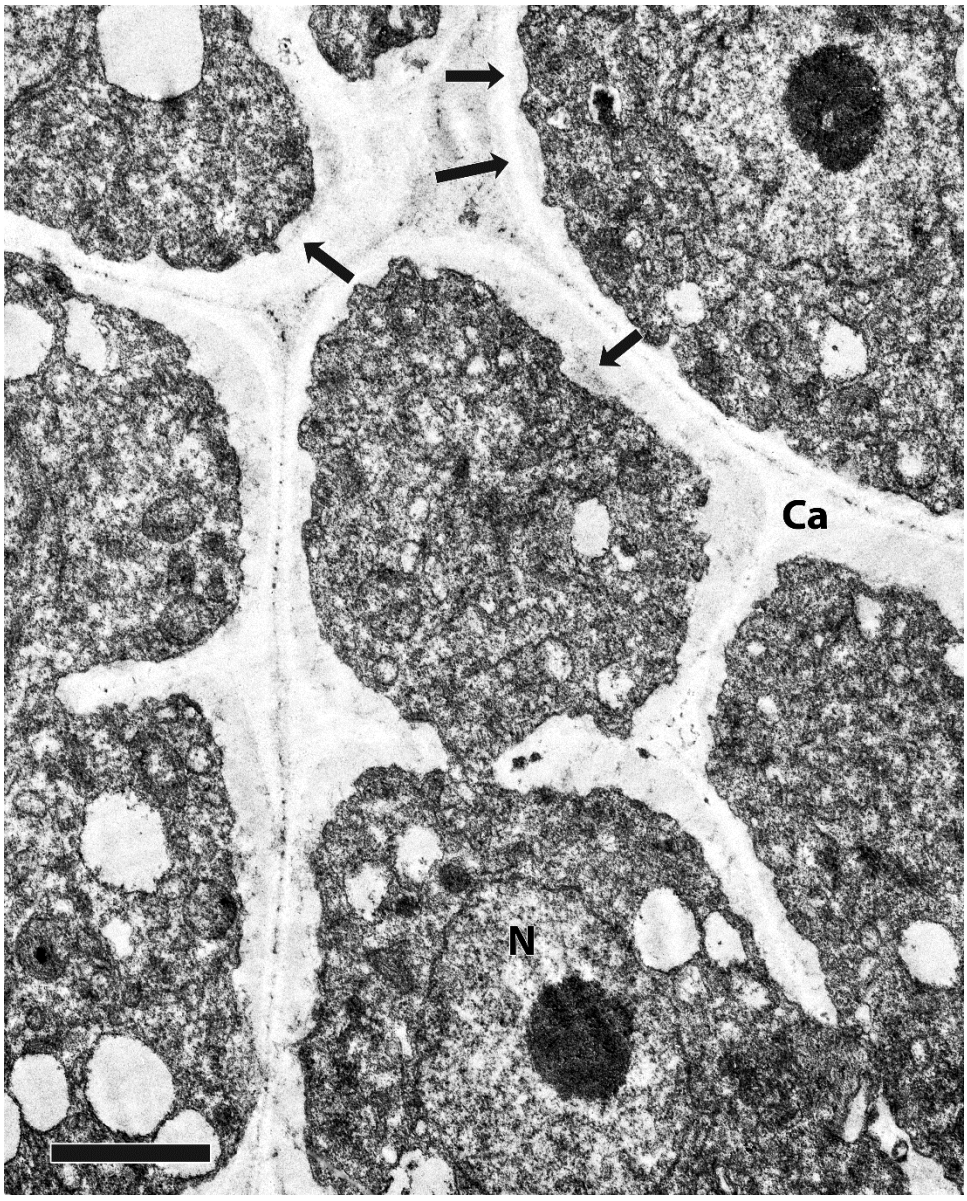

Fig. 25 Transmission electron micrograph of cross- section thru anther of mutant line 6491 *A. thaliana* grown at 16^{o} C during cytokinesis. Undulations in the plasma membrane (arrows) are evident. A callose wall (Ca) separates microsporocytes. Bar = 2 µm.

in the depressions of the plasma membrane undulations. The haploid microspores in tetrad stage are now encased fully within a callose wall (Fig. 24 B). The microspores are uneven in size and irregular in shape. The cytoplasm is vacuolated with a prominent nucleus and nucleolus. A large amount of rough endoplasmic reticulum is present, concentrated in close proximity to the nuclear envelope. Undulations varying in depth and spacing are found within the plasma membrane and a layer of an electron-dense material is found at the interface of the callose wall and plasma membrane. Deposits of very electron-dense material are beginning to accumulate at the peak portions of the membrane undulations (Fig. 26). This material seems to be produced by the microspores and is transported as far as the beginning of the callose wall (Fig. 27), where it accumulates in fibrillar strings possibly attaching to the plasma membrane.

The resulting pollen grains (Fig. 24 C) within the locule of the anther are lacking most cellular structure found within WT pollen grains. As the tapetum disintegrates, fibrillar electron dense material is found throughout the locule, and what appears to be a similar substance is accumulating on the developing grains (Figs. 28-30). The amount of electron dense material on the grain surface increases as development proceeds. The exine portion of the pollen grain wall appears to be a solid, somewhat smooth layer, although there are a few areas of slight reticular structure (Fig. 29). A thin intine is visible in some portions of the grain wall (Fig. 30). Other pollen grains from the same treatment appear to be aborted at an earlier stage (Fig. 30).

E. Discussion

An ultrastructural study of WT and temperature-sensitive mutant 6491 *A. thaliana* was used as a means to examine differences between the two lines in early development, and as a means to further elucidate the function of the mutated gene found in 6491. This study built upon

information gathered while examining semi-thin sections of the same lines, using the more general data to pinpoint specific areas of interest involved in development of the pollen grain wall.

As noted from the previous study of semi-thin sections (Chapter 2), ambient temperature changes resulted in multiple structural differences in both WT and 6491 lines. Taking this into consideration, the lowest temperature of the three studied was chosen, with the expectation that the fewest and least severe structural changes should be evident in the temperature-sensitive 6491 line in comparison to WT. At a growing temperature of 16° C, 6491 appears normal, rather than reduced-fertile or sterile as demonstrated at higher temperatures.

However, when the semi-thin sections of WS WT grown at 16° C were compared with semi-thin sections in a previous developmental study of WS WT grown at 20° C results were unexpected in the severity of differences (Peirson, Owen, Feldmann, & Makaroff, 1996) in development. This factor will be taken into consideration in discussion of the results, focusing the discussion primarily on differences between WT and 6491 grown at 16° C. This bears mentioning because the developmental stages and structural benchmarks of WT here may be different from those commonly referenced in literature based on plants grown in the mid-range of temperature considered optimal for *Arabidopsis* (20 - 22 ° C).

The complex interplay of genes, structures, and processes resulting in the species-specific differences in exine patterning found across the plant world are far from being understood. It has been shown the components necessary for proper exine patterning are in place by the end of meiosis (Dickinson & Sheldon, 1986; Sheldon & Dickinson, 1968, 1983) and many of the structures involved in pollen wall development have been described previously (Heslop-Harrison, 1971b; Owen & Makaroff, 1995; Paxon-Sowders, Owen, & Makaroff, 1997).

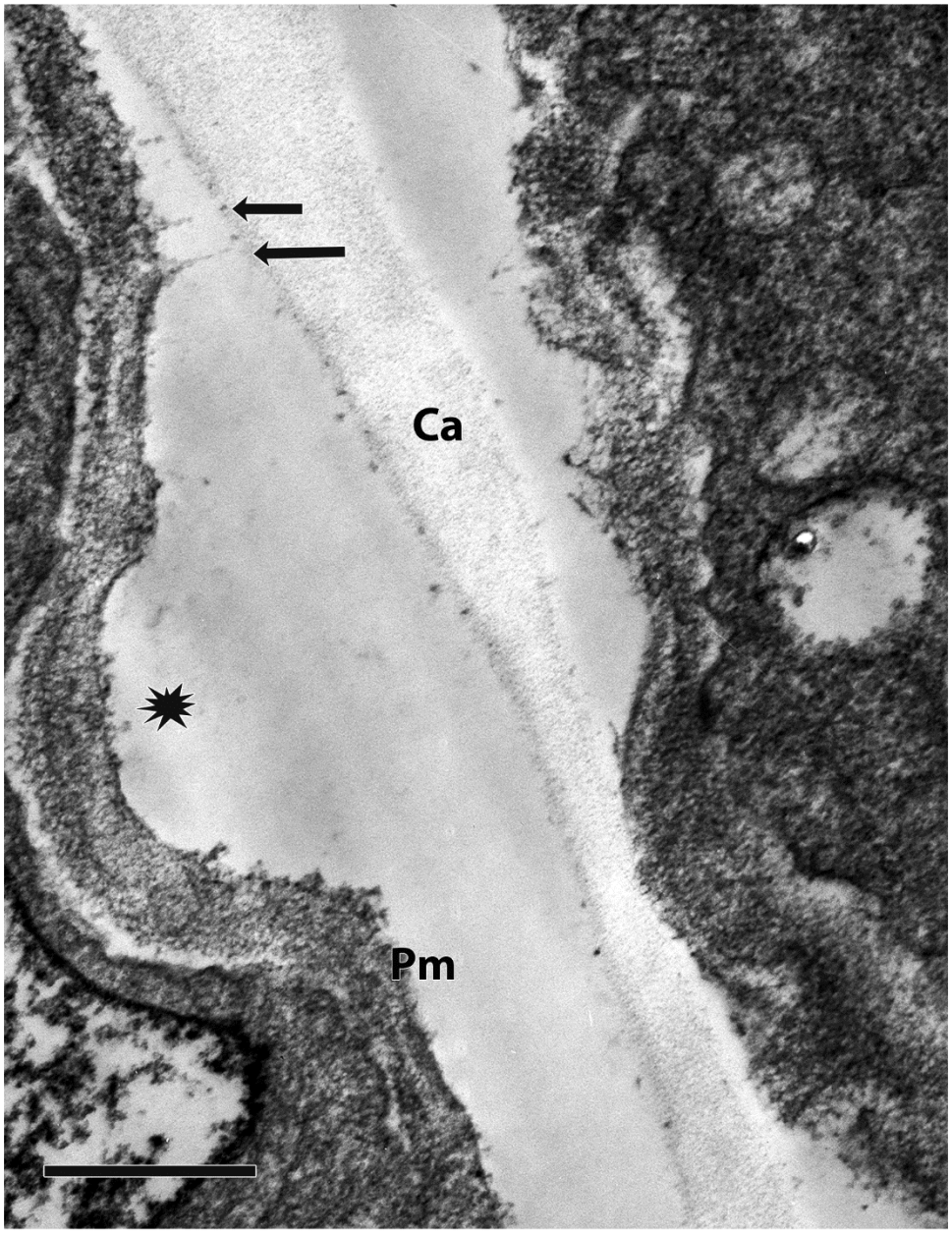

Fig. 26 Transmission electron micrograph of cross- section thru anther of mutant line 6491 *A. thaliana* grown at 16^{o} C during tetrad stage. Undulations in the plasma membrane (Pm) are filled with material of different electron density than surrounding areas (asterisk). Peaks of fibrillar electron dense material (arrows) are between the callose wall (Ca) and plasma membrane. Bar = 0.5 µm.

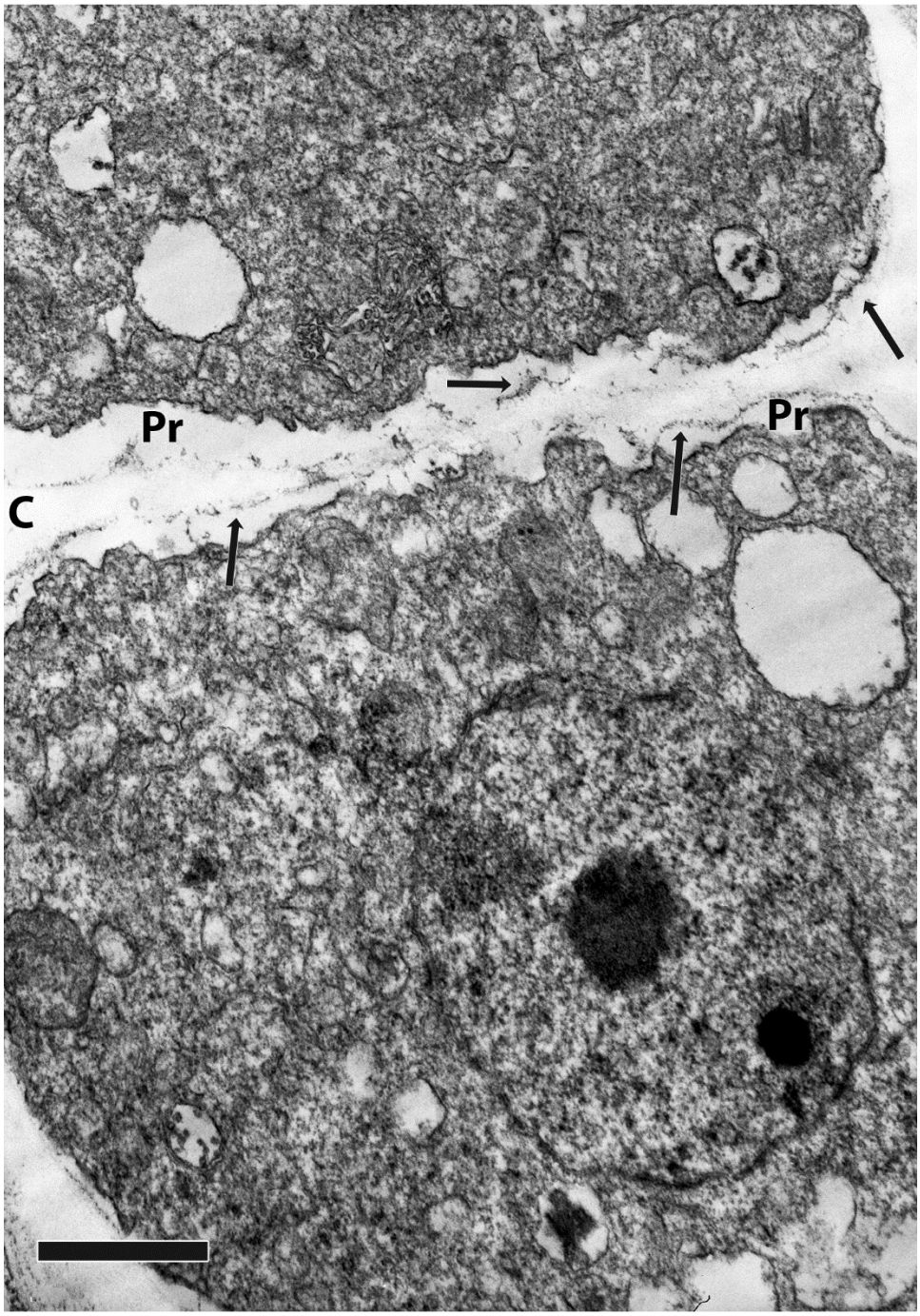

Fig. 27 Transmission electron micrograph of cross- section thru anther of mutant line 6491 *A. thaliana* grown at 16^{o} C during tetrad stage. Deposits of electron dense material (arrows) are noted at callose wall edge. A slightly electron-dense layer (Pr) has formed between the callose and plasma membrane. Bar = 1 µm.

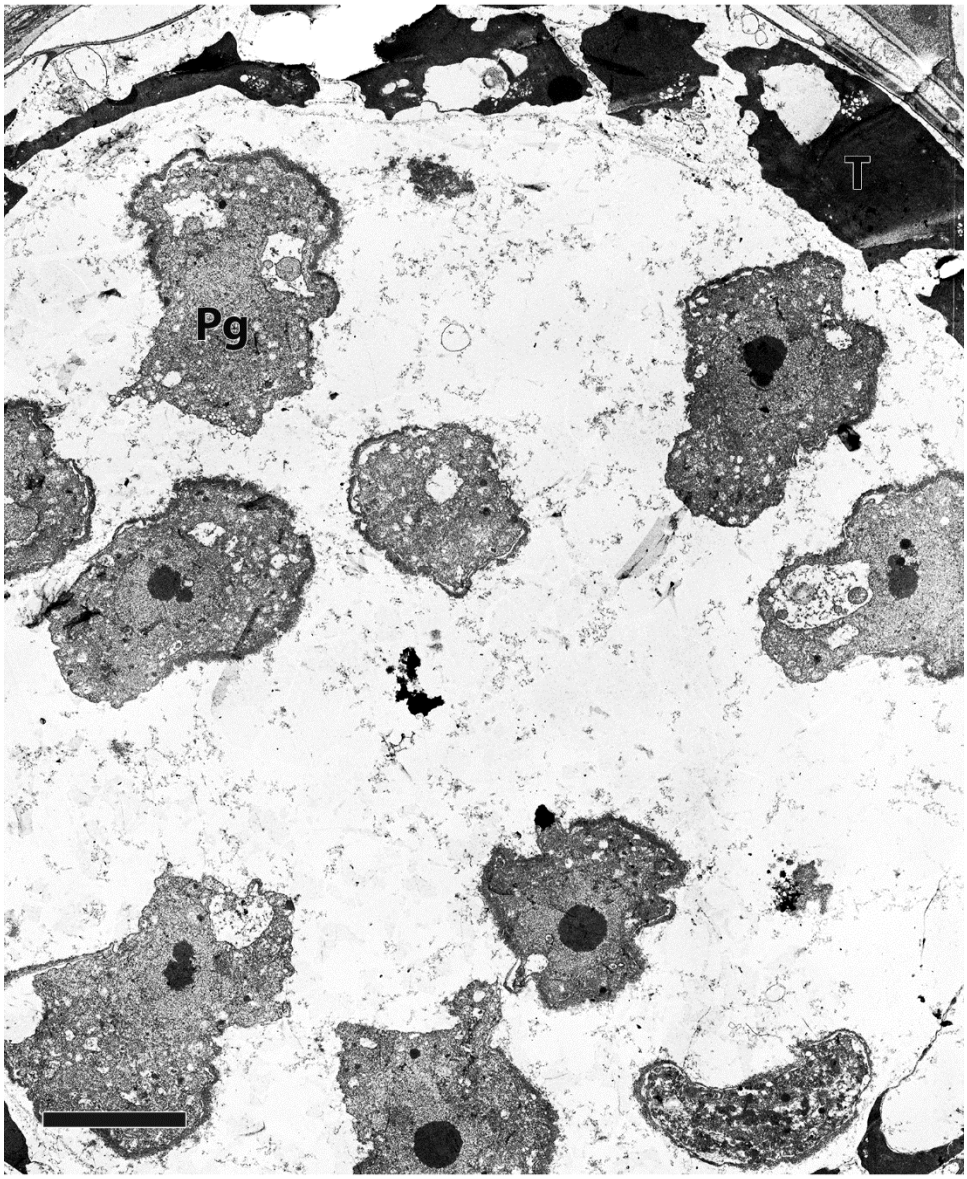

Fig. 28 Transmission electron micrograph of cross- section thru anther of mutant line 6491 *A. thaliana* grown at 16º C during released microspore stage. The tapetum (T) is disintegrating. Fibrillar material is present within the anther locule. Developing pollen grains (Pg) are misshapen. Bar = 1 µm.

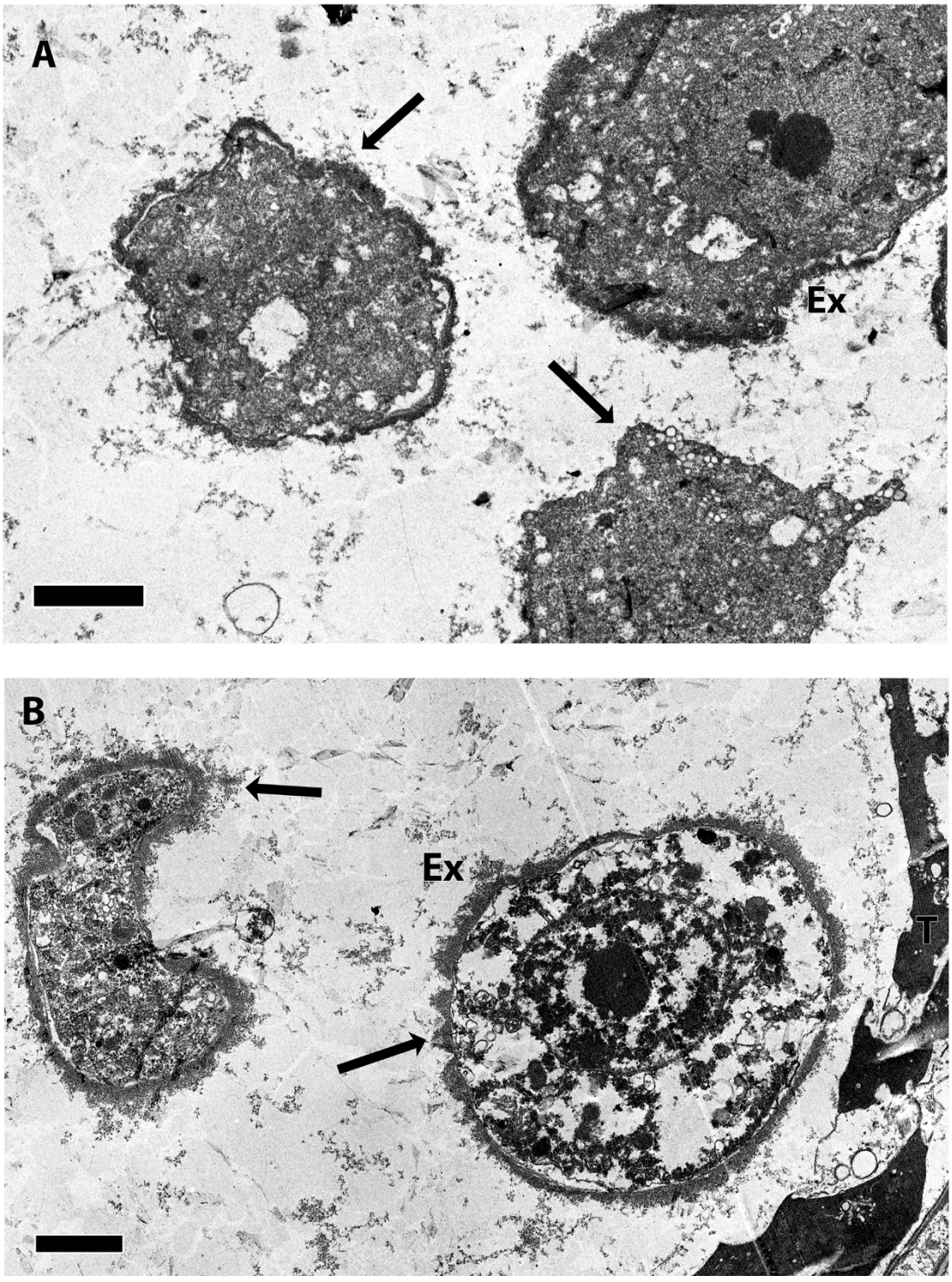

Fig. 29 Transmission electron micrographs of cross- section thru anther of mutant line 6491 *A. thaliana* grown at 16º C during late development. **A** Electron-dense material within anther locule appears to be accumulating on the exine surface of released microspores (arrows). **B** Areas of possible reticulate pattern are developing on some pollen grain surfaces (arrows). The tapetum (T) remains as fragments within the locule. Bar = 1 µm.

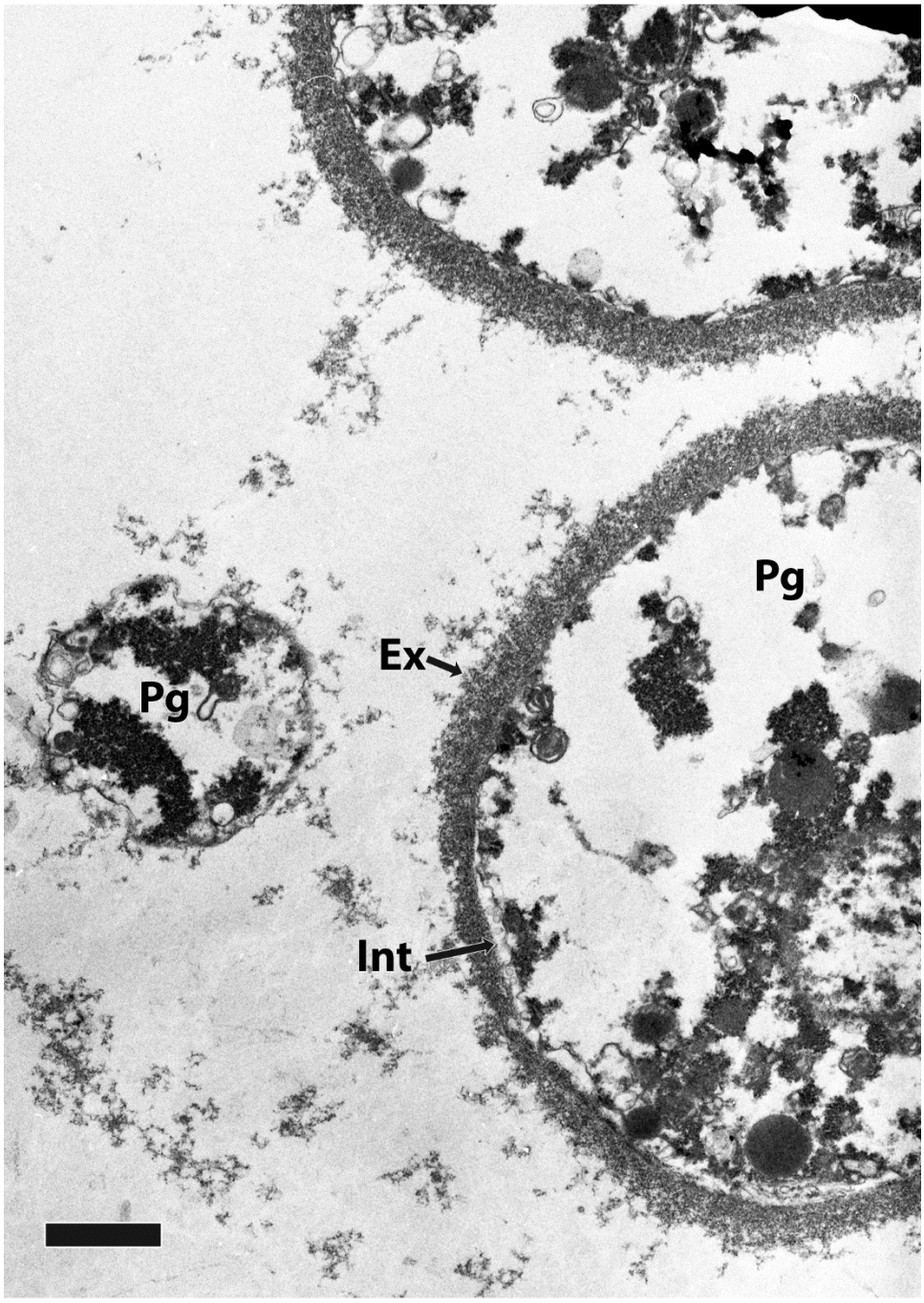

Fig. 30 Transmission electron micrograph of cross- section thru anther of mutant line 6491 *A. thaliana* grown at 16º C. Mature pollen grains (Pg) have an exine (Ex) which lacks pattern and an intine (Int) that is thin or not visible. Few well-formed cellular structures are apparent. Bar = 1 µm.

consideration, the lowest temperature of the three studied was chosen, with the expectation that the fewest and least severe structural changes should be evident in the temperature-sensitive 6491 line in comparison to WT. At a growing temperature of 16^{o} C, 6491 appears normal, rather than reduced-fertile or sterile as demonstrated at higher temperatures.

In many meiotic mutants, the blueprint is there, but the tools necessary to carry out the plans may be missing or dysfunctional. In studying the mutant 6491 and WT *Arabidopsis*, as well as the effect changes in temperature have upon both lines, I am inclined to think the mutated 6491 gene is involved with one of the primary tools in wall development, the delivery system of callose.

The differences between WT and 6491 are first evident in premeiosis II (Figs. 13 B and 22 B). There is a distinct difference in degree of separation between microsporocytes of WT and 6491. This separation is due in part to the deposition of callose, as confirmed by aniline blue fluorescence. Callose in 6491 is thin until meiosis, resulting in less of a separation. As development continues, the callose wall in 6491 appears more uneven in thickness than WT. As noted previously in Chapter 2, several problems can arise with the incorrect distribution or degradation of callose. One of the most visible of these problems is improper exine formation, such as found in 6491(Fig. 28). In examining the callose issue, one must also consider the cytoskeleton that is responsible for translocation of the callose components, primarily callose synthases. It is my belief that at least some of the phenotype changes apparent in 6491 arise from disruption of this cytoskeleton machinery.

The *GLUCAN SYNTHASE-LIKE* protein family has been widely studied as callose synthases. In particular, callose synthases encoded by *GSL1, 2, 5, 8,* and *10* are found during callose synthesis in pollen formation (Enns et al., 2005; Richmond & Somerville, 2000; Toller,

Brownfield, Neu, Twell, & Schulze-Lefert, 2008). All of these are found localized to the microsporocyte and microspore plasma membrane. GSL2 is also localized to Golgi-related endomembranes (Dong et al., 2005). GSL2 and 5 have been found in vesicles through the use of immunolocalization (Drakakaki et al., 2012). Vesicles shown in WT (Fig. 15) appear to be traveling from the microsporocyte plasma membrane to the layer of callose. Golgi bodies (Fig. 15) are found under the plasma membrane, fitting in with the current model of translocation of callose synthase. Callose has not been found in golgi bodies nor associated vesicles during callose wall formation, but is positively identified thru both aniline blue fluorescence (Chapter 2) and immunolabeling in the final callose wall (Otegui & Staehelin, 2004). Callose synthases such as GSL2 and GSL 5 are found in vesicles, then activated by calcium signal at the forming callose wall (Verma & Hong, 2001). Experiments that have used calcium chelators show an inhibition of callose formation (Aidemark, Andersson, Rasmussen, & Widell, 2009).

In tobacco pollen tubes, callose synthases are synthesized and processed in endoplasmic reticulum. The enzymes then integrate into golgi bodies and travel along tubulin and actin filaments to the pollen tube (Cai et al., 2011). Endoplasmic reticulum (Fig. 14 A) is found throughout WT and 6491 samples, at all stages in early development. In many cases endoplasmic reticulum is in close proximity to the nuclear envelope, perhaps beginning the process of callose synthase biosynthesis. Immunolabeling for callose synthase may help clarify as to whether or not the translocation of callose synthase is indeed occurring within this part of the endoplasmic reticulum-golgi body pathway in both WT and 6491.

Several structural changes found in meiotic mutants are similar to those resulting from disruption of the cytoskeleton. These changes from WT include imperfectly separated microspores (Figs. 24 A and B), alterations in the expected exine pattern (Figs. 24 C and 29) and

misplaced apertures (Fig. 4 B) (Dickinson & Sheldon, 1986; Heslop-Harrison, 1971b; Sheldon & Dickinson, 1983). All of these structural changes are also associated with improper formation of the callose wall.

The effects of alterations in callose deposition in 6491, when compared to WT, were shown in the continued development of the pollen wall. As the microsporocytes/microspores transitioned from cytokinesis through tetrad stage the rest of the components of the pollen wall were developed. Figures 17 (WT) and 25 (6491) show the differences in primexine deposition and plasma membrane undulations. Undulations are irregular in spacing and depth in the plasma membrane of 6491, as are deposits of primexine (Fig. 25).

In late cytokinesis the plasma membrane should be held tight to the callose wall, as primexine is deposited in regular intervals. More primexine is deposited as undulations are formed in the membrane, with the thickest primexine found within the “valley” portion of the waves. (Fig. 26). It is at peak portions of the membrane undulations where sporopollenin should be deposited. An electron dense material thought to be sporopollenin is shown first gathering at the plasma membrane, then traversing the primexine layer until it stops at the interface between callose and primexine (Figs. 26 and 27). In WT, sporopollenin continues to accumulate at the peak portions only, forming the probacula of the exine wall (Fig. 18). In 6491 this accumulation is irregular, with little pattern appearing as sporopollenin continues to be added. One would assume the sporopollenin comes back from the inner periphery of the callose layer then binds to the growing probacula, but that is not evident when examining the images. It is not possible to state conclusively that the sporopollenin does not gather at the callose periphery and the probacula are somehow pushed up to attach to the accumulated sporopollenin. This seems unlikely, but is a possible scenario.

At the end of the tetrad stage, the callose layer is dissolved, releasing microspores into the locule of the anther. Additional sporopollenin from the tapetum should be added to the probacula as the intine and nexine layers develop. The fibrillar electron dense material found throughout the locule may be sporopollenin released from the disintegrating tapetum. Sporopollenin continues to accumulate on the surface of some of the grains, adding to the exine layer. The appearance of the exine is variable from grain to grain, some having a smooth surface, while others exhibit a bit of pattern. This would coincide with the smooth surface noted when 6491 pollen grains are visualized with SEM (Fig. 4B).

In WT, the intine is secreted by the microspores (Huang et al., 2009) and has 2 distinct layers, the endintine and exintine (Fig. 19). Vesicles from the microspore cytoplasm clearly visible at the edge of the endintine support this manner of secretion. This build-up of intine would normally occur after the bulk of the exine was developed. Both the endintine and exintine in 6491 appear different from WT, to a point where it is mostly indistinguishable (Fig. 30) from the exine layer. Pollencoat accumulates on the surface of the pollen grain (Figs. 19 and 20). Elaioplasts and tapetosomes from the tapetum (Wu et al., 1997) are released into the anther locules. The remnants of the tapetum attach to the spaces within the bacula and, in conjunction with pollencoat already present, becomes the tryphine of the pollen wall. Electron-lucent structures appear within the tryphine of WT, but the function and composition of these structures is unknown.

What is responsible for the interaction between plasma membrane, primexine and callose wall that results in first the undulations, then the anchoring and accumulation of sporopollenin has not been determined. The cytoskeleton most likely facilitates the undulations within the plasma membrane, but the numerous proteins, structures and pathways resulting in the exine are not yet

understood. It has been shown that the callose wall may play a part in the final patterning found on a mature pollen grain. The callose wall is deposited beginning in late premeiosis, lending credence to the idea that components necessary for exine pattern are in place prior to meiosis. At this point, I think the 6491 callose is either not being delivered or deposited properly. In addition, the callose may not have the same composition in 6491 as in WT.

In chapter 2 of this body of work, I examined the changes that occurred within an acceptable growth temperature range of WT and 6491. Cytoskeleton components are affected by both cold and heat stress (De Storme, Copenhaver, & Geelen, 2012; De Storme & Geelen, 2014; Mamun, Alfred, Cantrill, Overall, & Sutton, 2006; Sharma & Nayyar, 2016; Thakur, Kumar, Malik, Berger, & Nayyar, 2010), which could explain the morphological differences not only in 6491, but also the lesser differences in WT. Given that 6491 is much more affected by a range of temperature changes and becomes sterile as growth temperature increases, the delivery system of callose should be examined in more detail in 6491.

References

Aidemark, M., Andersson, C., Rasmussen, A., & Widell, S. (2009). Regulation of callose synthase activity in situ in alamethicin-permeabilized Arabidopsis and tobacco suspension cells. *BMC Plant Biology, 9*(27), 1-13.

Albert, B., Ressayre, A., & Nadot, S. (2011). Correlation between pollen aperture pattern and callose deposition in late tetrad stage in three species producing atypical pollen grains. *American Journal of Botany, 98*, 189-196.

Ariizumi, T., Hatakeyama, K., Hinata, K., Inatsugi, R., Nishida, I. S., Shusei, & Kato, T. (2004). Disruption of the novel plant protein NDF1 affects lipid accumulation in the plastids of the tapetum and exine formation of pollen, resulting in male sterility in *Arabidopsis thaliana*. *The Plant Journal, 39*, 170-181.

Ariizumi, T., Kawanabe, T., Hatakeyama, K., Sato, S., Kato, N., Tabata, S., & Toriyama, K. (2008). Ultrastructural characterization of exine development of the *transient defective exine 1* mutant suggests the existence of a factor involved in constructing reticulate exine architecture from sporopollenin aggregates. *Plant and Cell Physiology, 49*, 58-67.

Cai, G., Faleri, C., Del Casino, C., Emons, A., & Cresti, M. (2011). Distribution of callose synthase, cellulose synthase, and sucrose synthase in tobacco pollen tube is controlled in dissimilar ways by actin filaments and microtubules. *Plant Physiology, 155*, 1169-1190.

Chen, X.-Y., Liu, L., Lee, E., Han, X., Rim, Y., Chu, H., Kim, S.-W., Sack, F., & Kim, J.-Y. (2009). The Arabidopsis callose synthase gene *GSL8* is required for cytokinesis and cell patterning. *Plant Physiology, 150*, 105-112.

De Storme, N., Copenhaver, G. P., & Geelen, D. (2012). Production of diploid male gametes in Arabidopsis by cold-induced destabilization of postmeiotic radial microtubule arrays. *Plant Physiology, 160*, 1808-1826.

De Storme, N., & Geelen, D. (2014). The impact of environmental stress on male reproductive development in plants: biological processes and molecular mechanisms. *Plant Cell Environ, 37*(1), 1-18.

Dickinson, H. G., & Sheldon, J. M. (1986). The generation of patterning at the plasma membrane of the young microspore of *Lilium Pollen and Spores: Form and Function* (pp. 1-17). London: Academic Press.

Dong, X., Hong, Z., Sivaramakrishnan, M., Mahfouz, M., & Verma, D. P. S. (2005). Callose synthase (CalS5) is required for exine formation during microgametogenesis and for pollen viability in Arabidopsis. *The Plant Journal, 42*, 315-328.

Drakakaki, G., van de Ven, W., Pan, S., Miao, Y., Wang, J., Keinath, N. F., Weatherly, B., Jiang, L., Schumacher, K., Hicks, G., & Raikhel, N. V. (2012). Isolation and proteomic analysis of the SYP61 compartment reveal its role in exocytic trafficking in Arabidopsis. *Cell Research, 22*, 413-424.

Ellis, E. A. (2006). Solutions to the problem of substitution of ERL 4221 for vinyl cyclohexene dioxide in Spurr low viscosiy embedding formulations. *Microscopy Today, 14*, 32-33.

Enns, L. C., Kanaoka, M. M., Torii, K. U., Comai, L., Okada, K., & Cleland, R. E. (2005). Two callose synthases, GSL1 and GSL5, play an essential and redundant role in plant and pollen development and in fertility. *Plant Molecular Biology, 58*, 333-349.

Feldmann, K. A., & Marks, M. D. (1987). *Agrobacterium*-mediated transformation of germinating seeds of *Arabidopsis thaliana*: A non-tissue culture approach. *Molecular and General Genetics, 208*, 1-9.

Guan, Y.-F., Huang, X.-Y., Zhu, J., Gao, J.-F., Zhang, H.-X., & Yang, Z.-N. (2008). *RUPTURED POLLEN GRAIN1*, a member of the MtN3/saliva gene family, is crucial for exine pattern formation and cell integrity of microspores in Arabidopsis. *Plant Physiology, 147*, 852-863.

Heslop-Harrison, J. (1963). An ultrastructural study of pollen wall ontogeny in *Silene pendula*. *Grana Palynologica, 4*, 7-24.

Heslop-Harrison, J. (1963). An ultrastuctural study of pollen wall ontogeny in Silene pendula. *Grana Palynol, 4*, 1-24.

Heslop-Harrison, J. (1966). Cytoplasmic continuities during spore formation in flowering plants. *Endeavour, 25*, 65-72.

Heslop-Harrison, J. (1968). Pollen wall development. *Science, 161*, 230-237.

Heslop-Harrison, J. (1971a). The pollen wall: Structure and development. In J. Heslop-Harrison (Ed.), *Pollen: Development and Physiology* (pp. 75-98). London: Butterworths.

Heslop-Harrison, J. (1971b). Wall pattern formation in angiosperm microsporogenesis. *Society for Experimental Biology Symposium, 25*, 277-300.

Holdorf, M. M., Owen, H. A., Lieber, S. R., Yuan, L., Adams, N., Dabney-Smith, C., & Makaroff, C. A. (2012). Arabidopsis ETHE1 encodes a sulfur dioxygenase that is essential for embryo and endosperm development. *Plant Physiol, 160*(1), 226-236.

Hong, Z., Delauney, A. J., & Verma, D. P. S. (2001). A cell plate-specific callose synthase and its interaction with phragmoplastin. *The Plant Cell, 13*, 755-768.

Hu, J., Wang, Z., Zhang, L., & Sun, M. X. (2014). The Arabidopsis Exine Formation Defect (EFD) gene is required for primexine patterning and is critical for pollen fertility. *New Phytol, 203*(1), 140-154.

Huang, L., Cao, J., Zhang, A., Ye, Y., Zhang, Y., & Liu, T. (2009). The polygalacturonase gene BcMF2 from Brassica campestris is associated with intine development. *J Exp Bot, 60*(1), 301-313.

Lu, P., Chai, M., Yang, J., Ning, G., Wang, G., & Ma, H. (2014). The Arabidopsis *CALLOSE DEFECTIVE MICROSPORE1* gene is required for male fertility through regulating callose metabolism duing microsporogenesis. *Plant Physiology, 164*, 1893-1904.

Mamun, E. A., Alfred, S., Cantrill, L. C., Overall, R. L., & Sutton, B. G. (2006). Effects of chilling on male gametophyte development in rice. *Cell Biology International, 30*, 583-591.

Nishikawa, S.-i., Zinkl, G. M., Swanson, R. J., Maruyama, D., & Preuss, D. (2005). Callose (b-1,3 glucan) is essential for *Arabidopsis* pollen wall patterning, but not tube growth. *BMC Plant Biology, 5*, 22.

Otegui, M. S., & Staehelin, L. A. (2004). Electron tomographic analysis of post-meiotic cytokinesis during pollen development in *Arabidopsis thaliana*. *Planta, 218*, 501-515.

Owen, H. A., & Makaroff, C. A. (1995). Ultrastructure of microsporogenesis and microgametogenesis in *Arabidopsis thaliana* (L) *heynh* ecotype Wassilewskija (*Brassicaceae*). *Protoplasma, 185*, 7-21.

Paxon-Sowders, D. M., Dodrill, C. H., Owen, H. A., & Makaroff, C. A. (2001). DEX1, a novel plant protein, is required for exine pattern formation during pollen development in *Arabidopsis*. *Plant Physiology, 127*, 1739-1749.

Paxon-Sowders, D. M., Owen, H. A., & Makaroff, C. A. (1997). A comparative ultrastructural analysis of exine pattern development in wild-type *Arabidopsis* and a mutant defective in pattern formation. *Protoplasma, 198*, 53-65.

Paxson-Sowders, D. M., Dodrill, C. H., Owen, H. A., & Makaroff, C. A. (2001). DEX1, a Novel Plant Protein, Is Required for Exine Pattern Formation during Pollen Development in Arabidopsis. *Plant Physiology, 127*(4).

Peirson, B. N., Owen, H. A., Feldmann, K. A., & Makaroff, C. A. (1996). Characterization of three male-sterile mutants of *Arabidopsis thaliana* exhibiting alterations in meiosis. *Sexual Plant Reproduction, 9*, 1-16.

Richmond, T., & Somerville, C. (2000). The cellulose synthase superfamily. *Plant Physiology 124*, 495-498.

Sharma, K. D., & Nayyar, H. (2016). Regulatory networks in pollen development under cold stress. *Frontiers in Plant Science, 7*(402), 1-13.

Sheldon, J. M., & Dickinson, H. G. (1968). Pollen wall formation in Lilium: The effect of chaotropic agents, and the organisation of the microtubular cytoskeleton during pattern development. *Planta, 168*(1), 11-23.

Sheldon, J. M., & Dickinson, H. G. (1983). Determination of patterning in the pollen wall of *Lilium henryi*. *Journal of Cell Science, 63*, 191-208.

Thakur, P., Kumar, S., Malik, J. A., Berger, J. D., & Nayyar, H. (2010). Cold stress effects on reproductive development in grain crops: An overview. *Environmental and Experimental Botany, 67*(3), 429-443.

Toller, A., Brownfield, L., Neu, C., Twell, D., & Schulze-Lefert, P. (2008). Dual function of Arabidopsis glucan synthase-like genes GSL8 and GSL10 in male gametophyte development and plant growth. *Plant Journal, 54*(5), 911-923.

Verma, D. P. S., & Hong, Z. (2001). Plant callose synthase complexes. *Plant Molecular Biology, 47*, 693-701.

Wu, S. S. H., Platt, K. A., Ratnayake, C., Wang, T.-W., Ting, J. T. L., & Huang, A. H. C. (1997). Isolation and characteization of neutral-lipid-containing organelles and globuli-filled plastids from *Brassica napus* tapetum. *Proceedings of the National Academy of Sciences of the United States of America, 94*, 12711-12716.

Zhang, Z. B., Zhu, J., Gao, J. F., Wang, C., Li, H., Li, H., Zhang, H. Q., Zhang, S., Wang, D. M., Wang, Q. X., Huang, H., Xia, H. J., & Yang, Z. N. (2007). Transcription factor AtMYB103 is required for anther development by regulating tapetum development, callose dissolution and exine formation in Arabidopsis. *Plant J, 52*(3), 528-538.

Chapter IV

Developmental Study of Interaperture Pollen Tube Breakout

A. Introduction

Pollen grain development takes place in the male portion of the plant called the anther. The anther and filament together comprise the stamen of the flower. The primary female structures involved in plant reproduction are the ovary, style and stigma, collectively known as the gynoecium (or pistil). After dehiscence, pollen grains are released from the anther and transported to the stigma via biotic and abiotic vectors. The *Arabidopsis* stigma contains approximately 150 elongated epidermal cells, specialized for recognition of compatible pollen grains (Sessions & Zambryski, 1995). Upon contact a series of interactions occur between the desiccated pollen grain and stigma with the pollen-stigma interface physically changing and becoming stronger as pollination continues. The initial contact and binding is thought to be exine-mediated, possibly of a chemical basis involving polymers in the exine (Edlund, Swanson, & Preuss, 2004). The process has not yet been fully studied and remains an unknown in the pollination pathway. What is known is that the compatibility response is different depending upon whether the stigma is of the dry or wet type. A wet stigma is covered in a layer of secretions containing carbohydrates and lipids (Zinkl, Zwiebel, Grier, & Preuss, 1999). Any pollen grain landing on the stigma has the ability to be hydrated. The compatibility response is initiated later in development rather than at the point of contact. In a dry stigma such as that of *Arabidopsis*, at the point of adhesion between the pollen grain and stigma, the pollen coat mobilizes from its original place between the tectum and bacula of the grain to form a "foot layer" between the two structures (Edlund et al., 2004). Other components such as water and

nutrients pass from the papillae through the pollen coat to contact the grain and contribute to the formation of the foot layer.

The point of adhesion is where the pollen tube germinates and either comes through the aperture or breaks through the exine, then travels down the stigma. Pollen tubes of many species will exit only through the thinned areas of the pollen wall, where the exine is absent. However, recent studies have shown that pollen tubes in *Arabidopsis* will breakout through inter-aperture spaces in some ecotypes, despite the presence of the thick sporopollenin in these patterned regions (Edlund et al., 2004; Edlund, Zheng, et al., 2016; Hoedemaekers, Derksen, Hoogstrate, Wolters-Arts, Oh, Twell, et al., 2015). In *Arabidopsis thaliana* Landsberg *erecta* accession, the breakout point seems to be determined by the most direct route to the point of adhesion in the ecotypes in which interaperturate breakout occurs. In order for the pollen tube to exit the pollen grain, the pollen wall must be weakened, a force or pressure must be present to push out through the wall, or a combination of the two must be present. While the pollen tube is breaking out, a pectin bulge forms underneath the point of adhesion to the stigma (Edlund, Zheng, et al., 2016). The pollen tube elongates and grows between the cell walls of the papillar cells of the stigma into the style. The two sperm travel down the tube until they reach the ovule, where one sperm fertilizes the egg and the other fuses with the 2N central cell nucleus to become the 3N endosperm. The inter-aperture breakout mechanism has now been found in *Arabidopsis thaliana* along with eight other members in the Brassicaceae family (Edlund, Zheng, et al., 2016). It is the goal of this project to lend supporting structural evidence to this mechanism of pollen tube germination and supplement the current knowledge base surrounding changes taking place in the pollen grain wall during the germination process. To avoid the need to emasculate flowers prior to pollination, the female parent chosen for the experiments was *ms-1*, a male-sterile line that

seldom produces mature pollen (Wilson, Morrol, Dawson, Swarup, & Tighe, 2001). The male parent was wild type. Both were in the Landsberg erecta background, which exhibits a frequent inter-aperturate pollen tube breakout.

B. Materials and Methods

Plant Growth

Arabidopsis thaliana ecotype Landsberg *erecta* (Ler) wild type plants and male sterile-1 (MS-1) mutant plants in the same background were used in this work. Seeds were grown on damp commercial potting mix in a growth chamber at 20℃ with a 16/8 light and dark cycle.

Specimen preparation for microscopy

WT pollen grains were manually pollinated onto the stigmas of *ms-1* flowers. Time periods of 8 to 12 minutes, 12 to 15 minutes, and 15 to 20 minutes were allowed to pass. The range of time indicates the longest and shortest times when pollen was on the stigma prior to having the flower placed in fixative. At the end of each specific waiting period, the pollinated flowers were removed from the plant and put into fixative (2.5% glutaraldehyde v/v, 0.02% Triton X-100 v/v, 0.1 M HEPES, pH7.2) for overnight fixation at room temperature. After rinsing twice in 0.1M HEPES pH7.2, the tissues were post-fixed in 1% OsO_4 w/v overnight. The flowers were then rinsed in water twice, followed by overnight fixation in 1% uranyl acetate. Tissue was dehydrated with 10% increments of acetone and infiltrated in modified Spurr's resin, as previously described. The stigma end of the gynoecium was removed from each individual resin-infiltrated flower and placed into a cavity of a silicon rubber flat embedding mold containing 100% modified Spurr's resin. The tissue was oriented so that the long axis of the gynoecium lay at the bottom of each cavity parallel to the truncated end of the mold. The filled molds were placed into a 60^{o} C oven and polymerized for 48 hours.

Sample preparation for semi-thin sections

Semi-thin sections (0.5 µm) were cut with a diamond knife on an RMC MT 7000 ultramicrotome and heat-fixed to microscope slides. Visualization of callose was completed on sections from which plastic had been removed with sodium methoxide (Fulcher, McCully, Setterfield, & Sutherland, 1976) followed by mounting in 0.05% (w/v) aniline blue in phosphate buffer (Smith & McCully, 1978).

All slides of semi-thin sections for callose visualization were examined with a Nikon 80i light microscope equipped with differential interference contrast and epifluorescence illumination with a Nikon UV-2E/C filter set (excitation filter 325-375, dichroic 400 LP, emitter 435-485) for callose imaging. Images were captured with a QImaging Retiga 2000-R digital camera using Q Capture Pro V.5.1 software.

Sample preparation for transmission electron microscopy

Ultrathin (silver to pale gold) sections were cut with a diamond knife on a RMC MT 7000 ultramicrotome and picked up on 200 mesh copper grids. Sections were stained with 1% aqueous uranyl acetate followed by Reynold's lead citrate, then imaged with a Hitachi H-600 transmission electron microscope operating at 75kv. Images were captured on Kodak 4489 electron microscope film. Following development, digital images were acquired by scanning the film with an Agfa V750 Pro flatbed scanner in transmitted light mode.

C. Results

In order to find the contact point between pollen grain and stigma, semi-thin sections from multiple pollinated flowers were first cut from blocks stained with azure blue. Once the contact point was found, ultrathin sections were taken from the same block for TEM. Within a single time point, multiple developmental stages were encountered. Results are arranged and

described in temporal and developmental sequence.

Pre-adhesion

Arabidopsis thaliana pollen is tri-aperturate (Fig. 31). Apertures are areas where exine has not developed as in the rest of the grain. The exine is an electron dense layer composed of bacula (radially organized) and tectum (transversely organized). Tryphine is found throughout the exine, between the bacula and covering most of the pollen grain surface. Deep to the exine is the bi-layered, electron lucent intine. The vegetative cell composes most of the entirety of the cell and contains several osmiophilic bodies spherical in shape. The cytoplasm of the pollen grain appears highly vacuolated with no apparent organization to the visible cellular structures. Sperm cells may be seen at this stage, but it is dependent upon the plane of section through the grain. The intine (Fig. 32 A) is composed of a thin layer of exintine with slightly electron dense inclusions. Deep to the exintine is endintine, which appears proportionally thicker to the exintine and contains some type of fibrillar material. The endintine lies adjacent to the plasma membrane of the pollen grain. Within the tryphine are white crystalline structures and thin fibrillar strands electron opaque in appearance.

Early adhesion

In the earliest stages of adhesion of grain to stigma, several changes occur in the appearance of the plasma membrane and intine. The intine is still held tight to the plasma membrane, but vacuolated areas containing multivesicular bodies (MVBs) appear to open or empty into the endintine (Fig. 32 B). The endintine continues to alter in appearance, having areas along its adjacent surface to the plasma membrane which travel deeper into the cytoplasm, forming what appear as pockets containing electron dense material (Fig. 32 C). Golgi bodies with numerous vesicles budding and endoplasmic reticulum appear in higher concentration close to the plasma

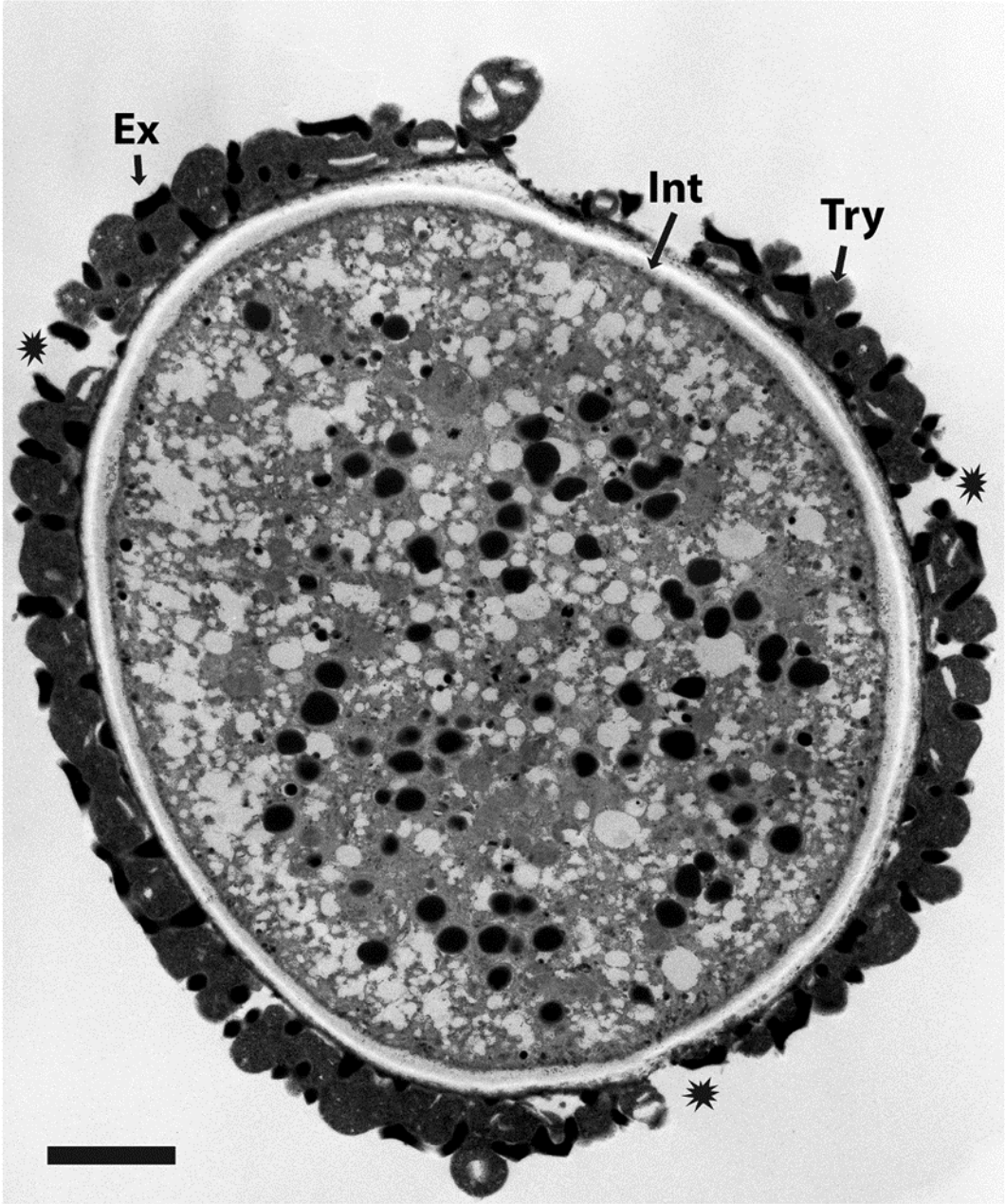

Fig. 31 Pollen grain prior to germination. Three apertures are present and also indicated are the three main cell wall components. Aperture (asterisk), Try (tryphine), Ex (exine), Int (intine). Bar = 2 µm

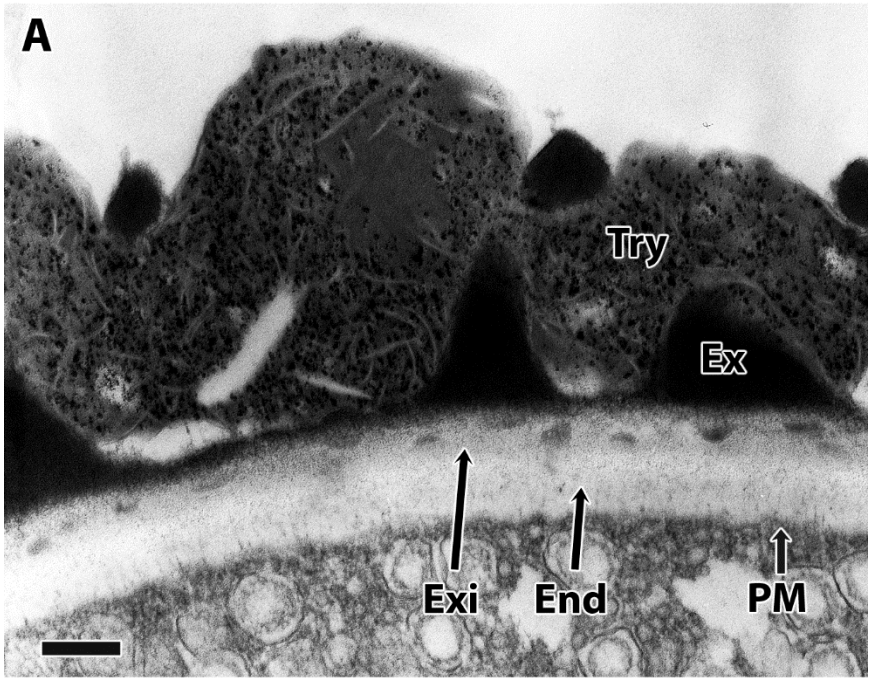

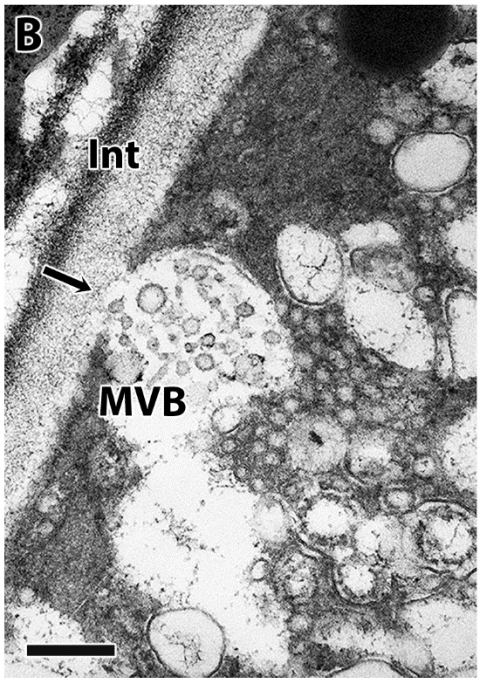

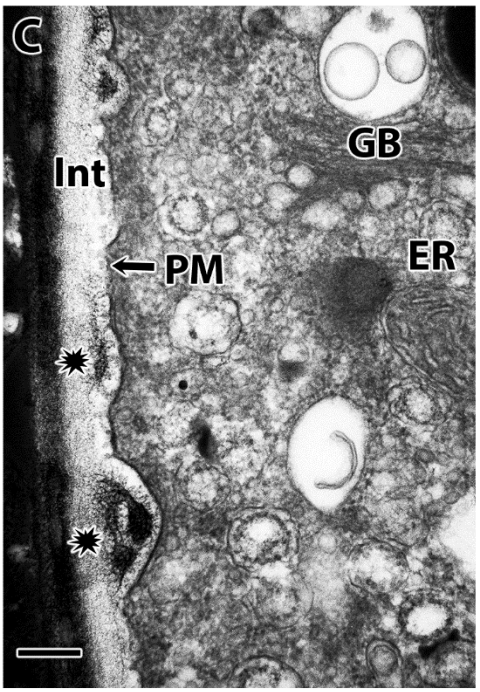

Fig. 32 A Pollen grain wall prior to germination showing bilayered intine. **B, C** Pollen grain wall 8-12 minutes post pollination, early adhesion stage with changes occurring in plasma membrane and intine. Try (tryphine), Ex (exine), Int (intine), Exi (exintine), End (endintine), MVB (multivesicular body), PM (plasma membrane), GB (golgi body), ER (endoplasmic reticulum). Bar = 200 nm

membrane by the point of adhesion.

After initial adhesion to the stigma surface, tryphine mobilizes toward the area of contact between grain and stigma (Fig. 33), forming a foot layer (Elleman & Dickinson, 1986). More undulations are noted in the endintine and some structural reorganization appears within the cytoplasm, most notably an area of small spherical bodies just deep to the plasma membrane in the vicinity of the contact point. As adhesion of grain to stigma proceeds (Figs. 34 A, B), the intine appears to thicken or the plasma membrane is retracting, leaving a broadening electron lucent layer with undulations more numerous toward the point of contact. Cytoplasmic reorganization is evident, as large areas of clearing are noted by the contact point. Fewer small osmiophilic bodies are apparent, although they may be coalescing into larger bodies. Tryphine continues to mobilize, increasing the foot layer.

Mid-adhesion

A widening electron lucent area or "plaque" forms directly under the point of contact (Fig. 35 A), with notable cytoplasmic clearing deep to the plaque. The foot now spreads and contacts both stigma surface and pollen grain (Fig. 35 B, C). What appear to be small vesicles are forming along the interface of plasma membrane and endintine.

As germination proceeds, the pollen grain takes on a more oblong appearance, with distortion in the shape toward the stigma (Fig. 36 A). Undulations in the intine appear to expand distally from the plaque. A polar reorganization of cytoplasmic material becomes more evident than in earlier stages.

Early pollen tube

In Figure 36 B the first notable extension of cytoplasmic material, plaque and pollen grain wall toward the stigma is evident. Portions of exine and foot layer are no longer visible by the

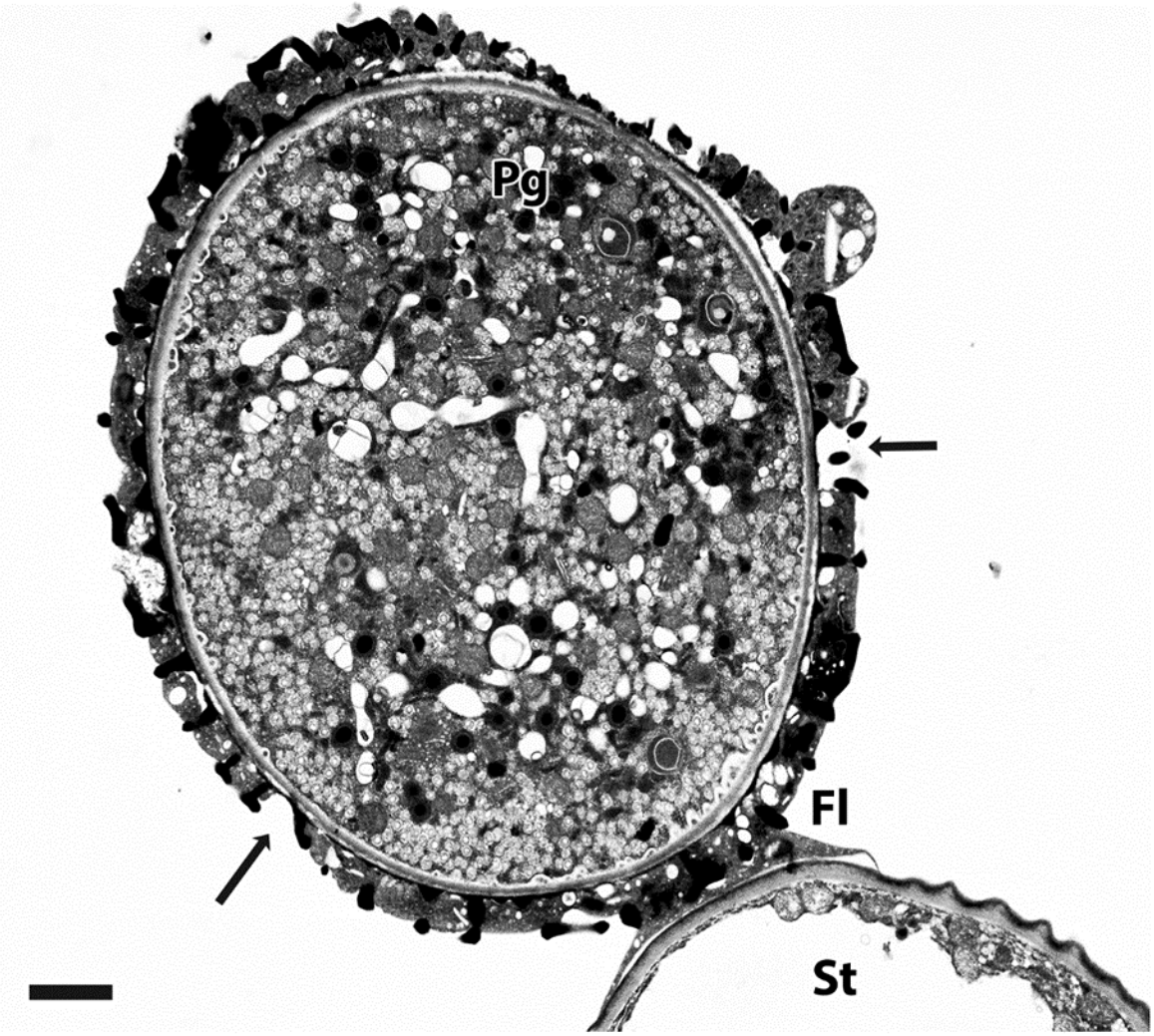

Fig. 33 Pollen grain and stigma early adhesion. A foot layer is visible at contact point between grain and stigma. Aperture (arrow), Pg (pollen grain), Fl (foot layer), St (stigma). Bar = 2 µm

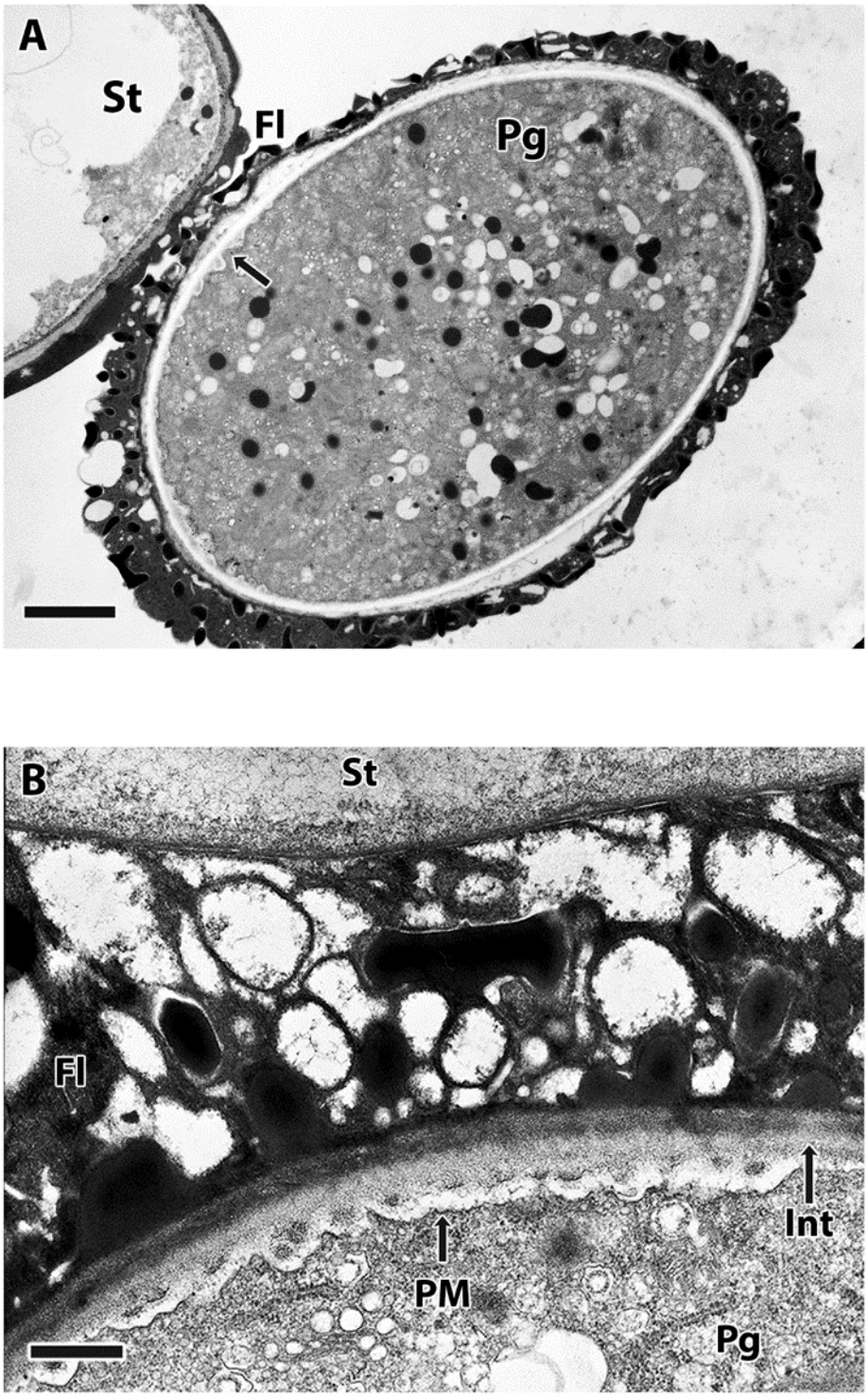

Fig. 34 A Pollen grain and stigma 8-12 minutes post-pollination. A foot layer is visible at contact point between grain and stigma. Bar = 2 µm. **B** Close-up of foot layer. Bar = 0.5 µm. Plasma membrane changes (arrow), Pg (pollen grain), Fl (foot layer), St (stigma).

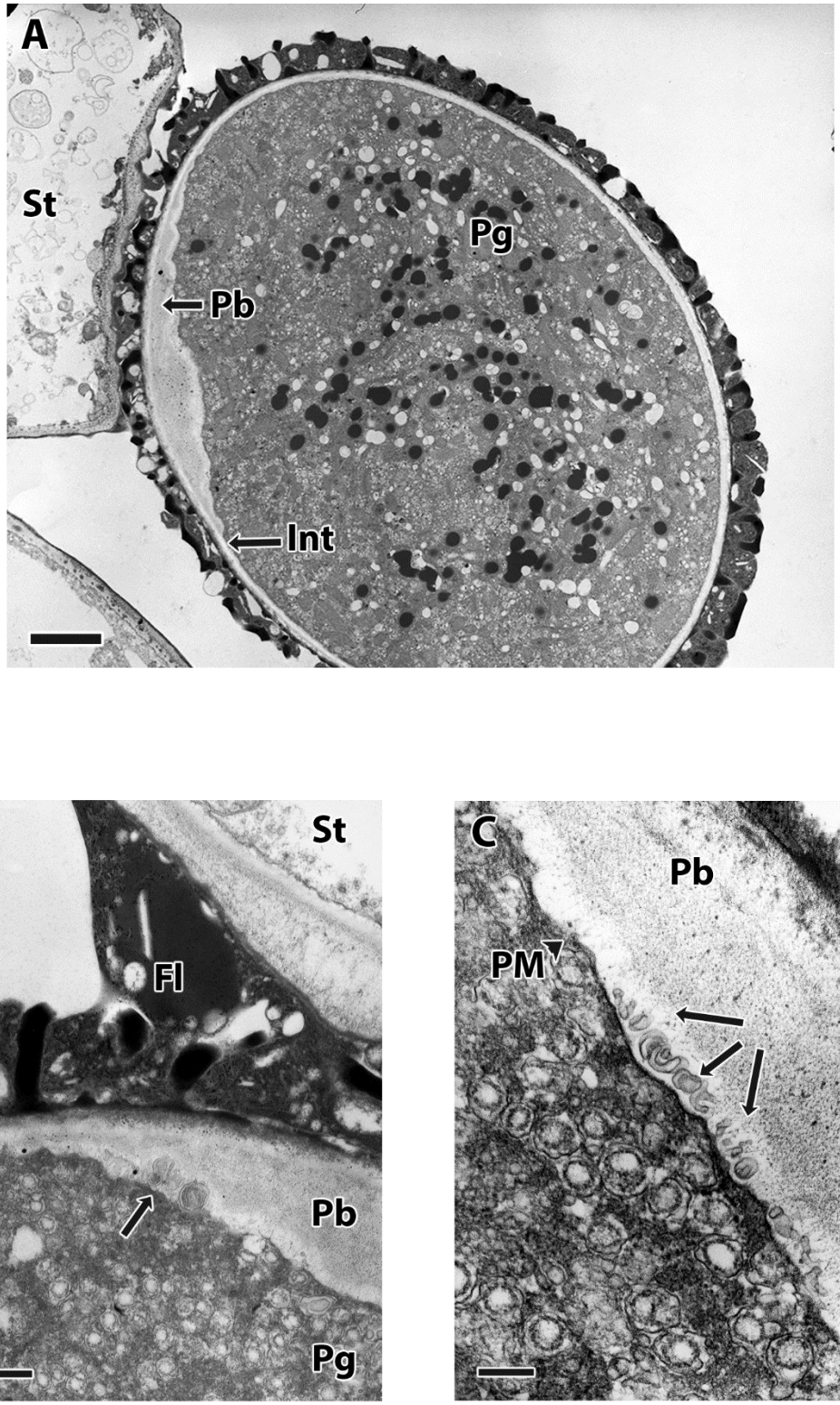

Fig. 35 A Pollen grain and stigma mid-adhesion. Thickening plaque (pectin bulge) present at contact point. **B, C** Pectin bulge by contact point and expanding foot layer. Vesicles (arrows) at interface of plasma membrane and intine. Pb (pectin bulge), Pg (pollen grain), Fl (foot layer), St (stigma), Int (intine). Bar (A) =2 µm, (B) = 0.5 µm, (C) = 200 nm

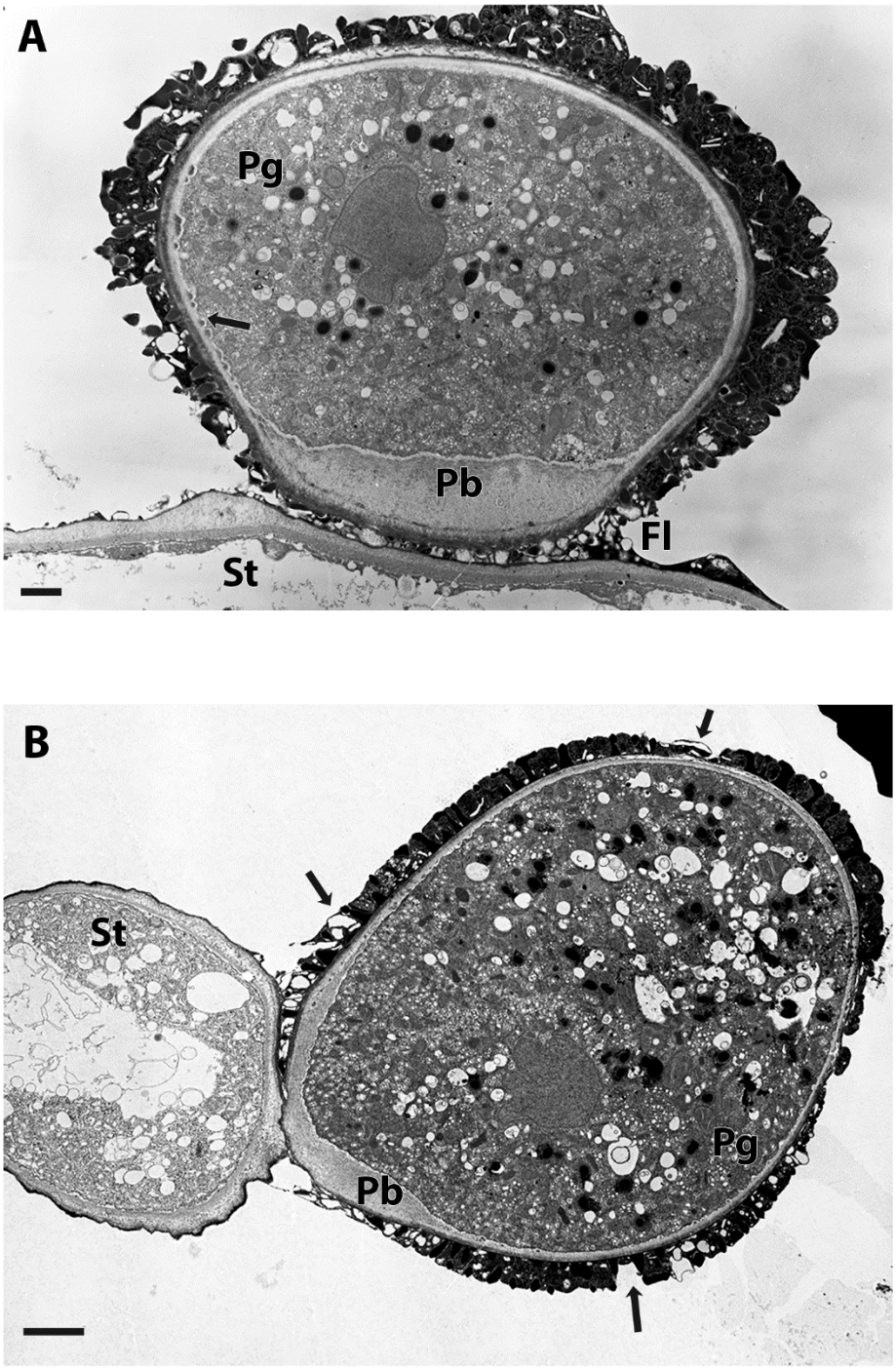

Fig. 36 A Pollen grain and stigma mid-adhesion. Undulations (arrows) in plasma membrane and cytoplasmic reorganization **B** Early emergence of pollen tube within inter-aperture space. Apertures indicated by arrows. Pb (pectin bulge), Pg (pollen grain), Fl (foot layer), St (stigma). Bar (A) =1 µm, (B) = 2 µm

contact point between stigma and pollen grain. Endoplasmic reticulum is more evident by the expanding distortion or extension of pollen grain material (Fig. 37 A). While the area immediately inferior to the plaque still shows clearing, more cellular structures, vacuoles and electron-dense spherical bodies are mobilizing toward the extension.

A distinct pollen tube now takes shape (Fig. 37 B), and there is a noticeable change in the wall of the grain. The intine appears to have expanded into a stratified fibrillar layer, wider on either side of the pollen tube where the breaching of grain wall occurs. Numerous small vesicles are present at the tip of the pollen tube extension. Present in the distal area of the pollen tube growth (Fig. 38) are Golgi bodies with attached vesicles, mitochondria, and spherical bodies which may be bound by endoplasmic reticulum. The exintine and endintine are no longer able to be distinguished from one another, as the stratified fibrillar layer expands within the intine.

Late pollen tube

The distal end of the pollen tube now appears to be filled with electron lucent spherical bodies (Fig. 39). Osmiophilic droplets have formed at the interface of the plasma membrane and intine. The pollen tube shows a narrowing some distance from the distal end, possibly from constriction by the expanded stratified fibrillar layer.

The pollen tube continues to expand in a distal direction from an inter-aperture space (Fig. 40 A), while the remainder of the pollen grain wall remains intact. An electron lucent layer appears between the plasma membrane and intine, but only in the constricted area of the pollen tube, not continuing distally down the tube. The bi-layered intine is clearly visible proximally from the constricted area of the pollen tube, toward the rest of the pollen grain (Fig. 40 B). The cytoplasm of the grain shows endoplasmic reticulum and small vacuoles throughout.

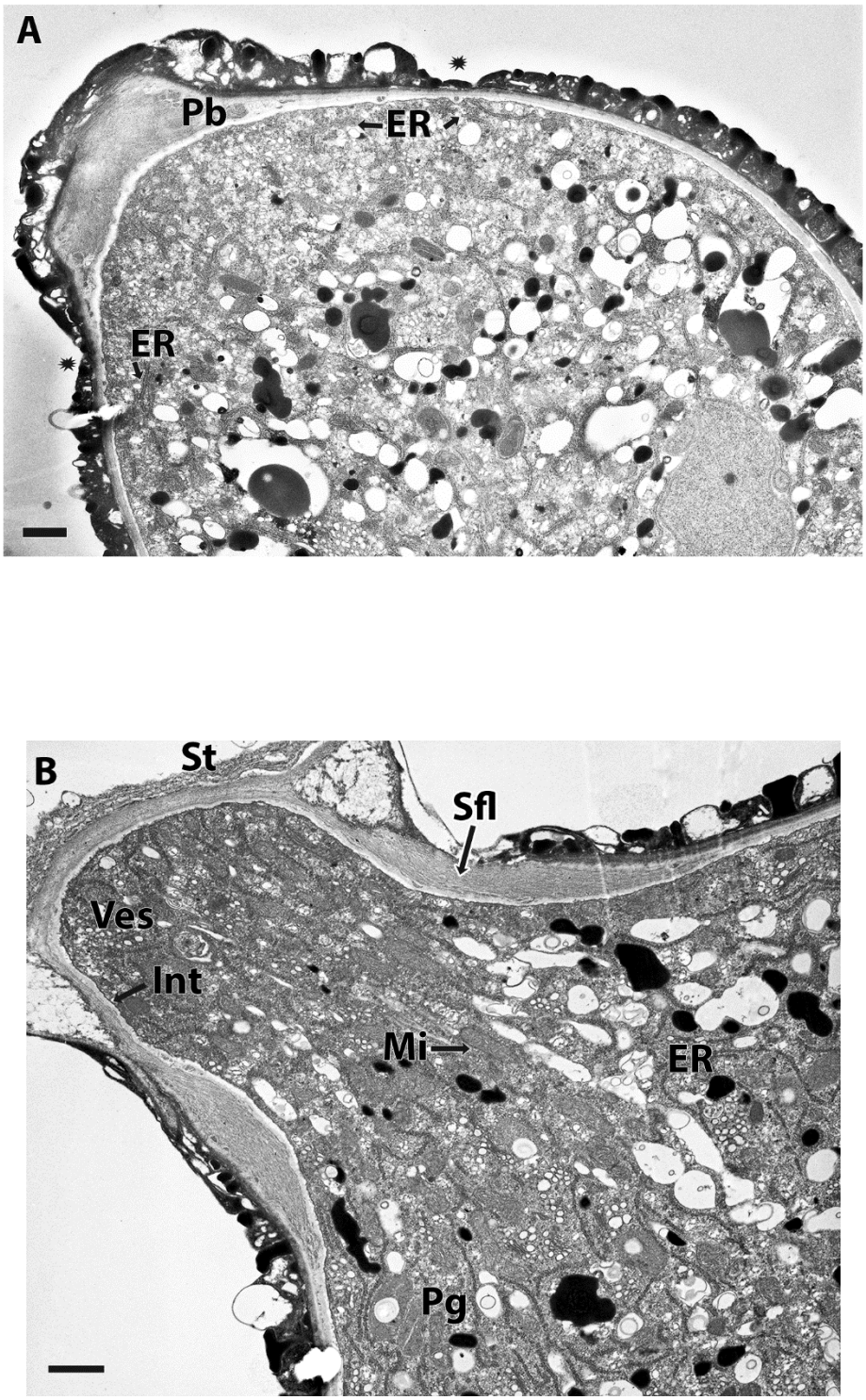

Fig. 37 A Emergence of pollen tube within inter-aperture space. Apertures indicated by asterisks. Endoplasmic reticulum in vicinity of pectin bulge. **B** Pectin bulge not as evident as stratified fibrillar layer in area of intine increases. ER (endoplasmic reticulum), Mi (mitochondria), Pb (pectin bulge), Pg (pollen grain), Fl (foot layer), St (stigma), Sfl (stratified fibrillar layer), Ves (vesicle), Int (intine). Bar (A) =2 µm, (B) = 1 µm

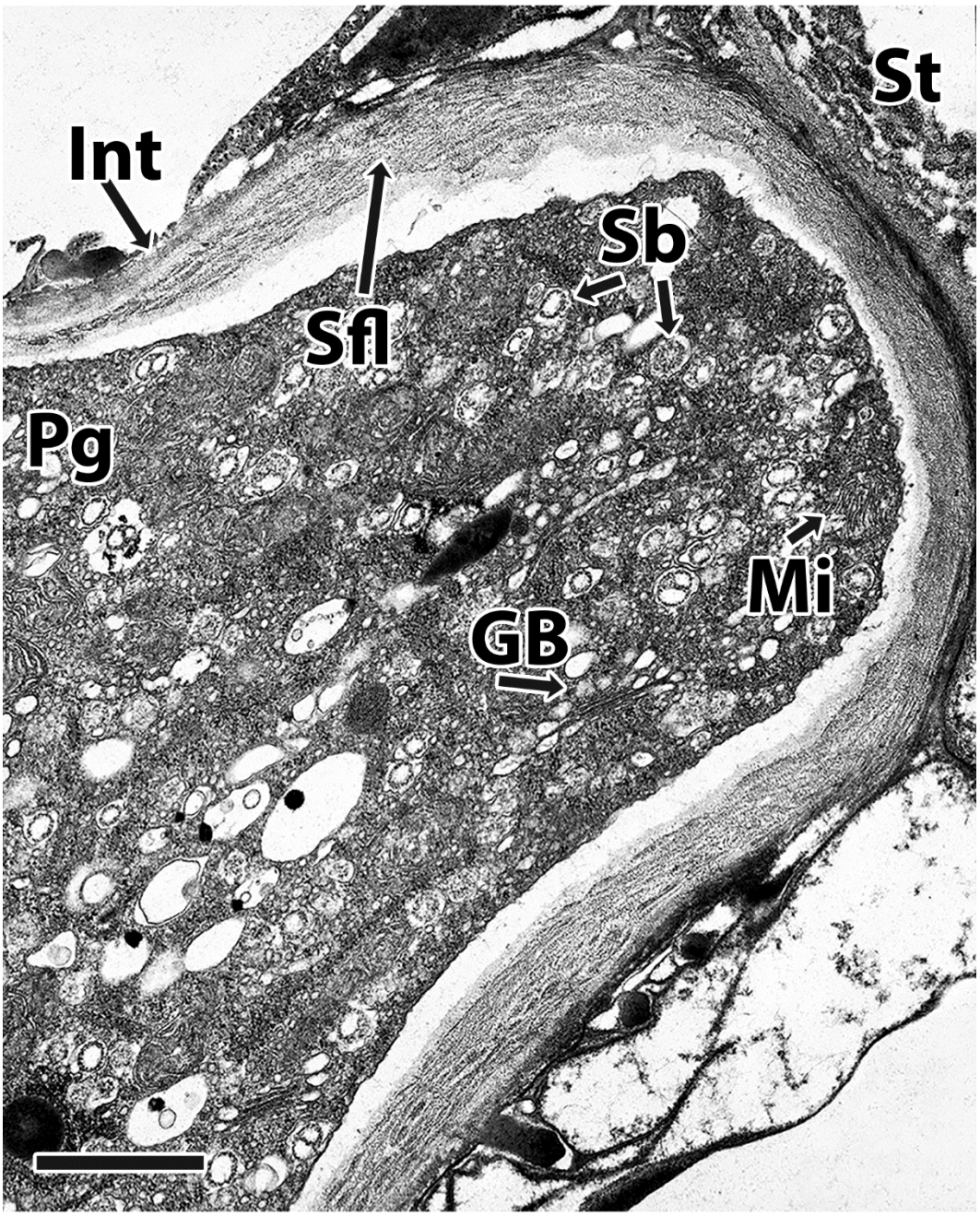

Fig. 38 Pollen tube with high magnification of pollen tube wall. Spherical bodies present by tip of pollen tube. Pg (pollen grain), St (stigma), Int (intine), GB (Golgi body), Sfl (stratified fibrillar layer), Mi (mitochondria). Bar =1 µm

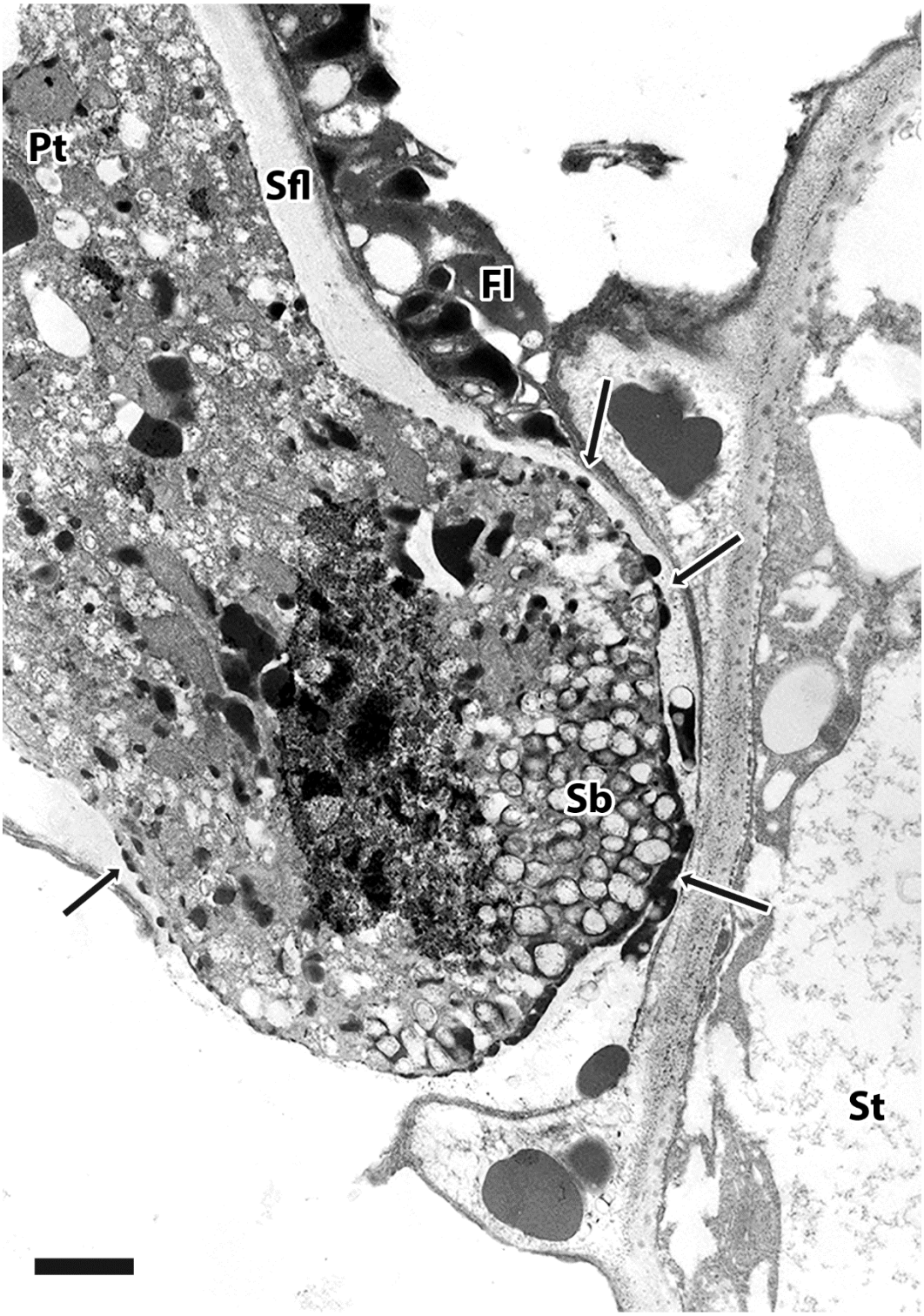

Fig. 39 Late pollen tube emergence with osmiophilic globules (arrows) at interface of plasma membrane and intine. Increase in spherical bodies by tip of pollen tube. Pt (pollen tube), St (stigma), Sfl (stratified fibrillar layer), Fl (foot layer), Sb (spherical bodies) Bar =1 µm

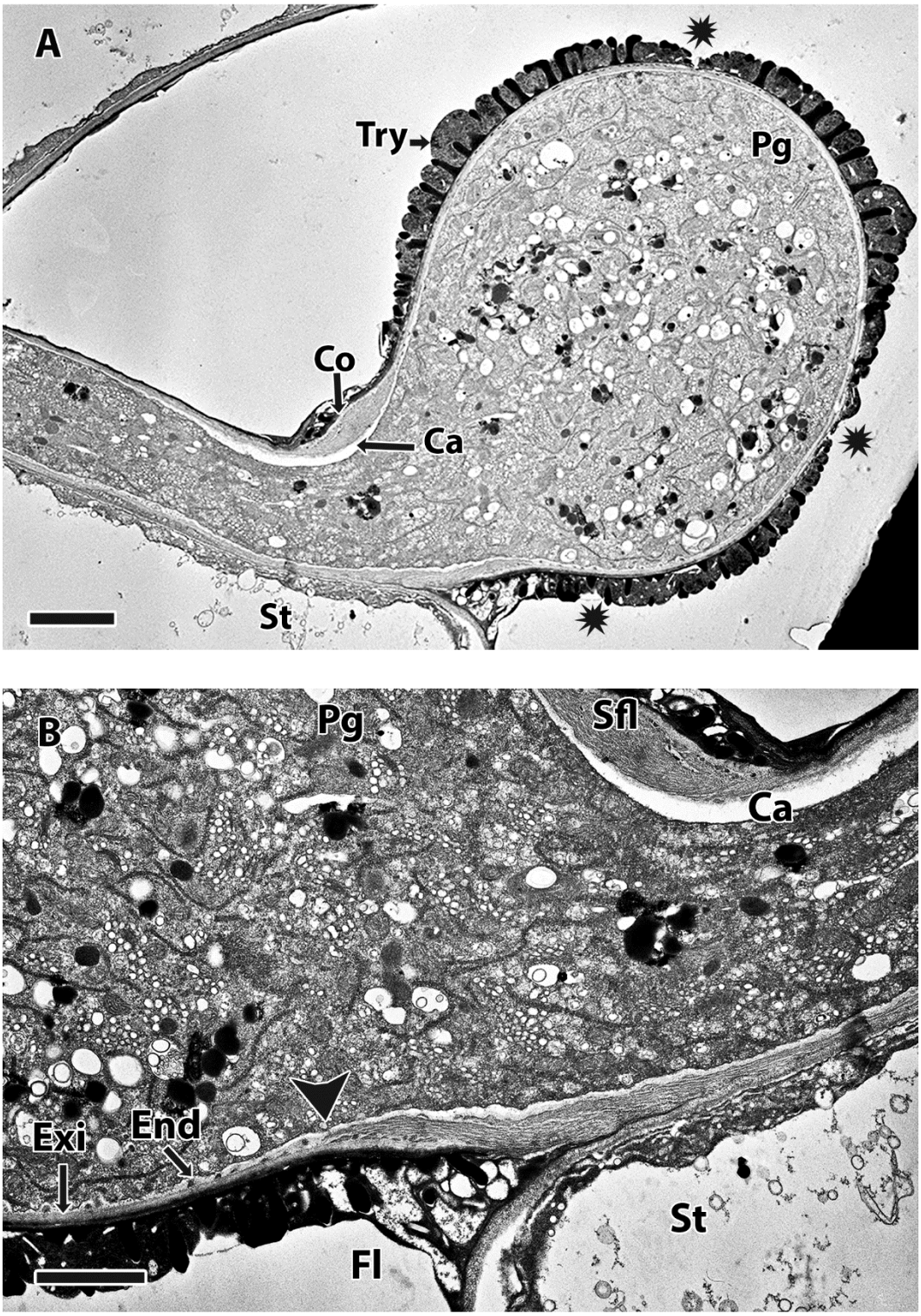

Fig. 40 A Late pollen tube within inter-aperture space showing callose collar. **B** High magnification of pollen tube shown in **A**. Asterisk (inter-aperture space), Pg (pollen grain), St (stigma), Try (tryphine), Sfl (stratified fibrillar layer), Ca (callose), Co (collar), Exi (exintine), End (endintine), Fl (foot layer). Bar (A) = 5 µm, Bar (B) =1 µm

Figures 41 A and B are images of semi-thin sections taken from the same pollinated material used for the transmission electron microscopy study (20 - 30 minutes). Figure 41 A is an image captured using differential interference contrast, showing the constricted area of the pollen tube, just distal from the tube's emergence from the pollen grain. Using the same material, the constricted area fluoresces when viewed by UV-excitation of aniline blue stained sections using epifluorescence microscopy (Fig. 41), confirming that the material is callose.

D. Discussion

The primary function of a pollen grain is to protect and deliver the sperm cell containing the male genetic information to the female ovule for fertilization. This process has been studied extensively, focusing largely on changes within the stigma, yet still containing large gaps of information. An objective of this project was to look at structural changes occurring as the pollen grain wall is expanded outward and then breached by the developing pollen tube. Carrying out an ultrastructural study of the pollen grain wall during germination informs understanding of the wall, pollen tube emergence through inter-aperture spaces, and the adhesion process.

The pollen grain wall of *Arabidopsis thaliana* consists of the pollen coat and two main layers, the outward facing and highly reticulate exine and inward facing bi-layered intine (Fig. 31 and 32 A). The exine is composed largely of sporopollenin, an electron-dense complex polymer that is resistant to non-oxidative degradation and insoluble in aqueous and organic solvents (Ahlers, Thom, Lambert, Kuckuk, & Wiermann, 1999). The pollen tube needs to emerge from within the grain, the intine and exine penetrating the stigma papillar cell wall of the female. Until recently, it was thought pollen tubes must emerge through apertures, which are areas on the pollen grain surface with reduced exine. It has now been shown the pollen tube of ecotype Landsberg *erecta* (Ler)

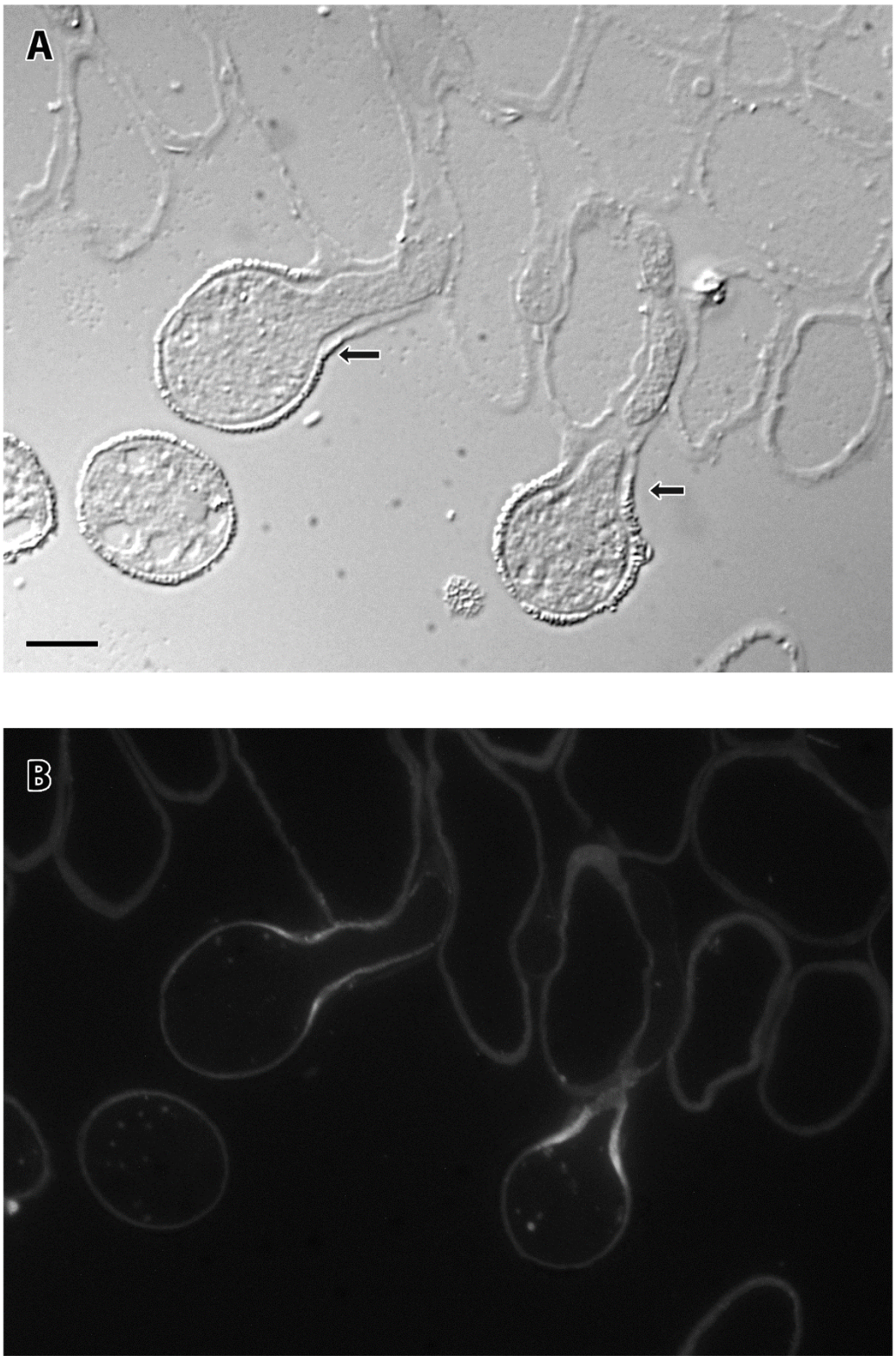

Fig. 41 A Differential interference contrast microscopy showing late pollen tube with collar (arrows). **B** Aniline blue staining with epifluorescence indicating callose within collar of pollen tube. Bar =10 µm

emerges through an inter-aperture space 67% of the time in situ (Edlund, Zheng, et al., 2016). The three apertures found on *Arabidopsis thaliana* pollen grains are arranged approximately equidistant from one another (Fig. 31). This unique arrangement, along with the reticulate and porous nature of the exine allows for rapid expansion when the desiccated grain is exposed to liquid.

Prior to adhesion the two layers of the intine are clearly delineated (Fig. 32 A). The exintine lies superficial to the endintine, which is adjacent to the plasma membrane. The intine is secreted by the microspores during ring vacuolate stage (Owen & Makaroff, 1995) and is formed via polysaccharide metabolism (Hess, 1993). The exintine is granular with pectin and protein inclusions and the endintine is a microfibrillar cellulosic layer (Huang et al., 2009; Regan & Moffatt, 1990). Changes in the wall began shortly after pollination, approximately eight to twelve minutes post-pollination in this project (Figs. 32 B, C). Actual adhesion and hydration between the dry stigma and pollen grain happens within five minutes (Dwyer et al., 1994; Preuss, Lemieux, Yen, & Davis, 1993), due to lipophilic molecules within the exine itself. These molecules are also thought to play a role in species-specific recognition and compatibility (Zinkl et al., 1999).

During the self-compatibility fertilization process, an *Arabidopsis* pollen grain can land on and may be fertilized by the dry stigma of an *Arabidopsis* plant. After initial adhesion, exudate formed and found as part of the foot layer (Figs. 34 A, B) serves to hydrate the grain and may help with penetration of the stigma (Carole J. Elleman & Dickinson, 1990). An exudate is formed during the self-incompatibility response found in *Brassica oleracea*, but this exudate contains signaling factors or determinants from both pollen grain and stigma that will stop pollination (Takayama et al., 2001). The male determinant is S-locus protein 11 or S-locus

cysteine rich protein (SP11/SCR), a small pollen coat protein that induces incompatible reactions in the stigma papilla cells (Schopfer, Nasrallah, & Nasrallah, 1999). While *A. thaliana* does not undergo the self-incompatibility response found in the Brassica, *A. lyrata, A. halleri, or A. arenosa,* it has retained the ability to produce necessary cytoskeleton elements to undergo this response (Nasrallah, Nasrallah, Liu, Sherman-Broyles, & Boggs, 2004). Gene sequences found in *A. thaliana* and transformation experiments demonstrated that evolutionary loss of self-incompatibility function was from an inactivation, not complete deletion of one of the compatibility response genes. Trafficking of substances necessary for the compatibility response, as well as the changes taking place in the pollen wall, require vesicular transport to the point of contact between stigma and grain. Because *A. thaliana* does not undergo the self-incompatibility response, those particular proteins (SCR) should not be found within the vesicles, although the timing and location would be appropriate. An opening to the intine from the plasma membrane (Fig. 32 B) appears filled with vesicles of various sizes, likely undergoing exocytosis. Possible components of the vesicles are enzymes used to degrade and breach the wall, cell wall components for extension of the pollen tube, or materials to be used in the synthesis of the pectin layer, but cytochemical tests need to be carried out in order to gain a better understanding of the contents.

Mobilization of the lipid and protein-rich tryphine helps form the foot layer between the stigma and grain at the point of contact (Fig. 34 A). In the vicinity of the foot layer but within the grain, a rippling of the plasma membrane and increasing thickness of the intine occurs. The rippling membrane continues distally, becoming less noticeable further from the contact point. The vegetative cell also becomes polarized, with a reorganization of osmiophilic bodies leaving a clearing toward the stigma contact point. Osmiophilic globules have been reported in many

species, with varying ideas as to what they are for. One thought was they contained calcium to be used as a resource for germinating pollen (Butowt, Rodríguez-García, Alché, & Gorska-Brylass, 1997), while another idea considered the globules to be autolytic in nature for mature pollen grains that did not undergo germination (Yamamoto, Nishimura, Hara-Nishimura, & Noguchi, 2003). A calcium repository for germination seems more likely, given that the results from this study indicated an increase in size and number of osmiophilic bodies as germination proceeded. The study that considered the globules autolytic in function did not examine actively germinating pollen grains that were adhered to stigmas, but rather isolated, mature grains from dehiscing anthers.

Approximately twelve to fifteen minutes post-pollination a large thickening of the intine occurs in the area of adhesion, resembling a lentil-shape or plaque (Figs 35-37). This structure contains pectin and cellulose (Hoedemaekers, Derksen, Hoogstrate, Wolters-Arts, Oh, & Twell, 2015) and remains until emergence of the pollen tube (Fig. 37 B). Figures 35 B and C show vesicles at the interface of the plasma membrane and the pectin bulge/ intine. At this point the borders of the endintine and exintine are not as clear, having been disrupted by the growing pectin bulge. According to micrographs at this stage, the exintine seems to be the area from which the pectin bulge arises. This conclusion is reinforced by a number of factors. The primary component of the pectin bulge is pectin, which is also the primary component in the exintine. The intine of immature and non-germinating mature grains contains highly methylesterified pectin, which is synthesized in the Golgi bodies and secreted in secretory vesicles (Carpita & Gibeaut, 1993; Hasegawa, Bressan, Zhu, & Bohnert, 2000). Upon hydration and germination of the pollen grain, the pectin is de-esterfied by pectin methylesterases (PME). Unesterified pectins can bind calcium ions and form a pectate gel that causes more rigidity in the

cell wall (Hasegawa et al., 2000). When considering the timing of the appearance of the vesicles by the intine and plasma membrane interface, as well as the growing pectin bulge (Figs. 36 A, B), it is certainly a possibility that the vesicles contain some of the components that result in the pectin bulge.

The pollen tube must breach the pollen wall in order to travel down the stigma and into the transmitting tract to deliver the sperm cells to the ovule. As shown previously, the pectin bulge through which the pollen tube emerges is not always at the site of an aperture, thus the pollen tube travels instead through the exine (Edlund et al., 2004; Edlund, Zheng, et al., 2016; Hoedemaekers, Derksen, Hoogstrate, Wolters-Arts, Oh, & Twell, 2015). Through the use of atomic force microscopy, exine stiffness was measured and determined to be between one and two orders of magnitude stiffer than the apertures. Atomic force microscopy makes use of extrapolated data from a cantilever that scans the surface of an object such as a pollen grain. Areas of indentation cause more deflection of the cantilever, which indicates a surface of less stiffness than around the indentation. (Edlund, Zheng, et al., 2016). Due to the stiffness of the exine, a considerable force must be in place for the tube to exit through an inter-aperture space (Figs. 33, 36 B, 37 A). Recently it has been established that a weakening of the exine wall in certain Brassicaceae members can be achieved through the use of a combination of hydrogen peroxide, peroxidase, and catalase, all found naturally occurring at the point of adhesion between stigma and grain. Hydrogen peroxide alone was able to cause degradation of the exine in *A. thaliana.* (Edlund, Olsen, et al., 2016).

Weakening of the exine wall is just one of the mechanisms needed for pollen tube emergence. Besides the influx of water continuing from the stigma, included in the emergence process is the force from within, the pectin bulge. The pectin bulge seems to have a force pushing, but what is

keeping it pushing in a unilateral direction, versus non-directional force? This may be explained by the presence of a "collar" found on either side of the pollen tube exit site. Constriction of the tube as it emerges from the grain (Fig. 37 B) appears to be associated with an increase in a stratified fibrillar layer that is a continuation of the intine (Fig. 38). By this stage the pectin bulge is no longer clearly visible at the tip of the growing pollen tube, but the stratified fibrillar layer is expanding as part of the tube wall.

Polarized reorganization of the cytoplasm occurs early in the adhesion process. The vegetative nucleus, followed by the two sperm cells are at the growing tip of the pollen tube, along with vesicles carrying more wall components for the expanding tube and collar. The inner wall of the pollen tube contains cellulose, pectin, and callose (Steer & Steer, 1989). Cellulose microfibrils are synthesized in the plasma membrane via the cellulose synthase complex, which contains cellulose synthase catalytic subunits (Chebli, Kaneda, Zerzour, & Geitmann, 2012). Cellulose synthase complexes are transported to the plasma membrane via the Golgi network, guided by microtubules (Mutwil, Debolt, & Persson, 2008). Crystalline cellulose has been found in cytoplasmic vesicles associated with golgi bodies (Fig. 38) in both the pollen tube and grain of *A. thaliana,* indicating it may be destined for exocytosis (Chebli et al., 2012). In tobacco, immunofluorescence microscopy and immunogold labeling of cellulose synthases were used to determine its distribution along the pollen tube. Cellulose synthase was found located along the length of the pollen tube and in highest concentration at the apex of the tube (Cai, Faleri, Del Casino, Emons, & Cresti, 2011), which could explain the numerous spherical bodies shown in figure 38.

Another possible component of the vesicles is callose synthase. Callose synthases are transmembrane proteins that produce callose. Callose is synthesized from a complex of UDP-

glucose transferase (UGT1), Rho1-like protein (Rop1), sucrose synthase, and annexin (Dong, Hong, Sivaramakrishnan, Mahfouz, & Verma, 2005; Hong, Zhang, Olson, & Verma, 2001; Nedukha, 2015). Callose synthases bind UGT1 which then binds to Rop1. Rop1 acts as a molecular switch to help regulate the production of callose (Verma & Hong, 2001). A generally accepted transport model suggests callose synthases are produced or processed in endoplasmic reticulum, sent to Golgi bodies and transported via actin filaments to the pollen tube apex and distal portions of the pollen tube (Cai et al., 2011). Another form of transport of callose is by multivesicular bodies (MVBs). At this point most of the research has been on callose transport in pathogen response, but the similarity in structures from research already done (An, Huckelhoven, Kogel, & Van Bel, 2006) and the structures noted in this research project are notable. MVBs carry vesicles of varying sizes to the plasma membrane for exocytosis.

The location of the callose synthases brings this discussion back to the collar which appears to be constricting the pollen tube at its emergence point from the grain (Figs. 40 A, B). In order to direct the turgor pressure from the pectin bulge, a collar first appears shortly after tube emergence from the grain (Fig. 37 B). This collar appears similar in composition to the stratified fibrillar layer from the intine which is composed primarily of cellulose (Regan & Moffatt, 1990). Late in the process of pollen tube emergence, a thin layer of callose forms deep to the stratified fibrillar layer of the collar. Presence of callose only at the narrowed portion of the tube has been supported by aniline blue staining (Fig. 41 B) and in previous studies (Parre & Geitmann, 2005). Callose likely acts not only to direct the turgor pressure, but also as a support for the pollen tube to help it withstand the outward forces of the tube growth process.

References

Ahlers, F., Thom, I., Lambert, J., Kuckuk, R., & Wiermann, R. (1999). H NMR analysis of sporopollenin from *Typha angustifolia*. *Phytochemistry, 50*, 1095-1098.

Butowt, R., Rodríguez-García, M. I., Alché, J. D., & Gorska-Brylass, A. (1997). Calcium in electron-dense globoids during pollen grain maturation in Chlorophytum elatum R. Br. *Planta, 203*, 413-421.

Cai, G., Faleri, C., Del Casino, C., Emons, A. M. C., & Cresti, M. (2011). Distribution of callose synthase, cellulose synthase, and sucrose synthase in tobacco pollen tube Is controlled in dissimilar ways by actin filaments and microtubules. *Plant Physiology, 153*(3), 1169-1190.

Carpita, N. C., & Gibeaut, D. M. (1993). Structural models of primary cell walls in flowering plants: Consistency of molecular structure with the physical properties of the walls during growth. *Plant Journal, 3*, 1-30.

Chebli, Y., Kaneda, M., Zerzour, R., & Geitmann, A. (2012). The Cell Wall of the Arabidopsis Pollen Tube—Spatial Distribution, Recycling, and Network Formation of Polysaccharides 1. *Plant Physiology, 160*, 1940-1955.

Dong, X., Hong, Z., Sivaramakrishnan, M., Mahfouz, M., & Verma, D. P. S. (2005). Callose synthase (CalS5) is required for exine formation during microgametogenesis and for pollen viability in Arabidopsis. *The Plant Journal, 42*, 315-328.

Dwyer, K., Kandasamy, M. K., Mahosky, D. I., Acciai, J., Kudish, B., Miller, J. E., Nasrallah, J. B. (1994). A superfamily of S locus-related sequences in Arabidopsis: diverse structures and expression patterns. *Plant Cell, 6*, 1829-1843.

Edlund, A. F., Olsen, K., Mendoza, C., Wang, J., Buckley, T., Nguyen, M., Owen, H. A. (2016). Pollen wall degradation in the Brassicaceae permits cell escape after pollination. *In preparation*.

Edlund, A. F., Swanson, R., & Preuss, D. (2004). Pollen and stigma structure and function: The role of diversity in pollination. *The Plant Cell, 16*, S84-S97.

Edlund, A. F., Zheng, Q., Lowe, N., Kuseryk, S., Lyles, R. H., Sibener, S., & D. Preuss, D. (2016). Pollen from Arabidopsis thaliana and other Brassicaceae are functionally omniaperturate. *American Journal of Botany, 103*(6), 1006-1019.

Elleman, C. J., & Dickinson, H. G. (1986). Pollen-stigma interactions in Brassica. IV. Structural reorganization in the pollen grains during hydration. *J Cell Sci, 80*, 141-157.

Elleman, C. J., & Dickinson, H. G. (1990). The role of the exine coatings in pollen-stigma interactions in *Brassica oleracea* L. *New Phytologist, 114*, 511-518.

Fulcher, R. G., McCully, M., Setterfield, G., & Sutherland, J. (1976). β-1,3-Glucans may be associated with cell plate formation during cytokinesis. *Canadian Journal of Botany, 54*(5-6), 539-542.

Hasegawa, P. M., Bressan, R. A., Zhu, J., & Bohnert, H. J. (2000). Plant cellular and molecular responses to high salinity. *Annual Review of Plant Physiology and Plant Molecular Biology, 51*, 463-499.

Hess, M. W. (1993). Cell-wall development in freezefixed pollen: intine formation of Ledebouria socialis (Hyacinthaceae). *Planta, 189*, 139-149.

Hoedemaekers, K., Derksen, J., Hoogstrate, S., Wolters-Arts, M., Oh, S.A., & Twell, D. (2015). BURSTING POLLEN is required to organize the pollen germination plaque and pollen tube tip in Arabidopsis thaliana. *New Phytologist, 206*, 255-267.

Hoedemaekers, K., Derksen, J., Hoogstrate, S. W., Wolters-Arts, M., Oh, S. A., Twell, D., Rieu, I. (2015). BURSTING POLLEN is required to organize the pollen germination plaque and pollen tube tip in Arabidopsis thaliana. *New Phytol, 206*(1), 255-267.

Hong, Z., Zhang, Z., Olson, J. M., & Verma, D. P. S. (2001). A novel UDP-glucose transferase is part of the callose synthase complex and interacts with phragmoplastin at the forming cell plate. *The Plant Cell, 13*, 769-779.

Huang, L., Cao, J., Zhang, A., Ye, Y., Zhang, Y., & Liu, T. (2009). The polygalacturonase gene BcMF2 from Brassica campestris is associated with intine development. *J Exp Bot, 60*(1), 301-313.

Mutwil, M., Debolt, S., & Persson, S. (2008). Cellulose synthesis: a complex complex. *Current Opinion in Plant Biology, 11*, 252-257.

Nasrallah, J. B., Nasrallah, M. e., Liu, P., Sherman-Broyles, S., & Boggs, N. A. (2004). Natural variation in expression of self-incompatibility in Arabidopsis thaliana: Implications for the evolution of selfing. *Proceedings of National Academy of Science, 101*(45), 16070-16074.

Nedukha, O. M. (2015). Callose: localization, functions, and synthesis in plant cells. *Cytology and Genetics, 49*(1), 49-57.

Owen, H. A., & Makaroff, C. A. (1995). Ultrastructure of microsporogenesis and microgametogenesis in *Arabidopsis thaliana* (L) *heynh* ecotype Wassilewskija (*Brassicaceae*). *Protoplasma, 185*, 7-21.

Parre, E., & Geitmann, A. (2005). More than a leak sealant. The mechanical properties of callose in pollen tubes. *Plant Physiology, 137*, 274-286.

Preuss, D., Lemieux, B., Yen, G., & Davis, R. W. (1993). A conditional sterile mutation eliminates surface components from *Arabidopsis* pollen and disrupts cell signaling during fertilization. *Genes & Development, 7*(6), 974-985.

Regan, S. M., & Moffatt, B. A. (1990). Cytochemical analysis of pollen development in wild-type *Arabidopsis* and a male-sterile mutant. *The Plant Cell, 2*, 877-889.

Schopfer, C., Nasrallah, M., & Nasrallah, J. B. (1999). The male determinant of of self-incompatibility in plants. *Science, 286*, 1697-1700.

Sessions, R., & Zambryski, P. (1995). Arabidopsis gynoecium structure in the wild and in ettin mutants. *Development, 121*(5), 1519-1532.

Smith, M., & McCully, M. (1978). Enhancing aniline blue fluorescent staining of cell wall structures. *Stain Technologies, 53*(2), 79-85.

Steer, M., & Steer, J. (1989). Pollen tube tip growth. *New Phytologist, 111*, 323-358.

Takayama, S., Shimosato, H., Shiba, H., Funato, M., Che, F. S., Watanabe, M., Isogai, A. (2001). Direct ligand-receptor complex interaction controls Brassica self-incompatibility. *Nature, 413*(6855), 534-538.

Verma, D. P. S., & Hong, Z. (2001). Plant callose synthase complexes. *Plant Molecular Biology, 47*, 693-701.

Wilson, Z. A., Morrol, S. M., Dawson, J., Swarup, R., & Tighe, P. J. (2001). The Arabidopsis MALE STERILITY1 (MS1) gene is a transcriptional regulator of male gametogenesis, with homology to the PHD-finger family of transcriptional factors. *Plant Journal, 28*(1), 27-39.

Yamamoto, Y., Nishimura, M., Hara-Nishimura, I., & Noguchi, T. (2003). Behavior of Vacuoles during Microspore and Pollen Development in Arabidopsis thaliana. *Plant Cell Physiology, 44*(11), 1192-1201.

Zinkl, G. M., Zwiebel, B. I., Grier, D. G., & Preuss, D. (1999). Pollen-stigma adhesion in *Arabidopsis*: a species-specific interaction mediated by lipophilic molecules in the pollen exine. *Development, 126,* 5431-5440.

Chapter V

General Conclusions and Future Work

In this genetics-centered world of science currently in favor, it is as important to visualize structural changes occurring as it is to find the genes responsible for those changes. Understanding the "normal" development and processes that lead to a continuation of a species such as *Arabidopsis thaliana* helps us decipher the problems that may arise and where a solution may be sought. This necessary interplay between structure and function can be better elucidated with a wide range of tools from the big old science toolbox that is ever changing.

One of the primary objectives of this research project was to examine the structural changes occurring during development of the pollen grain wall from its inception as part of a young microsporocyte to its demise upon delivery of the precious genetic cargo. Several microscopy methods were used to this end and valuable information was gained that could help fill in gaps of knowledge in the pathways presently in place. But there is always room not only for improvement but also for a much broader range of information to be collected, given that the tools necessary are available.

Developmental Study of a Temperature-Sensitive Meiotic Mutant

The *Arabidopsis thaliana* mutant line 6491has been shown to be reduced fertile at higher temperatures, exhibiting defects in the exine that were examined via brightfield and transmission electron microscopy. In carrying out a developmental study, several areas of interest were noted. Pollen grains from the mutant line 6491 that are able to fully mature lack the typical reticulate exine found in wild-type *A. thaliana* from the same line. Grains are inconsistent in size and shape and lack distinctive colpi. The inconsistency in grain size is one of the factors that suggest 6491 is a meiotic mutant. When undergoing meiosis, a callose wall should develop and

eventually separate microsporocytes. Callose is deposited between 6491 microsporocytes, but it is thinner than in wild-type. Looking at issues with callose deposition and timing became an integral part of this project, because it is conceivable that a defect in the callose synthesis process could lead to the resulting phenotype of 6491. The noted defects were seemingly dependent upon the temperature to which the growing source plants had been subjected. Structural differences were also found to be present in the wild-type line when subjected to temperatures on the extreme ends of the acceptable growing conditions.

Callose is formed by callose synthases that are produced by the endoplasmic reticulum and transported via the golgi network along bundles of actin filaments (Cai, Faleri, Del Casino, Emons, & Cresti, 2011). Any discussion regarding changes in callose should include possible alterations in the transport system as part of the mechanism that may be affected in both the 6491 mutant line and temperature affected wild-type line. But where does the story begin? Looking at what has gone wrong in meiosis would be the most appropriate starting place for work that could be done to further elucidate the mutated line 6491.

Examining meiocyte development would be an appropriate experiment to run when looking at a meiotic mutant. It would be beneficial to determine when during meiosis chromosomal changes take place. The use of confocal microscopy with young inflorescences (Stronghill, Azimi, & Hasenkampf, 2014) has shown a number of advantages that would be useful for gathering information related to this study. This method isolates meiotic stages in a more precise manner than in typical meiocyte spreads. It would be useful to know when in development the first abnormal meiotic changes in 6491 are occurring. It is also possible to determine whether a temporal change in meiotic progression is due to an early or late entrance, or extended period within a particular stage. This information can also be coupled with other tissue development,

such as callose or tapetal cells. My research project has shown that visible changes in microsporocytes occur later in development than when the actual damage is done. Being able to narrow down a time-frame when the mutation is most affecting development would better characterize the mutant line. Another benefit of this procedure would be to determine how a change in temperature affects the meiotic spindle (De Storme & Geelen, 2014). I would predict a noticeable change based on the increased fertility problems with increasing temperature associated with 6491.

Another way to examine the meiotic issue would be staining of anthers to compare number of large and small grains produced, or using scanning electron microscopy of dehisced anthers. Both methods could indicate the severity of the meiotic problem. A bigger increase in large versus small grains may show a more severe meiotic issue. Coupling this with Alexander staining (Peterson, Slovin, & Chen, 2010) would indicate not only the grain size, but also if the resulting pollen grains were viable. Undertaking these two methods on different temperature groups such as the ones used for this project would give a more quantitative measure of the changes seen with growth temperature increase in 6491.

Finding the gene affected in 6491 could open several other pathways for experimentation. Immunolabeling could indicate where in the tissues the protein encoded by the mutated gene is located. Pairing that with temperature studies may show an increase in the protein with an increase in temperature, which would lend even more support to the idea of ultrastructural changes being a direct result of the mutation.

Moving on to morphological studies, one of the most important procedures I would do in the examination of WT and 6491 grown at different temperatures would be a re-evaluation of the ultrastructure using high pressure freezing rather than chemical fixation (Kiss & Staehelin,

1995). There certainly are some known artifacts introduced in chemically fixed tissue, and those can be incorporated into the results (Paxon-Sowders, Dodrill, Owen, & Makaroff, 2001; Paxon-Sowders, Owen, & Makaroff, 1997). However, when looking at material that has not previously been studied, there is a factor of uncertainty as to what is real and what is artifact that is difficult to accept, especially as a microscopist. Whether or not possible artifacts would alter conclusions reached with chemically fixed tissue is impossible to know, but the opportunity to make that decision would be a huge step in characterization of 6491.

Use of high pressure freezing would also allow better visualization of cytoskeletal structures not easily preserved with chemical fixation, especially in plant cells within thick walls, such as the callose wall surrounding the meiocytes and tetrad stage microspores. This is important when dealing with 6491, because I believe part of the callose deposition and wall pattern problem is tied to the transport and deposition of callose synthases. It has been shown that callose synthases in pollen tubes are transported via microtubules (Cai et al., 2011). An assumption could be made that the same transport system may be in place in developing microsporocytes. High pressure freezing has the demonstrated ability to preserve microtubules in microsporocytes and tetrad-stage microspores. Comparing the presence, structure or concentration of microtubules in 6491 to wild-type, as well as how the microtubules change in altered growth temperatures, would add a great deal to the characterization of 6491.

Electron tomography in conjunction with high pressure freezing (Otegui & Staehelin, 2004) has shown promising results in examination of callose deposition and cell wall formation in coenocytic microsporocytes. There is an unanswered question as to why callose deposition is different in 6491 when compared to wild-type. Being able to better visualize where or when the callose is forming could help answer that question. Another technique is localization microscopy

in intact plant tissue (Eggert, Naumann, Reimer, & Voigt, 2014) that has shown promising results with resolution so high that individual callose microfibrils have been visualized, showing orientation of the microfibrils as well as interaction with surrounding tissue. Aniline blue fluorochrome can be used to stain callose fibrils. A laser is used to repeatedly stimulate fluorescence and then allow a return to a dark state. The emitted photons are collected and processed into a 3-D image with resolution to 20 nm. This process is repeated thousands of times until all of the fluorochromes have been processed. Nanoscale resolution such as this could help explain the altered thickness of callose wall in 6491 or, as part of pollen tube emergence, help show how the callose "collar" is deposited and interacts with surrounding tissues of the intine.

Structural Changes During Microgametogenesis and Megagametogenesis in Wild-Type *Arabidopsis thaliana* Subjected to Different Growth Temperatures

Changes in plants subjected to chilling and heating are seen on a daily basis, especially with extreme temperature fluctuations that are becoming more prevalent as our planet continues with climate change. Agricultural losses have the ability to decimate populations, both animal and human, or at the very least cause economic hardship. Understanding how changing temperatures can affect such vital systems as pollination will be of benefit to many. As part of this research project, wild-type *A. thaliana* was grown at three different temperatures covering the range of acceptable growth temperatures. Structural changes from pollen removed from plants grown outside the average growth temperature were noted. As mentioned previously, high pressure freezing would be a primary focus in re-examination of the plant tissue. A developmental study of chemically-fixed tissue is a necessary first step in order to find the stages of interest, much like examining semi-thin sections was necessary prior to moving onto electron microscopy. Completing a transmission electron microscopy developmental series of WT during early pollen

development, in conjunction with an expanded range of growth temperatures in smaller increments would be the next logical step. I would like to see what changes occur at more specific temperatures, ideally being able to determine the temperatures that are no longer healthy for pollen development. Also of interest would be the difference in healthy growth temperatures for a variety of ecotypes. *Arabidopsis* ecotypes such as Landsberg erecta (Ler), Cape Verde Islands (Cvi), or Columbia (Col) are from different geographical areas that represent a variety of climates. Ecotype Col from Germany would not be expected to have the same heat tolerance as ecotype Cvi from off the coast of Africa. Genomic information has been gathered in heat stress studies (Barah, Jayavelu, Mundy, & Bones, 2013), but comparison of ultrastructural differences between the ecotypes has largely been ignored. Finding what cellular structures are more tolerant to heat or more susceptible to cold under changes that are more in line with our temperature changes versus extremes could help develop crop lines that would better survive in our future environment.

Structural differences noted in WT grown at the cooler end of acceptable growth in this research project included hypertrophy of tapetal cells. The increase in tapetal cell size may be from reabsorption of products released by the disintegrating callose wall, but what those products are is unknown, as is the function of tapetal cell vacuoles that develop under cold stress (Mamun, Alfred, Cantrill, Overall, & Sutton, 2006). In studies with rice, carbohydrate metabolism and transport has been shown to be a key factor in cold-tolerant plants (Sharma & Nayyar, 2016). Nutrients such as carbohydrates necessary for microspore development come from tapetal cells, and programmed cell death (pcd) is part of the normal process by which products from the tapetum support microspores. Gibberillin acts as a signaling molecule that cues pcd and has also been found in large amounts in cold tolerant plants (Plackett, Thomas, Wilson, & Hedden, 2011).

The mechanisms involved with carbohydrate transport and regulation of gibberillins are known to be involved in cold stress response, but how it all works is not yet known. Structural changes in tapetal cells evident in WT within an acceptable growth temperature should indicate that the temperature optimum for viable pollen may not be as cool as originally thought. This brings the research back to needing an expansion of the original temperatures tested.

Another area to consider would be the examination of Callose Synthase mutants known to have defects in callose deposition and how they change structurally when grown at the temperatures tested in this project. It would be interesting to see if growth temperature differences exacerbated the defects or changed their severity in any way. This would also tie into the callose issues in 6491 and help fill gaps in unknown callose deposition pathways.

Novel Interaperture Breakout in *Arabidopsis thaliana*

Interaperture breakout in *A. thaliana* had not been characterized previously, nor was it determined until recently a possible mechanism for pollen tube escape through the resilient exine wall (Edlund et al., 2016). Endless questions have arisen in the examination of images collected for this project, with few concrete answers reached. As frustrating as this is, it has also exposed a chasm of unknowns so large that research can proceed in this area for a tremendously long time. Most structural research in germination seems to have been completed on the stigma end of things, not on the developing pollen tube. Considering that this is the delivery system of half of the genetic material for the zygote and one third of the genetic material for the endosperm, it should also be a focus as much as the stigma. One of the most challenging aspects of working with germinating pollen grains in situ is finding the exact stage needed in the few grains that are within ultrathin sections needed for TEM. Making use of the technique of array tomography (Micheva & Smith, 2007) in which a field emission SEM is used to obtain backscattered electron

images from ribbons of serial sections, and the Reconstruct software program to image changes in the exine wall at the point of escape would be a good addition to using just TEM. Ultrathin sectioning through an entire pollen grain adhered to a stigma would give a more complete picture of what is occurring, but the sheer scope of the number of serial sections and the limited size of the sections needed would make this an unlikely avenue to pursue by TEM. But again, the ability to image the entire area of large serial sections with SEM is more feasible, although resolution would not be as good at that of TEM.

After reading previous research on germination, it became quite evident that in vitro germination of pollen does not yield the same results as in situ. Keeping this in mind, any of the material for future studies of germinating pollen tubes should only come from pollen grains that are germinated in situ, or the results cannot be well supported.

One facet of the results had to do with changes in the intine layer of the pollen wall. The intine is actually composed of two layers, the exintine and endintine. The pectin bulge forms just under the area where the pollen tube will develop and escape and it appears as though the pectin bulge arises from the same area in which the exintine is located. Preliminary research indicated thickness of the exintine and endintine were in different proportions dependent upon where along the grain wall they were being examined. Knowing that the exintine most likely plays a part in the development of the pectin bulge, it would be interesting to see if that bulge changed in dimension if the exintine thickness was changed initially. Various plant stressors might lead to intine changes and this could possibly be indicated by a change in germination. The pectin bulge seems to be one of the forces behind the interaperture breakout. If that were too small, would the pollen tube still be able to escape or would it require more time to do so? Comparing the intine thicknesses of some of the *Arabidopsis* ecotypes that have been determined to have a high

frequency of interaperture breakout with those that have a low frequency of interaperture breakout might be of interest to complement some of the other studies. However, a very big issue to surmount would be how to ensure the grains were all arranged in the same position, so sections made at various angles would not give false indications of wall thicknesses. Using array tomography and 3-D reconstruction with a program such as Reconstruct may help alleviate these issues.

Probably the area most in question is that of the identity of vesicles in the germinating pollen grain and developing pollen tube. There are several types, shapes and sizes that appear throughout the process. It could be assumed that many of the vesicles are carrying wall components for the pollen tube, but some type of definitive labeling should be done on the vesicles. One possibility would be immunolabeling for callose synthase, a component of the callose collar formed within the pollen tube. Another possibility is affinity purification of the vesicles. If the vesicles are isolated in their natural state, then proteomics could be used to determine the proteins within vesicles of similar densities (Drakakaki et al., 2012). This could be carried further, by comparing proteins in vesicles involved in the self-incompatibility response to those in this project, which uses a line that does not undergo that response. Another avenue of exploration would be using immunogold localization for identification of the carbohydrate components of the intine, pollen tube wall and the various vesicles. JIM (John Innes monoclonal) antibodies such as JIM 5 could be used for direct immunolocalization of non-esterified pectin, determining where in the intine pectin is present.

Examination of a time course of mature grains to determine when callose deposition under the intine begins would be interesting when comparing interaperture to aperture breakout. Does it take as long to develop or is there as thick of a callose collar when not needing to breach the

exine? Rippling that changes along the inside of the pollen grain wall as the point of breakout approaches is yet another area of unknown mechanism. Is this a "loosening" of the intine to better facilitate the development of the pectin layer, or perhaps some part of the vesicular transport system allowing vesicles to bind with and release cell wall components for the growing tube? Going back to immunolabeling of known wall components might lend insight into what is actually occurring. One more point of contention is the presence of electron opaque structures that appear within the tryphine, especially as it mobilizes toward the place of adhesion of grain to stigma. There have been very few mentions of these structures in past literature, and even then it was simply to point out their presence. I have found no speculation as to what they might be nor a possible function. I am unsure if they could be isolated by removing the tryphine from the grain, but it would be a start. Another possibility would be to examine the Callose Synthase Five (CalS5) mutant using TEM. The CalS5 mutant produces tryphine (Dong, Hong, Sivaramakrishnan, Mahfouz, & Verma, 2005), but it is deposited in irregular clumps. Would these same electron lucent structures be present in tryphine that is formed irregularly? If not, could they have something to do with how tryphine is attached or situated within the exine?

Perhaps one of the most relevant ideas as far as practical use of information gathered from the interaperture germination project has to do with removal of sporopollenin. It has been shown that a mixture of three different reactive oxygen species was able to digest sporopollenin (Edlund et al., 2016). *Chlorella protothecoides* is a microalgae that shows promise in the production of biodiesel, and it is now known that sporopollenin is outside the layer of the polysaccharide wall (He, Dai, & Wu, 2016). Removal of the sporopollenin layer increases biodiesel production, but it is not an easy process. It would be interesting to see if application of any of the combination of the three reactive oxygen species would safely remove sporopollenin and increase biodiesel

production. Of course this would have to be done in a manner that was not harmful to the environment, nor prohibitive in cost.

There are several avenues that could come from this research project and lead to information that would positively affect our future in agricultural areas. Understanding the mechanisms that lead to heat or cold tolerance through further study of 6491 may allow for incorporation of these ideas into production of more "weather resistant" crops. Safely growing *Arabidopsis* plants at the optimum temperature for each specific ecotype could lessen structural variability that may be impacting research data in a manner previously unknown. Finding better ways to isolate and identify the components taking part in pollen tube development would also help us understand how the grain wall itself develops, since this needs to quickly and efficiently expand along with the growing pollen tube. Certainly once more research is completed and it is no longer an initial foray into all of the different aspects this project has touched upon, expansion of knowledge of the molecular pathways and structural components will be greatly increased.

References

Barah, P., Jayavelu, N. D., Mundy, J., & Bones, A. (2013). Genome scale transcriptional response diversity among ten ecotypes of Arabidopsis thaliana during heat stress. *Frontiers in Plant Science, 4*(532).

Cai, G., Faleri, C., Del Casino, C., Emons, A. M. C., & Cresti, M. (2011). Distribution of callose synthase, cellulose synthase, and sucrose synthase in tobacco pollen tube Is controlled in dissimilar ways by actin filaments and microtubules. *Plant Physiology, 153*(3), 1169-1190.

De Storme, N., & Geelen, D. (2014). The impact of environmental stress on male reproductive development in plants: biological processes and molecular mechanisms. *Plant Cell Environ, 37*(1), 1-18.

Dong, X., Hong, Z., Sivaramakrishnan, M., Mahfouz, M., & Verma, D. P. S. (2005). Callose synthase (CalS5) is required for exine formation during microgametogenesis and for pollen viability in Arabidopsis. *The Plant Journal, 42*, 315-328.

Drakakaki, G., van de Ven, W., Pan, S., Miao, Y., Wang, J., Keinath, N. F., Weatherly, B., Jiang, L., Schumacher, K., Hicks, G., & Raikhel, N. V. (2012). Isolation and proteomic analysis of the SYP61 compartment reveal its role in exocytic trafficking in Arabidopsis. *Cell Research, 22*, 413-424.

Edlund, A. F., Olsen, K., Mendoza, C., Wang, J., Buckley, T., Nguyen, M., Callahan, B., & Owen, H. A. (2016). Pollen wall degradation in the Brassicaceae permits cell escape after pollination. *In preparation*.

Eggert, D., Naumann, M., Reimer, R., & Voigt, C. (2014). Nanoscale glucan polymer network causes pathogen resistance. *Scientific Reports, 4*(4159).

He, X., Dai, J., & Wu, Q. (2016). Identification of Sporopollenin as the Outer Layer of Cell Wall in Microalga Chlorella protothecoides. *Frontiers in Microbiology, 7*(1047).

Kiss, J. Z., & Staehelin, A. (1995). High pressure freezing. In N. J. Sever & D. M. Shotton (Eds.), *Techniques in Modern Biomedical Microscopy; Rapid freezing, freeze fracture, and deep etching* (pp. 89-104). New York: Wiley-Liss, Inc.

Mamun, E. A., Alfred, S., Cantrill, L. C., Overall, R. L., & Sutton, B. G. (2006). Effects of chilling on male gametophyte development in rice. *Cell Biology International, 30*, 583-591.

Micheva, K. D., & Smith, S. J. (2007). Array tomography: a new tool for imaging the molecular architecture and ultrastructure of neural circuits. *Neuron, 55*(1), 25-36.

Otegui, M. S., & Staehelin, L. A. (2004). Electron tomographic analysis of post-meiotic cytokinesis during pollen development in *Arabidopsis thaliana*. *Planta, 218*, 501-515.

Paxon-Sowders, D. M., Dodrill, C. H., Owen, H. A., & Makaroff, C. A. (2001). DEX1, a novel plant protein, is required for exine pattern formation during pollen development in *Arabidopsis*. *Plant Physiology, 127*, 1739-1749.

Paxon-Sowders, D. M., Owen, H. A., & Makaroff, C. A. (1997). A comparative ultrastructural analysis of exine pattern development in wild-type *Arabidopsis* and a mutant defective in pattern formation. *Protoplasma, 198*, 53-65.

Peterson, R., Slovin, J., & Chen, C. (2010). A simplified method for differential staining of aborted and non-aborted pollen grains. *International Journal of Plant Biology, 1*(e13).

Plackett, A. R. G., Thomas, S. G., Wilson, Z. A., & Hedden, P. (2011). Gibberellin control of stamen development: a fertile field. *Trends in Plant Science, 16*, 568-578.

Sharma, K. D., & Nayyar, H. (2016). Regulatory networks in pollen development under cold stress. *Frontiers in Plant Science, 7*(402), 1-13.

Stronghill, P., Azimi, W., & Hasenkampf, C. (2014). A novel method to follow meiotic progression in Arabidopsis using confocal microscopy and 5-ethynyl-2′-deoxyuridine labeling. *Plant Methods, 10*(33).

KATRINA L. OLSEN

Department of Biological Sciences
University of Wisconsin - Oshkosh
800 Algoma Boulevard
Oshkosh, WI 54901
olsenk10@uwosh.edu

Education:

University of Wisconsin-Milwaukee; Milwaukee, WI; Ph.D. Cell Biology/ Botany, December 2016.
Dissertation: Ultrastructural Changes during Pollen Wall Development and Germination in *Arabidopsis thaliana*. Advisor: Heather Owen, PhD

University of Wisconsin-Oshkosh; Oshkosh, WI; M.S. Microbiology, May 2005.
Thesis: The Effect of Heat Stress on the Plastoglobuli Proteome of *Gossypium Barbadense.* Advisor: Robert Wise, PhD

Alverno College; Milwaukee, WI; B.A. Biology, May 2003.

Presentations:

Anna F. Edlund, Sumana Rao, Katrina Olsen, April Wang, Qin Zheng, Andre Rafizadeh, Lenny Nguyen, Skye Kuseryk and Heather A. Owen. 2014. How and why some pollen tubes don't germinate through apertures. Annual Meeting of the Research Co-ordination Network on Integrative Pollen Biology. May 14 - 15, 2014. Charlotte, NC.

Edlund, A.F., Rao, S., Olsen, K., Wang, A., Nguyen, M., Rafizadeh, A., Nguyen, L., and Owen, H. A. 2013. Environmental sensitivity of pollen germination behaviors in the Brassicaceae. Third Annual Meeting of the Research Co-ordination Network on Integrative Pollen Biology Workshop. March 1 – 3. Tucson, AZ.

Edlund, A., Olsen, K., Wang, A., Rao, S., Rafizadeh, A., Zheng, Q. and Owen, H. 2012. Exine degradation during escape from the pollen wall of *Arabidopsis thaliana*. Linnean Society Palynology Specialist Group's Annual Meeting – Understanding Pollen and Spore Diversity. Burlington House, London.

Edlund, A.F., Olsen, K., Wang, J., Zheng, Q. and Owen, H.A. 2011. Variations in pollen germination: How do *Arabidopsis thaliana* pollen tubes escape sporopollenin walls? Plant Biology 2011. Minneapolis, MN.

Olsen, K. 2005. The Effect of Heat Stress on the Plastoglobuli Proteome *of Gossypium Barbadense.* Thesis Defense, University of Wisconsin-Oshkosh, Oshkosh, WI.

Olsen, K., Kostman, T. 2004. Calcium Sequestration and Transport within Calcium Oxalate Crystal Forming Cells. Research Colloquium. University of Wisconsin-Oshkosh, Oshkosh, WI.

Olsen, K. 2004. The Ultrastructure of Crystal Idioblast Cells in *Amaranthus spp.* Research Colloquium, University of Wisconsin-Oshkosh, Oshkosh, WI

Manuscripts (in review):

Edlund, AF, Olsen, K, Mendoza, C, Wang, J, Buckley, T, Nguyen, M, Callahan, B, and Owen, HA. (2016) Pollen wall degradation in the Brassicaceae permits cell escape after pollination. Nature Scientific Reports.

Teaching Experience

University of Wisconsin - Oshkosh
- Human Anatomy Laboratory
- Human Physiology Laboratory
- Animal Physiology Laboratory
- Unity in Biology Laboratory

University of Wisconsin-Milwaukee
- Human Anatomy and Physiology Laboratory

Marian University
- Transmission Electron Microscopy Lecture and Laboratory
- Cell Biology Lecture
- Biology in Society Lecture and Laboratory
- Microbiology Lecture
- Microbiology Lecture Online Course

Professional Experience

August 2005 to the present; Senior Lecturer (Academic Staff), Department of Biological Sciences, University of Wisconsin - Oshkosh.

August 2011 to May 2013; Teaching Assistant, Department of Biological Sciences, University of Wisconsin-Milwaukee.

August 2005 to June 2008; Adjunct Faculty and Director, Electron Microscope Laboratory, Department of Biological Sciences, Marian University.

September 2002 to January 2003; Internship, Department of Neuroscience, Medical College of Wisconsin.